UNIVERSITY OF LIVERPOOL

Institute of Integrative Biology

# Analysis of Fibroblast Growth Factor-Heparin Interactions

**Thesis submitted in accordance with the requirements of the University of Liverpool for the degree of Doctor in Philosophy**

**Written**

**By**

**Ruoyan Xu**

**December 2012**

# Abstract

The functions of a large number (> 435) of extracellular regulatory proteins are controlled by their interactions with heparan sulfate (HS). In the case of fibroblast growth factors (FGFs), HS binding controls their transport between cells and is required for the assembly of a high affinity signaling complex with the cognate FGF receptor. However, the specificity of the interaction of FGFs with HS is still debated. In this thesis, a panel of FGFs (FGF-1, FGF-2, FGF-7, FGF-9, FGF-18 and FGF-21) spanning five FGF sub-families were used to probe their specificities for HS/heparin at different levels: recombinant FGF proteins were expressed and purified and their biological activities tested in a DNA synthesis assay. Then, the proteins were tested for their heparin binding specificity using a variety of complementary approaches: 1. Measurement of the binding parameters of FGFs and a model heparin sugar in an optical biosensor or by microscale thermophoresis; 2. Identification of the heparin binding site (HBS) in the proteins using a Protect and Label strategy; 3. Determination of stability changes in FGFs when bound to different heparin sugars and related glycosaminoglycans employing differential scanning flurometry; 4. Measurement of the conformational changes in FGFs when binding to a variety of molar ratios of heparin and chemically modified heparins using synchrotron radiation circular dichroism (SRCD); 5. Measure directly the binding of FGF-2 to cellular HS using nanoparticles (NPs) to label the FGF-2 and transmission electron microscopy. For interaction with heparin, the FGFs have $K_D$s varying between 38 nM (FGF-18) and 620 nM (FGF-9) and association rate constants spanning over 20-fold (FGF-1, 2,900,000 $M^{-1}s^{-1}$, FGF-9, 130,000 $M^{-1}s^{-1}$). The canonical HBS in FGF-1, FGF-2, FGF-7, FGF-9 and FGF-18 differs in its size and these FGFs have a different complement of secondary HBS, ranging from none (FGF-9) to two (FGF-1).

Differential scanning fluorimetry identified clear preferences in these FGFs for distinct structural features in the polysaccharide. SRCD revealed conformational changes in FGFs induced by binding to heparin and the changes were distinct at different heparin concentrations. Moreover, there was evidence that the conformational changes of FGFs differed with chemically modified heparins, indicating that the conformational change caused by binding to heparin is related to the sulfation pattern. At the cellular level, FGF-2 labeled with nanoparticles allowed the distribution of FGF-2 to be determined in the pericellular matrix of Rama 27 fibroblasts. The results showed that the FGF-2-NPs were specifically bound to cellular HS and were clustered. Taken together, these data suggest that the differences in heparin binding sites in both the protein and the sugar are greatest between FGF sub-families and may be more restricted within a FGF sub-family in accord with the known conservation of function within FGF sub-families, which supports the idea that heparin binding of these proteins is specific, but in terms of consensus sites on the GAG chain, rather than precisely defined chemical structures.

**To my parents with love**

# Acknowledgements

First and foremost, I would like to express my deep and sincere gratitude to my supervisors: **David Fernig and Ed Yates**! Your wealth of learning and millions of ideas, have been of great value for me, and for supporting this work.

I am deeply grateful to my assessors, **Mark Wilkinson** and **Jerry Turnbull** for your help during four years to guide me to the right position.

I wish to express my warm and sincere thanks to **Ori Alessandro** and **Katarina Uniewicz** for your help with lab work and correction of my writing.

Thanks to **Timothy R Rudd**, **Yassir A Ahmed**, **Scott E Guimond**, **Mark A Skidmore** and **Giuliano Siligardi** for editing my paper.

To **everyone in the lab**, a big thank you for all your help, advice, understanding and friendship.

Thanks to my family: **my grandfather,** who is an old scientist, to treat my young brain with scientific ideas from my childhood. I really benefited a great deal from your wide knowledge, which continues to help me.

Special thanks to **my parents**, without your help and support, I could never go so far.

Thanks to you, **Ye**, I am really indebted from your encouragement and care, which I will never forget.

# Contents

# List of Figures

# List of Tables

# List of Abbreviations

2D: 2-dimensional

3D: 3-dimensional

$BS_3$: bissulfosuccinimidyl suberate

BSA: bovine serum, albumin

CS: chondroitin sulfate

DMSO: dimethyl sulphoxide

DMEM: Dulbecco's modified Eagle medium

DP: degree of polymerization

DS: dermatan sulfate

DSF: differential scanning fluorimetry

DTT: dithiothreitol

ECM: extracellular matrix

$ED_{50}$: 50 % effective dose

EDTA: ethylenediamine tetra-acetic acid

FCS: foetal calf serum

FGF: fibroblast growth factor

FGF-2-NP: FGF-2 conjugated to a gold nanoparticle

FGFR: fibroblast growth factor receptor

HA: hyaluronic acid

HBS: heparin binding site

HCD: higher collision decomposition

HEPES: N-2-Hydroxyethylpiperazine-N'-2-ethanesulphonic acid

HS: heparan sulfate

GAG: glycosaminoglycans

GPI: glycosyl-phosphatidyl-inositol

IdoA: L-iduronic acid

IPTG: isopropyl β-D-1-thiogalactopyranoside

$k_a$: association rate constant

$k_d$: dissociation rate constant

$K_D$: equilibrium dissociation constant

$k_{off}$: off rate

$k_{on}$: on rate

LB: lysogeny broth

MST: microscale thermophoresis

MWCO: molecular weight cut-off

nhRNA: heterogeneous nuclear RNA

NHS: N-hydroxysuccinimide

Tris-Ni-NTA: tris-nickel nitrilo-tri-acetic acid

NP: nanoparticle

NRE: non reducing end

$OD_{600}$: optical density at 600 nm

PAGE: polyacrylamide gel electrophoresis

PBS: phosphate-buffered saline

PC: principal component

PCA: principal component analysis

PCR: polymerase chain reaction

PDB: protein data bank

PFA: paraformaldehyde

PI: phosphatidylinositol

RE: reducing end

RM: routine medium

PMHS: porcine mucosal heparan sulfate

Rama: rat mammary

RM: routine medium

SD: standard derivation

SDM: step down medium

SDS: sodium dodecyl sulphate

SE: standard error

SRCD: synchrotron radiation circular dichroism

TAE: tris-acetate-EDTA

TB: terrific broth

TCA: trichloroacetic acid

TEM: transmission electron microscopy

TEMED: N,N,N’,N’,Tetramethylethylenediamine

TFA: trifluoroacetic acid

$T_M$: melting temperature

Tris: tris(hydroxymethyl)methylamine

Tris-NTA: tris-nitrilo-tri-acetic acid

Tween 20: polyoxyethylenesorbitan monolaurate

# Chapter 1 General Introduction

## 1.1 Overview

Fibroblast growth factors (FGFs) and their receptors comprise an integrated signaling system in multicellular organisms. These systems allow the continual exchange of information between cells and their internal and external environments in the developing embryo and adult organisms [1]. The archetypal FGFs, basic fibroblast growth factor (bFGF now FGF-2) and acidic fibroblast growth factor (aFGF now FGF-1) were first isolated from pituitary and brain [2-6]. Thereafter, the genes for FGF-1 and FGF-2 were found to be widely expressed in adult tissues and in the developing embryo. FGFs possess two types of receptors, heparan sulfate (HS) and tyrosine kinases (FGFR), which are involved in transducing the FGF signal into the cell [7]. Twenty-two *fgf* genes and five *fgfr* genes have been identified so far in human and mouse, *fgf*1-23 and *fgfr*1-5; human *fgf*15 and mouse *fgf*19 have not been identified. They may have been lost or diverged during gene evolution.

## 1.2 Evolution of FGFs

*fgf* genes have not been identified in unicellular organisms, by contrast, they have been identified in multicelluar organism: two *fgf* genes and one *fgfr* gene have been identified in *C.elegans*, however, twenty two *fgf* genes and five *fgfr* genes have been identified in human and mouse, and the zebra fish *fgf* gene family has twenty seven members [1]. This indicates that the *fgf* gene family expanded greatly during the evolution of primitive metazoa to vertebrates [8]. Over the course of evolution, the *fgf* gene family has expanded in two phases. In the first phase, during early metazoan evolution, *fgf* genes expanded more than once, from two or three to six genes by gene duplication. In the second phase, during the evolution of early vertebrates, the FGF family expanded via two large-scale genome duplications to result in two to four members in each of the seven sub-families of FGFs [8] (**Figure 1.1**). However, the detailed history of their expansion and the reasons that they form such a large

family is still uncertain, because the functional differences between different FGFs are not always apparent [7, 8].

## 1.3 FGF sub-families

By phylogenetic analysis, the 22 human FGFs can be divided into 7 sub-families: FGF-1, FGF-4, FGF-7, FGF-8, FGF-9, FGF-11 and FGF-19, with each sub-family containing 2 to 4 different FGFs (**Figure 1.1 and Table 1.1**).

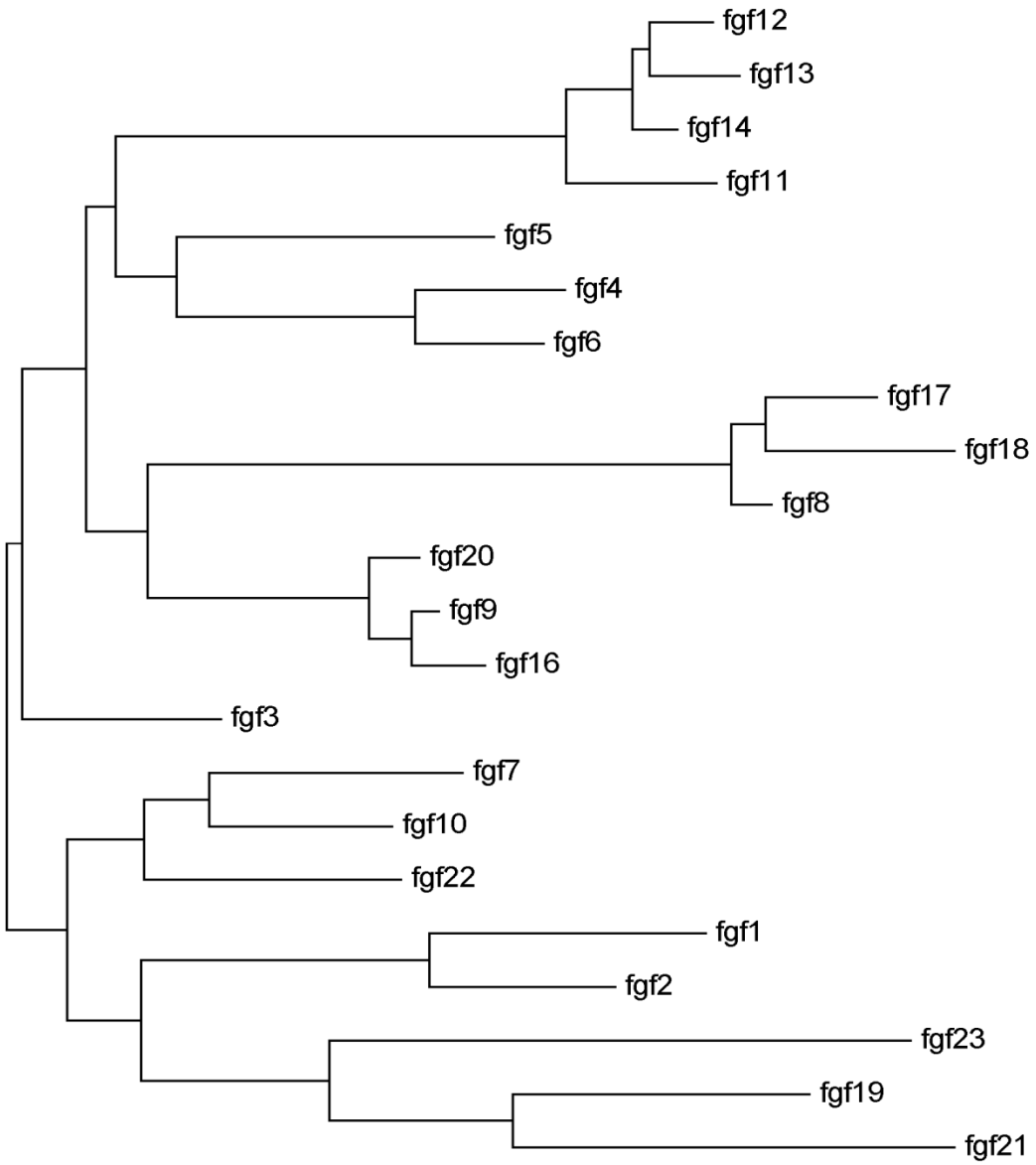


**Figure 1.1 Evolutionary tree of the FGF family.**

The protein sequences of 22 human FGFs were aligned using Cluster X software and the tree was constructed by automatic likelihood method.

# 1.4 FGF gene structure and localization

## 1.4.1 Gene localization

Following the sequencing of the human genome, the 22 human *fgf* gene locations are all known. These 22 human FGFs comprise ~150-300 amino acids and have a conserved core

structure containing about 120 amino acids with ~30-60 % identity [1, 9]. Although, FGFs share similar amino acid sequences, most of the genes have different localizations in humans (**Table 1.1**), e. g., *fgf-2* is located on human chromosome 4 [10] and *fgf-1* is located on chromosome 5, between bands 5q 31.3 and 5q 33.2 [10]. If other members in other sub-families are compared, there seems little relation between them, e.g. in the FGF-4 sub-family, FGF-4 is located in human chromosome 11, however, the FGF-5 gene is located in chromosome 4 and FGF-6 in chromosome 12 (**Table 1.1**).

### 1.4.2 Gene structure

FGF gene structure dictates protein structure. FGF genes contain 2-5 different exons to form mRNA, which are separated by 1-4 large introns, e.g., in *fgf*-2 gene structure, three exons are separated by two relatively large introns [11]. Within sub-familes FGFs have similar numbers of exons and introns, e.g., all *fgf*-4, *fgf*-8, *fgf*-9 and *fgf*-11 sub-family members have the same exon and intron numbers in each sub-family.

| | ***fgfs*** | **Localization** | **Exons** | **Introns** | **Total gene length** |
|---|---|---|---|---|---|
| *fgf*-1 sub-family | *fgf*-1 | 5q31 | 4 | 3 | 125.88 kb |
| | *fgf*-2 | 4q26-27 | 3 | 2 | 91.53 kb |
| *fgf*-4 sub-family | *fgf*-4 | 11q13.3 | 3 | 2 | 22.38 kb |
| | *fgf*-5 | 4q21 | 3 | 2 | 90.08 kb |
| | *fgf*-6 | 12p13 | 3 | 2 | 37.46 kb |
| *fgf*-7 sub-family | *fgf*-3 | 11q13 | 3 | 2 | 28.8 kb |
| | *fgf*-7 | 15q15-21.1 | 4 | 3 | 454.05 kb |
| | *fgf*-10 | 5p12-p13 | 3 | 2 | 106.16 kb |
| | *fgf*-22 | 19p13.3 | 3 | 2 | 23.78 kb |
| *fgf*-8 sub-family | *fgf*-8 | 10q24 | 5 | 4 | 25.75 kb |
| | *fgf*-17 | 8q21 | 5 | 4 | 26.41 kb |
| | *fgf*-18 | 5q34 | 5 | 4 | 57.97 kb |
| *fgf*-9 sub-family | *fgf*-19 | 11q13.1 | 3 | 2 | 26.41 kb |
| | *fgf*-21 | 19q13.1-qter | 3 | 2 | 22.24 kb |
| | *fgf*-23 | 12p13.3 | 3 | 2 | 31.50 kb |
| *fgf*-19 sub-family | *fgf*-9 | 13q11-q12 | 3 | 2 | 53.12 kb |
| | *fgf*-16 | Xq13 | 2 | 1 | 23.12 kb |
| | *fgf*-20 | 8p21.3-p22 | 3 | 2 | 30.01 kb |
| *fgf*-11 sub-family | *fgf*-11 | 17q13.1 | 5 | 4 | 27.69 kb |
| | *fgf*-12 | 3q28 | 5 | 4 | 645.87 kb |
| | *fgf*-13 | Xq26.3 | 5 | 4 | 611.21 kb |
| | *fgf*-14 | 13q34 | 5 | 4 | 699.09 kb |

**Table 1.1 Human *fgf* location**

Twenty two human gene locations on different chromosomes, numbers of exons, numbers of introns and total gene lengths (data from Ornitz *et al.* 2001 and Ensembl database, (Cambridge, UK. http://www.ensembl.org/index.html) [12].

## 1.4.3 FGF secretion

Except for FGF-1, FGF-2, FGF-9, FGF-11-15, FGF-20 and FGF-22, all other FGFs have classic cleavable N-terminal signal peptides and are secreted from cells via the endoplasmic

reticulum/Golgi pathway [1]. Although, FGF-9, FGF-16 and FGF-20 lack cleavable N-terminal signal peptides, they are still secreted through this pathway [1]. FGF-1 and FGF-2 do not have signal peptides and can be released from damaged cells or by an exocytotic mechanism that is independent of the endoplasmic-reticulum-Golgi pathway [13]. FGF-11, FGF-12, FGF-13 and FGF-14 do not have signal sequences and are thought to remain intracellular.

### 1.4.4 Alternative splicing

*fgf* genes contain 2-5 coding exons, the size of the coding portion of the genes ranges from under 5 kb (in *fgf*-3 and *fgf*-4) to more than 100 kb (in *fgf*-12) [12]. In *fgf-1* and *fgf-2* the position of the boundaries between introns and exons are similar [14]. Exon 1 of *fgf* usually contains the initiation methionine, except in *fgf-2* and *fgf-3*, which have additional 5' transcribed sequences that initiate from upstream CUG codons [12, 15, 16].

The total lengths of most of *fgfs* are between 22 to 126 kb (**Table 1.1**). However, *fgf-7* is 454.05 kb and three FGF-11 subfamily members also have large genes (*fgf*-12, 645.87 kb; *fgf*-13, 611.21 kb; *fgf*-14, 699.09 kb).

In several *fgf* sub-families, there are other similarities: exon 1 can be divided into 2-4 alternatively spliced sub-exons, e.g., *fgf-8*, sub-exon 1A-1D, in which an initial codon (ATG) in sub-exon 1A is used to start coding [12]. The organization of *fgf* is conserved in mouse, zebrafish and humans, however, its functional significance is not understood [12]. In some other cases, such as the *fgf*-11 sub-family, there exist alternative amino termini, because of alternative 5' exons. However, whether a common 5' untranslated exon splices to exons in these sub-families, or an alternative promoter and regulatory sequences are active, remains uncertain [12].

# 1.5 FGF ligand structure

## 1.5.1 Core structure of FGFs

The FGF family exhibits a folding pattern similar to the cytokine interleukin-1β, as first revealed by X-ray crystallography of FGF-2 [17]. The overall structure of the core of FGF-2 is a cylindrical barrel made up of 12 anti-parallel β-strands. The backbone of the structure can be described as a pyramid, where the three sides are built of two β-strands together forming a β-sheet barrel of six anti-parallel strands (**Figure 1.2**). The base of the pyramid is built of six additional, β-strands extending from the three sides of the pyramid to close one end of the barrel [17]. The core structure of the FGF family also includes the regions of the molecules that are required for binding to FGFR and HS [18].

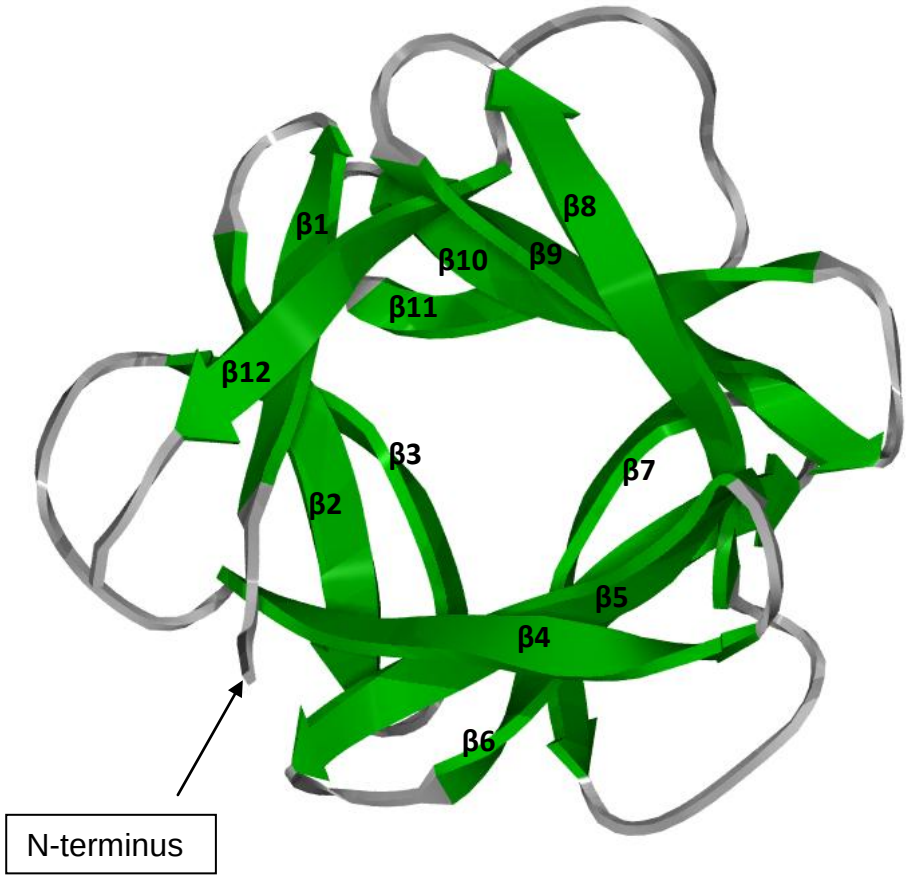


**Figure 1.2 FGF-2 3-dimensional structure ribbon diagram.**

Crystal structure of FGF-2 (PDB: 2FGF [18], residues 28-153) is shown using a ribbon diagram. The structure was rendered with SPDBV and exported using PRO-RAY (Persistence of Vision Ray tracer Pty. Ltd. Victoria, Australia, http://www.povray.org/).

## 1.5.2 The structural similarities and differences of the FGF ligands

The core structures of FGFs are quite similar according to the known 3-D structures of FGFs and sequence alignment, so, therefore, the main differences are due to the lengths of loops, the amino acid side chains and the N- and C-termini, which are not part of the core structure.

The crystal structure of FGF-9 (PDB: 1IHK) [19] indicates that the main difference between FGF-9 and FGF-1 subfamily members are the loops between β stand 1-2 and 9-10 [20]. Loop 1-2 of FGF-9 is one amino acid shorter than loop 1-2 of FGF-1 and FGF-2, however, loop 9-10 is 6 residues longer than the corresponding loop in FGF-2 and 4 residues more than the one in FGF-1 [20]. Because of the longer sequence, loop 9-10 bulges out from the main structure of FGF-9 [20]. Another difference between the structures of these FGFs is the conformational differences in N- and C-termini. The two termini in the FGF-1 sub-family are disordered in crystal structures to the extent that these proteins are expressed as truncated variants in order to obtain crystals. In contrast, in FGF-9, the N-terminal contains an α helix and the C-terminal of FGF-9 (17 amino acids), which is much longer than that of FGF-1 (4 amino acids) and FGF-2 (3 amino acids) also contains a short helical structure [20].

In the FGF-7 subfamily, FGF-7 and FGF-10 have a longer β1 strand than FGF-1 and FGF-2, [21-23]. Also, FGF-7 and FGF-10 have a single hydrogen bond between the β10 and β11 strands to link them, which is different from other FGFs [23]. The consequent conformational restrictions may be a hallmark of the FGF-7 sub-family [23]. Like FGF-9, FGF-7 and FGF-10 were also reported to be much longer at loop β1-2 and β9-10 compared to FGF-1 and FGF-2 [23].

FGF-8 has a larger N-terminus compared to other FGFs, which contains an α helix and some disordered sequence, and so has a very different structure from the N-termini of other FGFs, It is predicted that FGF-17 and FGF-18 may also have similar N-termini [24].

The 3-D structures of FGFs determined by crystallography are quite similar to the NMR derived models, but they are not exactly the same. For example, the FGF-1 crystal structure (PDB: 2AFG) [25] has a shorter β1 (LLYC) and β12 (LPL) than the corresponding NMR structure (PBD: 2ERM [26], β1: KPKLLYCS, β12: LFLPLPVS). This indicates that the FGF solution structures may differ from the crystal structures. Taken together, the main differences between these FGF structures are the loop regions, and also the N- and C-termini. Alongside, there are differences in amino acid sequence, which do not affect the overall structure. It is proposed that these differences are the reasons for FGFs having distinctive receptor binding specificities, allowing FGFs to activate distinct signaling pathways.

# 1.6 Heparin/HS structure

## 1.6.1 Heparin/HS disaccharide structure

Heparin is found *in vivo* in mast cells; HS is found at the cell surface and in ECM of most cells [27]. Heparin and HS together, hyaluronic acid (HA), chondroitin sulphate (CS), dermatan sulfate (DS) and keratan sulfate all belong to the family of glycosaminoglycans (GAG), which are long unbranched polysaccharides. HS and heparin have the same repeating disaccharide architecture composed of a uronic acid, α-L-iduronic or β-D-glucuronic and D-glucosamine (**Figure. 1.3**) [28]. The initial product of biosynthesis is a repeating disaccharide of glucuronic acid and N-acetyl glucosamine of 50 to 300 disaccharides. This is then modified, initially by N-deacetylase / N-sulfotransferase activity, which replaces the N-acetyl group of glucosamines with a N-sulfate. This modification is clustered along the chain and acts as a marker for the other modifications: epimerization of glucuronic acid to iduronic acid, O-sulfation of C2 on iduronic acid and of C6 and C3 of glucosamine [29].

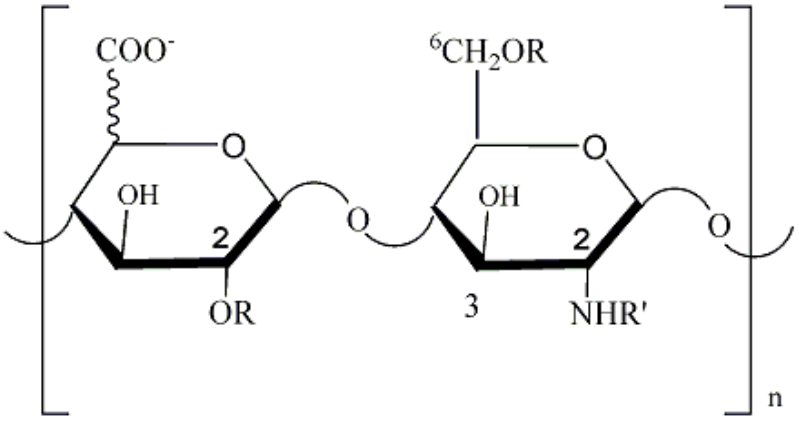


**L-iduronic acid or D-glucuronic acid** **D-glucosamine**

**Figure 1.3 Heparin/HS repeating disaccharides unit.**

The repeating disaccharide unit contains two parts: a L-iduronic acid or D-glucuonic acid and a D-glucosamine. R can be H or $SO_3^-$, R' can be $SO_3^-$or $COCH_3$.

## 1.6.2 HS chain

The structure of HS chains is a consequence of their biosynthesis. The chains are not homogenously sulfated, so they possess domains of varying sites that are not sulfated (NA domains) containing one glucosamine in two N-sulfated (transition or NAS domain) and sulfated domains in which every glucosamine is N-sulfated (S-domain). The latter look more like heparin, but are generally less O-sulfated [27]. S and NAS domains of HS chains are the sites where proteins bind [30].

HS polysaccharides are synthesized as covalent complexes with core proteins forming heparan sulfate proteoglycans (HSPGs). The sugar attachment consensus sequence consists of a Ser-Gly sequence flanked by at least two acidic amino acid residues. Three major families of HSPGs have been characterized. They include the transmembrane syndecans (four members in mammals), the glypicans, proteins attached to the cell membrane by a glycosyl-phosphatidyl-inositol (GPI) anchor (six members) and ECM proteins such as

perlecan, agrin and collagen XVIII. There are other core proteins, which carry HS chains facultatively, sometimes as a result of alternative splicing of their mRNA. The core protein addresses the HS chains to different locations; syndecan and glypicans to the plasma membrane, matrix core proteins to the extracellular matrix/basement membrane [31].

### 1.6.3 Heparin *vs* HS

Each disaccharide unit of heparin chains contains an average of 2.7 sulfates, in contrast, HS contains less than 1 sulfate in each disaccharide. So, heparin has a higher charge density for binding to proteins than HS [32]. However, the domain structure of HS means that S-domains in particular have a charge density that is considerably higher than the average for an HS chain, though still lower than that of heparin. Thus, heparin and HS share similar structures, so, heparin can mimic the binding activity of HS towards FGFs [33].

## 1.7 FGFR binding

### 1.7.1 FGFR structures

FGFR1-4 are transmembrane proteins, their structure comprises three parts: an extracellular portion, which binds ligands and HS, a transmembrane helix and a tyrosine kinase domain [34]. FGFR1-4 have a degree of identity of between 55-72 % of the total amino acids sequences and ~ 32 % identity of the extracellular domain. For FGFR1-4, the extracellular region contains two or three immunoglobulin Ig-like domains (D1, D2, and D3) (**Figure 1.4**) [34, 35]. There is an unusual sequence of acidic amino acids (the acid box) between D1 and D2 [36]. There are also up to six possible N-glycosylation sites on D2 and D3, which affect ligand and heparin binding *in vitro* [37] and receptor activity *in vivo* [38]. Heparin and HS bind to D2 while the FGF ligand interacts with residues in D2 and D3 [39]. The intracellular part of the FGFR has a large juxtamembrane region to which the adaptor FRS2 binds, a split tyrosine kinase domain and a COOH terminal tail. There are two Tyr residues in the activation loop of the FGFR kinase and around six other Tyr residues which, when

phosphorylated, serve as docking sites for signaling molecules. The alternative splicing results in many isoforms of FGFR. For example, alternative splicing of exon 6 of FGFR hnRNAs produces the corresponding protein structures in D3 determining the ‘a’, ‘b’ and ‘c’ isoforms, with the ‘a’ isoform lacking an intracellular domain (**Figure 1.4**). The two FGFR5s (FGFR5β and FGFR5γ) were found later and they have a different structure compared with the other four FGFRs. FGFR5 does not have an acid box between D1 and D2 and it lacks a tyrosine kinase domain (**Figure 1.4**) [40]. .

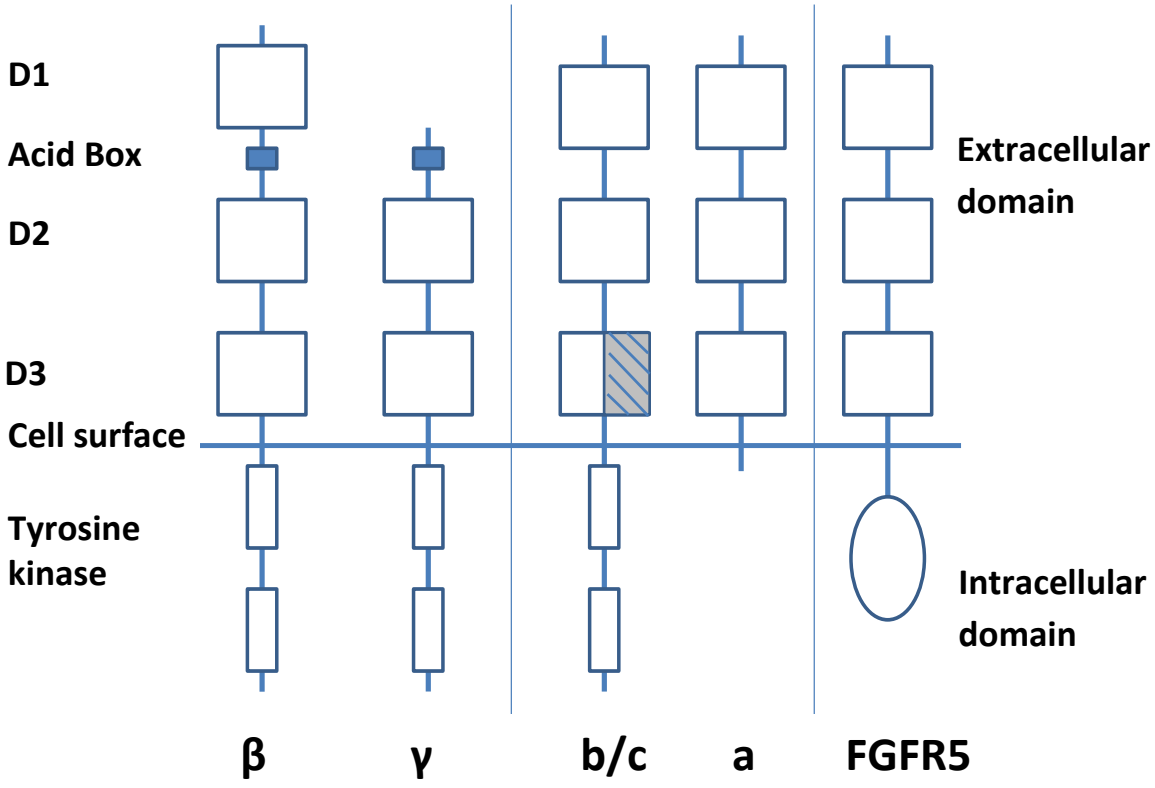


**Figure 1.4 Schematic of the domains of FGFR [40].**

FGFRs have 5 family numbers and each member has different isoforms. The major differences between these FGFR isoforms are shown. The main difference between isoforms β and γ, is that γ is missing the mRNA encoding the D1 domain and maybe also the acid box, and the acid box can be found in FGFR 1-4 [41-43]. The alternative splicing of exon 6 of FGFRs, for which the corresponding protein structures in D3 are coloured in grey, determine the "b" and "c" isoforms, and isoform "a" does not have an intracellular domain. FGFR5 does not have tyrosine kinase. Minor isoforms, though with some functional significance are formed as a result of exon slippage at splicing sites.

**Table 1.2 Isoelectric point (pI) and FGFR binding specificities of FGFs**

| FGF subfamily | FGF | PI | FGFR binding specificity |
|---|---|---|---|
| **FGF-1 sub-family** | FGF-1 | 6.52 | All FGFRs |
| | FGF-2 | 9.58 | FGFR 1c, 3c>2c, 1b, 4Δ, 5β[a], 5γ[a] |
| **FGF-4 sub-family** | FGF-4 | 9.73 | FGFR1c, 2c>3c, 4Δ |
| | FGF-5 | 10.54 | |
| | FGF-6 | 10.00 | |
| **FGF-7 sub-family** | FGF-3 | 10.88 | FGFR2b>1b |
| | FGF-7 | 9.29 | |
| | FGF-10 | 9.61 | |
| | FGF-22 | 11.81 | |
| **FGF-8 sub-family** | FGF-8 | 10.44 | FGFR3c>4Δ>2c>1c>>3b |
| | FGF-17 | 10.43 | |
| | FGF-18 | 9.86 | |
| **FGF-9 sub-family** | FGF-9 | 7.06 | FGFR3c>2c>1c, 3b>>4Δ |
| | FGF-16 | 9.22 | |
| | FGF-20 | 8.89 | |
| **FGF-19 sub-family** | FGF-19 | 6.55 | FGFR1c, 2c 3c, 4Δ (weak activity) |
| | FGF-21 | 5.01 | |
| | FGF-23 | 9.17 | |
| **FGF-11 sub-family** | FGF-11 | 9.92 | No known activity |
| | FGF-12 | 9.98 | |
| | FGF-13 | 9.92 | |
| | FGF-14 | 10.11 | |

The theoretical pI was calculated using the online software protparam tool (http://web.expasy.org/protparam/) [44] and the FGFR binding specificities in sub-families are from Ornitz, *et al*. and Zhang, *et al.* [45, 46]. [a.] FGF-2 can bind to the FGFR5β and FGFR5γ, the binding affinity is less than FGFR2c, but was not compared to other FGFRs [47].

## 1.7.2 Binding of FGFs to their receptors

FGFs mediate their biological effects by binding to, dimerizing, and activating their FGFR, through transphosphorylation of their kinase domains. This initiates intracellular biochemical signal transduction by FGFs at the cell surface [48]. FGFs have distinct binding specificities for FGFRs (Table 1.4) [45, 46]. However, the selective binding of FGF ligands to their

receptors is far from absolute. Only FGF-7 shows a high degree of fidelity, binding only to FGFR2c, whereas all other extracellular FGFs are capable of binding more than one FGFR isoform. At the other extreme is FGF-1, which is often called the "universal ligand", because it can bind all FGFRs to some extent. Nonetheless, specificity within each sub-family is conserved, except in the FGF-1 sub-family, due to the promiscuity of FGF-1 (**Table 1.4**) [45, 46]. FGF-2 binds to FGFR5, but FGF-7 cannot [47], which again highlights the specificity of FGF-7. The binding specificity of other FGFs for FGFR5 is not known.

### 1.7.3 FGFR binding site

The binding sites of FGF ligands in FGFR are focused on parts of Ig loops D2 and D3, and also the linker between these two loops. The first studies into the sites of interactions of FGFs and FGFR involved synthetic peptides [49], site-directed mutagenesis and isothermal titration calorimetric [50]. Subsequently, the structures of co-crystals of FGF ligand and the extracellular domain of FGFRs were solved. In the crystal structure of FGF2-FGFR1 (PDB: 1CVS) [51], a large number of amino acids residues in FGF-2 were reported to be involved in FGFR binding by hydrogen bonds, van der Waals and hydrophobic interaction. These interactions included 4 areas in FGF-2: F26, K30, Y33 and K35, located at the N-terminus, β1 stand and loop β1-2. The sequence 65-QAEER-69, which includes part of β4 and of loop β4-5 was also proposed to be part of the FGFR binding. Further along the sequence, V97, 111-NYN-113, E105, L107, 108-DSN-110, located between loops β7-8 and strand β9 were observed to make contact with the receptor. Another five amino acids, 141-PG-142, L147, L149, M151 in loop β11-12 and also strand 12 interacted with the FGFR. Subsequently, another crystal structure, comprising a FGF-2-FGFR1-DP6 complex (PDB: 1FQ9) supported these binding sites [52].

In the asymmetric FGF-1-FGFR2-heparin DP10 crystal structure (PDB: 1E0O) [53], there were also four areas with binding residues reported, which are quite similar to the sites of

interaction of FGF-2. The first one is located at β1 and loop β1-β2 (Y30, Y35 and Y37). Another three residues are located at loop β3-4 (R50 and R52) and loop 4-5 (V66). The third one includes E102, and two sequences 104-LEE-106 and 108-HYN-109, which are located between β8 to loop β8-9. The last one is located at β12, consisting of only two residues (L148 and L150). Later, in another crystal structure (FGFR3c-FGF1, PDB: 1RY7), another three residues, which are located at N-terminals were also reported (G21, Y23 and K24).

In the FGF-10-FGFR2b crystal structure (PDB: 1NUN) [54], the amino acids reported to have interactions directly with FGFR again mapped to four areas on the molecular surface, which are at similar positions as those in FGF-1 and in FGF-2. The first one is between the N-terminus and β1 (71-HLLQGDVR-78, R80, F83 and F85). The second one is quite large from loop β3-4 to strand 6, which includes K102, E104, 113-ITSVEIG-119, V121 and Y131. Another area includes F146, 154-ERI-156 and 159-NGY-161, located between loop β7-8 to strand 9 [54]. The last one includes just two residues, which are L202 and M204 in strand 12.

The crystal structure of FGF-8b-FGFR2c (PDB: 2FDB) also showed that the FGFR binding site is contributed to by four areas, which are similar to those in FGF-1 and FGF-2 [24]. The first one contains 11 residues: F50, H53, V54, Q57, D62, L64, R66, L68, R70, Y75 and R77, which map to part of the N-terminus and the whole of strand 1. The second one is between stands 4 to 5 and includes V106, T108, F111 and S113. The third one is located between β8 to β9 and comprises E159, V161, L162 and 165-NYT-167. The last one is located at β12 and consists of 193-MKR-195.

### 1.7.4 Activation of FGFR: binding models

In pioneering studies, FGFs were shown to require heparin to stimulate cell division [55, 56]. Since then, many growth factors, including other FGFs have also been shown to be dependent on heparin/HS. It should be noted that there is evidence to show that FGFs can activate their receptors in the absence of the polysaccharide. However, the outcome of

signaling in the absence of the sugar is different to that in the presence of sugar, and only in the latter case can FGFs exert their full range of effects, including the stimulation of cell division [57-61]. To explain this dependence on the sugar in the formation of a signaling complex, three different binding models have been proposed. The first model was established by Pantoliano, *et al*. in 1994 using isothermal titration calorimetry (ITC), site directed mutagenesis and molecular modeling. This is usually called the growth hormone model [62]. Later, crystallographic analysis of binary FGF-FGFR and ternary FGF-FGFR-heparin complexes has provided another two models for FGFR dimerization, the symmetric (dimer of dimers) model and the asymmetric model [52, 63, 64].

### 1.7.4.1 Growth hormone model

In the growth hormone model the FGF-2 ligand is bivalent, with one high and one low affinity binding site binding two receptors, with the heparin glueing the complex together; the low affinity binding site of the FGF-2 that binds to the second FGFR is effective because this second stage of complex formation occurs in the 2-dimensional confines of the membrane [62]. So, the FGF-2 and HS are like bridges, linking the two FGFRs [62]. Also, site mutagenesis showed that while the disruption of the secondary FGFR binding site did not decrease the binding of the high affinity site to the FGFR and HS, it reduced the mitogenic potency [50]. Later, a site-directed mutagenesis and loop replacement study of the FGF-7 binding complex with FGFR2c also supported this model [65].

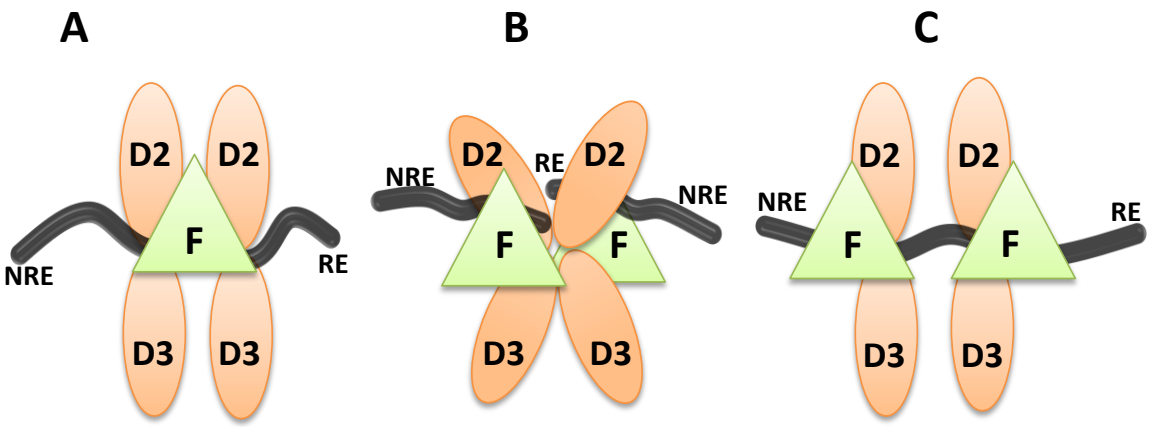


**Figure 1.5 Three models of the FGFR signaling complex.**

The "F" is FGF, which is coloured in green. Only receptor Ig D2 and D3 are shown in these models, which are coloured in orange. Heparin chains are coloured in black, NRE: non reducing end, RE: reducing end. A. Growth hormone model. B. Symmetric model. C. Asymmetric model.

### 1.7.4.2 Symmetric dimer model

In the symmetric two-end model, heparin promotes dimerization of two FGF-FGFR complexes by stabilizing bivalent interactions of the ligand and receptor through primary and secondary sites and by stabilizing direct receptor-receptor contacts [52]. The two FGF-FGFR-HS/heparin complexes arise from back-to-back interactions, with reducing ends of sugar chains facing each other (**Figure 1.5**). The symmetric dimer model is based on the crystal structure of the FGF-2 bound to D2-D3 of FGFR1 (PDB: 1FQ9) [51, 52, 63]. In this model, two 1:1(FGF: FGFR) complexes form a symmetric dimer. FGF ligand to receptor interactions include both the interaction directly between the two molecules and the interaction of the FGF bound to the FGFR of the adjoining complex, which is proposed to help stabilize the dimer. However, no FGF to FGF interactions were observed. Later another dimeric assembly of two 1:1 (FGF1:FGFR2) complexes was determined, which supports this

model [66]. Another two FGF-FGFR crystal complexes were established afterwards, FGF-10-FGFR2b and FGF-8b-FGFR2c, again supporting this model.

### 1.7.4.3 Asymmetric model

A fundamentally different model (asymmetric model) for FGF signaling complex was proposed based on the crystal structure of a FGF-1-FGFR2c-heparin complex (PDB: 1E0O) [53]. In the asymmetric model, there are no protein-protein contacts between the two FGF-FGFR complexes and these are linked only by the sugar [53] (**Figure 1.5**). Heparin binds to both FGFs, but binds only one FGFR. Also, each FGF binds to only one FGFR and there are no contacts between the two FGFRs.

### 1.7.4.4 Symmetric vs. Asymmetric

The major differences between the asymmetric and the symmetric model include an invariant proline in the D2-D3 linker region of the FGFR form in *cis* conformation, whereas in the symmetric 2:2:2 model, this proline is in a *trans* conformation [52, 53, 67].

Following the publication of these proposed models, there was considerable argument as to which was correct. Harmer *et al.* used a combination of size-exclusion chromatography, analytical ultracentrifugation and mass spectrometry to present data suggesting that both types of dimer can coexist [68]. However, these models may not explain other biochemical and biophysical data, such as the ability of at least FGF-2 to induce the transient activation of the MAP kinase pathway in the absence of sugar [57, 59-61]. The asymmetric model, which relies on the linkage by the sugar chain, may have difficulty accommodating a tetrasaccharide, which is the shortest oligosaccharide capable of allowing FGF-2 to stimulate cell proliferation [57]. Moreover, site-directed mutagenesis that reduces the secondary FGF-FGFR interactions results in diminished FGFR activation, presumably due to decreased dimerization, without affecting ligand-receptor binding [69]. This can be explained by the symmetric two-end model, but not the asymmetric model. However, since many of the

receptor-receptor contacts in the symmetric two-end model are due to the peptide backbone, such experiments are not necessarily as conclusive as they appear at first sight.

## 1.8 Non-signaling Functions of HS binding

Since heparin was found to promote the activity of FGF-1 on endothelial cells [70], the binding of FGFs to HS/heparin has been progressively investigated. As well as promoting the growth stimulatory activity of FGFs by forming ternary complexes with the FGFR, the interaction of these growth factors with the polysaccharide influences other important aspects of their activity: conformation, stability and transport.

*Conformational change and stabilization of FGFs*-The interaction of FGF-2 with heparin and HS has long been associated with conformational change in the protein. Thus, it was established that heparin protected FGFs against pH-dependent degradation and proteolysis, and increased the thermal stability of the proteins [71, 72]. Some conformational change in FGFs has also been reported in experiments that measured the secondary structure of FGFs in solution by infra-red spectroscopy [73]. However, the structures derived from X-ray crystallography do not support these effects of heparin, because in co-crystals of FGFs with oligosaccharides derived from heparin, the alpha carbon backbone is superimposable on that observed in crystals made from the protein alone [74-77]. Nonetheless, the earlier biochemical and biophysical data cannot be disregarded and the question of the extent of conformational change in FGFs induced by their binding the sugar needs to be re-addressed.

*Transport and storage*-Not long after FGFs were found to bind to heparin and HS, the storage of FGFs in HS of the extracellular matrix was noted [78-80] and various mechanisms for the release of such stored FGF were discovered [31, 78, 81-84]. These include release of FGF-2 from the HS chains of PGs in the matrix by the action of heparanase, as observed in a skin wound healing model [85]. The released FGF-2 was proposed to be a key early component in the signaling required to heal skin wounds. In development, differences in the

storage capacity of HS in resting *versus* developing tissue were observed in the developing rat mammary gland. The high storage capacity of HS along resting ducts was attributed to their quiescent state, whereas the lack of any storage in terminal end buds, a site of active ductal elongation, was suggested to relate to the active transport of FGFs between the stroma and the epithelium [80].

## 1.9 The interaction of FGFs with heparin

Owing to the importance of the interactions of FGFs with HS and its experimental proxy heparin these have been subject to a large amount of experimental analysis. Most data relate to the archetypal FGFs, FGF-1 and FGF-2.

Heparin was found to increase FGF-1 mitogenic activity first in the 1980s [70, 86]. Later, Lys-118 in FGF-1 was found to strongly bind heparin and it was reactive because it was in a unique micro environment. This work also showed that clusters of basic residues are important for heparin binding [87]. One of the first systematic analyses was of a series of nested peptides derived from the sequence of FGF-2 [49]. This study identified sequences of FGF-2, 24-68 and 106-115 as having the ability to bind heparin. Subsequently, the interaction of FGF-2 with heparin was probed by a combination of site directed mutagenesis, heparin chromatography and isothermal titration calorimetry [88]. This study showed that wild-type FGF-2 was eluted at 1.38 M NaCl [88], whereas FGF-2 with mutations of selected arginines and lysines eluted with 0.46-0.26 M NaCl. The binding of FGF-2 to heparin was characterized by a single binding constant ($K_D$=0.47 μM) in 0.1 M NaCl, and 30 % of the free energy of binding derived from ionic bonding [88]. Subsequent quantification of the biophysical binding parameters of FGF-2 binding to heparin-derived oligosaccharides of different lengths in an optical biosensor showed that there is no interaction with DP2 [57]. FGF-2 did bind with DP4 ($K_D$=62±28 nM), the highest affinity being for DP8 ($K_D$=11±2 nM), which then decreased as the sugar length increased. The kinetics of interaction had a

fast association rate constant (~$10^6$ $M^{-1}s^{-1}$), characteristic of ionic interactions, where coulombic steering increases the collision cross section of the molecules. The very different affinities found in these two studies highlights some of the difficulties in the field. In calorimetry, binding sites must be saturated, whereas in kinetic measurements in optical biosensors only the highest affinity site is probed. Since heparin and HS are polydisperse, presenting different qualities of binding sites to FGF-2, the two techniques report quite different affinities.

## 1.10 Complexity and Specificity

The regulation of FGF activity by HS represented the second major biological function for these glycosaminoglycans, the first being the regulation of coagulation. There are now at least 435 proteins that bind heparin/HS in the plasma membrane and extracellular matrix of mammalian cells [89, 90]. Their interactions with HS controls many facets of their activities. The FGFs remain a key model for these protein-sugar interactions; ideas derived from experiments on the FGF ligand-receptor system become the starting hypotheses for these other protein-HS interactions. Therefore, questions relating to the specificity of the interactions of FGFs with HS/heparin are important beyond the FGF field. In the FGF signaling system heparin/HS was shown to be essential for FGF signaling and there is evidence for the FGF ligand-receptor system possessing a high degree of specificity. For example, HS from different tissues is clearly able to support the assembly of specific FGF ligand-receptor complexes [91]. According to other evidence, specific minimal chain length and selective of sulfation of heparin-derived sugars are needed for assembly of FGF-FGFR complexes. For example, DP8 has been suggested to be the minimal length required to enable FGF-1 and FGF-2 interactions with FGFR1 or FGFR2 and to induce ligand-receptor dimerization; 6-O-sulfate, though not required for ligand binding is thought to be essential for complex assembly and receptor dimerization [92, 93]. By removing 2-O- and 6-O-

sulfates, heparin can be reduced to activating only FGF-1 with FGFR-2, but not FGF-1 with FGFR-1 or FGF-7 with FGFR2b [93]. In other studies heparin oligosaccharides of different sizes or of modified structure were tested with FGF-1, FGF-2 and FGF-4. The results showed that at least a decasaccharide was required for high affinity interaction with FGF-1, FGF-2 and FGF-4 [94, 95] and that FGF-2 required both 2-O-sulfate groups and the negative charge of the carboxy group in iduronate residues to bind to oligosaccharides, whereas 6-O-sulfate was required for FGF-1 and FGF-4 binding. However, DP4, though not as effective as DP8, has been shown in other experiments to be sufficient for assembly of a signaling complex and able to bind FGF-2 with good affinity [57].

At the level of binary complexes, *in vitro*, HS isolated from different cell types has different binding kinetics for FGF-1 and FGF-2, spanning from 22±6 to 290±70 nM for FGF-2 and 400±130 to 8600±2500 nM for FGF-1 [96], suggesting that FGF-1 and FGF-2 bind differently to different HS structures. However, there are other views, which state that different FGFs bind to HS oligosaccharides with similar relative affinities and low selectivity, such that the strength of these interactions relies more on the overall level of sulfation than other characteristics [97]. Also, different members of the FGF family have been suggested to share binding sites on HS chains [98, 99]. The constrasting biophysical data from ITC and opitical biosensor, where a 10-fold difference in $K_D$ was measured (**Section 1.9**) highlights a key issue. These experiments are quantitative and their differences readily explained by the necessary differences in experimental design. A clear conclusion from this work and later studies on HS [96] is that FGFs do indeed recognize a range of sites in the polysaccharide. Many other studies have used indirect and qualitative measurements of affinity. One of the most common is the concentration of NaCl required for elution from heparin. Such approach, as has been reviewed [27] may confound it over interpreted. Thus, although the broad picture of the activity of FGFs being controlled by HS is accepted, there is considerable

inconsistency as to how specific the interaction of FGFs with the sugar are, what is the affinity and how ligand, receptor and sugar come together to form a signaling complex.

## 1.11 Rationale & Aims

Most of the FGF family members mediate their bioactivity by binding to HS. There is evidence for FGFs possessing different specificities with respect to their interactions with HS and the assembly of receptor-ligand complexes. However, studies have been heavily biased to the first members of the family to be discovered, FGF-1 and FGF-2, which belong to the same subfamily and experiments have often employed techniques that report the ionic component of the interaction rather than the actual affinity. Since the FGFs are all related, and arose through genome duplication and natural selection, they provide an excellent system for the analysis of whether protein structure specifies heparin binding specificity. Importantly, the functional consequences of a particular mode of heparin binding can be tested. The aim of this thesis is to produce a panel of FGFs from different subfamilies and determine the structure in the proteins responsible for heparin binding and their preferred sugar structures. This information can then be used to interpret the structural basis for different binding specificities and assemblies. Moreover, it should allow a critical test of whether FGF-sugar interactions do indeed exhibit a degree of specificity, since this would be expected to be under positive selection pressure and so follow, at least to some extent, the functional diversification of the FGFs. That is, sugar binding specificity, like FGFR binding specificity (**Table 1.2**), would be expected to be retained within FGF families, but to differ between sub-families.

# Chapter 2 General Materials and Methods

## 2.1 Electrophoresis

### 2.1.1 Materials

2-log DNA marker (New England Biolab, Herts, UK)

SDS-PAGE markers (Bio-Rad, Laboratories Ltd, Hemel Hempstead, UK)

Coomassie brilliant blue (CBB) (R) (Bio-Rad)

### 2.1.2 Agarose gels

Agarose gels (1.2 %, w/v) were made as follows:

Agarose (1.2 g) was diluted and melted in 100 mL TAE (tris-acetate-EDTA) buffer (40 mM Tris, 20 mM acetic acid, and 1 mM EDTA, pH 8), then 10 μL 10,000× SYBR (New England, Biolab) was added into the agarose. The liquid agarose was added to the gel making kit and allowed to cool. Electrophoresis was carried out at 100 V, 30 min for each gel.

### 2.1.3 SDS PAGE and Western blot

#### 2.1.3.1 Buffers

Sample buffer (5×): 50 % (v/v) glycerol, 10 % (w/v) SDS, 25 % (v/v, freshly made) 2-mercaptoethanol in 315 mM Tris-HCl, pH 6.8 and coloured with bromophenol blue.

Running buffer: 50 mM Tris, 192 mM glycine and 0.1 % (w/v) SDS.

#### 2.1.3.2 SDS-PAGE

SDS-PAGE (15 % (w/v) acrylamide resolving gels and 4 % (w/v) acrylamide stacking gels) was made according to a published method [100]. The following (**Table 2.1**) were mixed together; gels were poured in a Bio-Rad (Bio-Rad) mini protein gel system apparatus with 0.75 mm spacers. Electrophoresis was carried out at 200 V, 1 h/30 mA for each gel.

**Table 2.1 SDS-PAGE**

**A, Resolving gel.**

| | |
|---|---|
| Acrylamide/ bis-acrylamide stock (30 %, w/v) | 5 mL |
| Tris-HCl (3 M), pH 8.85 | 2.5 mL |
| Water | 2.5 mL |
| 10 % Sodium dodecyl sulphate (SDS) w/v | 100 µL |
| TEMED (N,N,N',N',Tetramethylethylene diamine) | 10 µL |
| Ammonium persulphate 50 mg/mL (freshly made) | 100 µL |

**B, Stacking gel.**

| | |
|---|---|
| Acrylamide/ bis-acrylamide stock (30 %, w/v) | 1.3 mL |
| Tris-Cl (1.25 M), pH 6.8 | 1 mL |
| Water | 3.7 mL |
| 10 % Sodium dodecyl sulphate (SDS) w/v | 100 µL |
| TEMED | 20 µL |
| Ammonium persulphate 50 mg/mL (freshly made) | 100 µL |

Ingredients for 15 % (w/v) gel. A, 10 mL for 2 resolving gels; B, 6.22 mL for 2 stacking gels (**Section 2.1.3.2**).

Clear liquid samples were mix in the ratio 4:1 (v/v) with 5× sample buffer. Five µL cell samples were mixed into 50 µL of 1× sample buffer. The mixed samples were heated to 100$^{o}$C for 2 min and centrifuged at 10,000 ×g for 5 min to remove any insoluble material. Electrophoresis was carried out at 30 mA, 200 V, 1 h for each gel.

## 2.1.3.3 Coomassie Stainning

The gels were soaked in Coomassie Stain (0.25 % (w/v) CBB (R), 40 % (v/v) methanol, 10 %

(v/v) acidic acid) for up to 20 min, then destained in destain buffer (30 % (v/v) methanol, 10 % (v/v) acidic acid) until the background became clear.

### 2.1.3.4 Silver staining

The gel was incubated in fixer (40 % (v/v) ethanol, 10 % (v/v) acetic acid, 50 % (v/v) $H_2O$) for 1 h. Then, the gel was washed in 10 % (v/v) ethanol 3 × 5 min and in $H_2O$ for 3 × 5 min to reduce background staining and increase sensitivity. The gel was incubated in 0.02 % (w/v) silver nitrate solution for 30 min with gentle shaking. After washing in $H_2O$ for 5 s, the gel was washed once with freshly made developer (3 % (w/v) $Na_2CO_3$, 0.05 % (v/v) formaldehyde) and then incubated in developer until the level of staining was sufficient. Staining was stopped with a 5 min incubation in 1 % (v/v) acetic acid. The gel was left to wash in $H_2O$ for 6×5 min. The gel was cleaned by reducer (12 mM $Na_2S_2O_3$, 4.6 mM $K_3[Fe(CN)_6]$, 4.7 mM $Na_2CO_3$), and then with another 6×5 min wash with water until dry.

### 2.1.3.5 Gel drying

The gels and two pieces of cellophane were wetted in gel drying buffer (2 % (v/v) glycerol, 20 % (v/v) ethanol). Gels were placed between two pieces of cellophane and clipped on the gel drying kit until dry.

## 2.2 Mutagenesis

Polymerase Chain Reaction (PCR) (KOD Hot Start DNA polymerase, Novagen) was undertaken to alter DNA sequences in plasmids with designed primers.

The mutagenesis PCR system conditions with a total volume of 50 μL, followed by the general PCR method as shown in (**Table 2.2**).

One μL Dpn1 was then used to digest the PCR product, at 37$^{o}$C 1 h. Competent DH5α *E.coli* cells were thawed on ice. Ten μL of ligation product was mixed with 70 μL bacterial cells and incubated on ice for 30 min. Plasmids were permeated into cells by heat shock (1 min at 42$^{o}$C). After incubation for 2 min on ice, cells were rescued with 1 mL LB broth and incubated at 37$^{o}$C for 60 min. Bacteria were collected by centrifugation at 3,500 ×g for 5 min

and resuspended with 100 mL of LB. Ten µl was plated out onto LB-amp plates (LB supplemented with 100 mg/mL of ampicillin (Sigma-Aldrich Ltd. Dorset, UK)). Plates were incubated overnight at 37$^{o}$C.

A single colony from the plates was added to 10 mL LB culture (ampicillin), grown overnight (37$^{o}$C, 250 rpm). Cells from the overnight culture were collected by centrifugation (5 min, 2,500 ×g).

# 2.3 Cloning

## 2.3.1 PCR

cDNAs were amplified by PCR using 50 µL systems, PCR conditions are shown in **Table 2.2**

**Table 2.2 PCR conditions.**

**A,** PCR reaction mixture

| **Contains** | **Volume** |
|---|---|
| 25 mM $MgCl_2$ : | 3 µL |
| dNTPs : | 5 µL |
| Primers (forward and reverse): | 2.0 µL each (30 µM) |
| Hot start polymerases: | 1 µL |
| DNA template: | 2 µL (30-300 ng/µL) |
| Hot start polymerase buffer | 5 µL |
| $H_2O$ : | 30 µL |

**B,** PCR cycle setting

| | **Stage 1** | **Stage 2** | | **Stage 3** | | |
|---|---|---|---|---|---|---|
| Cycle number: | 1 | 30 | | | 1 | finish |
| Temperatures ($^{o}$C) | 98 | 95 | Tm | 72 | 72 | 4 |
| Time (s) | 120 | 15 | 15 | 40/120 | 600 | forever |

A, PCR reaction mixture; B, PCR cycle setting

### 2.3.2 Digestion

Double restriction enzyme digests were conducted at 37°C in a water bath for at least 2 h, and the conditions are shown in Table 2.3.

**Table 2.3 PCR products restriction digests and plasmids**.

| **Contains** | **Volume** |
|---|---|
| DNA | 5 μL |
| Buffer (according to manufacturer's instruction) | 2 μL |
| Nco1 | 2 μL |
| Kpn1 (Sal1 or EcoR1) | 2 μL |
| 10× BSA (1 mg/mL) (according to manufacturer's instruction) | 2 μL |
| water | 11 μL |

### 2.3.3 Ligation

FGF cDNAs were ligated with vector plasmid by T4 ligase (T4 DNA ligase M0202L, New England Biolabs, UK) 15 min at room temperature, the ligation condition is shown in **Table 2.4**.

**Table 2.4 Digest FGF cDNAs and pETM-11 plasmid ligation conditions**

| | |
|---|---|
| Vector pETM11 (digested with enzymes) | 1.5 μL |
| DNA (from the digest) | 2.5 μL |
| ×2 buffer | 5 μL |
| T4 ligase | 1 μL |
| Total | 10 μL |

## 2.4 Bacterial culture strains

### 2.4.1 Bacterial culture

Lysogeny Broth (LB) culture was made following the instructions of the manufacturer (Merk, East Yorkshire, UK).

Terrific Broth (TB) culture: 1 L contained: 2.4 % yeast extract (w/v), 1.2 % tryptone (w/v), 0.4 % glycerol (v/v), 17 mM $KH_2PO_4$, 72 mM $K_2HPO_4$, 50 µM $FeCl_3$, 10 µM $MgCl_2$, 10 µM $ZnCl_2$, 2 µM $NiCl_2$, 1 µM $CoCl_2$.

## 2.4.2 Competent cells

### 2.4.2.1 Competent cells list

DH5α cells (stored in -80$^o$C); CL41 cells (stored in -80$^o$C); BL21 (DE3) plysS cells (kind gift from Dr. Roger Barraclough). T1, RG (blue) and Rosetta Competent cells (ORIGAMI $^{TM}$ Technology).

### 2.4.2.2 Preparation of stocks of CL41 (DE3), DH5α and BL21 (DE3) plysS competent cells

A single colony was added to 5 mL LB and incubated overnight at 30$^o$C, 250 rpm. Five mL overnight culture was transferred into 100 mL LB, and incubated at 30$^o$C, then incubated at 250 rpm for 1.5 h (until the $OD_{600}$ reached 0.3-0.6). Cells were centrifuged 10 min, 3,500 ×g, at 4$^o$C. The supernatant was removed and 20 mL 50 mM $CaCl_2$ (chilled) was added and then the tube was left on ice for 30 min. Cells were then centrifuged as above after which 8.5 mL 50 mM $CaCl_2$ (4$^o$C), and 1.5 mL 50 mM glycerol (15 %, v/v) were added to resuspend the cells, which were then stored at -80$^o$C in aliquots.

## 2.4.3 Transformation

One hundred ng of plasmids were placed on ice together with 70 µL competent cells for 30 min, 1 mL LB culture was added and the mixture incubated at 37$^o$C for 1 h in a shaker culture (250 rpm). Then, the cells were collected by centrifugation and 1 in 5 of the cells were plated onto a LB Aar plate with antibiotic (dependent on the plasmids).

## 2.4.4 Miniprep

A single colony from the plates was added to 10 mL LB-Kanamycin (LB-Kan) culture, grown overnight at 37$^o$C, 250 rpm. The overnight culture was then centrifuged 5 min, 2,500

×g, to collect the cells. Plasmids in the cells were purified using a Qiagen miniprep kit, according to the manufacturer's instructions (Qiagen, UK).

### 2.4.5 Sequencing

Plasmid DNAs (30-100 ng/μL) were sent to Dundee Sequence (University of Dundee, UK) or GATC sequence service (GATC, UK) for sequencing.

## 2.5 Protein expression

A single colony was inoculated into 10 ml of LB with antibiotic (according to plasmids) overnight at 37$^{o}$C in a shaking incubator (250 rpm).

### 2.5.1 IPTG induction

Three mL of the overnight culture were inoculated into 500 mL LB culture with antibiotic (according to plasmids). Several flasks of culture were set up, depending on the amount of protein required. Cultures were grown at 37$^{o}$C (250 rpm) until an $OD_{600}$ of 0.5~0.8 was reached. The expression of the protein was then induced with IPTG (Bioline UK, London, UK) at a final concentration of 1 mM under shaking at 250 rpm, for 3 h at 37$^{o}$C or 16 h at 16$^{o}$C, depending on the FGF.

### 2.5.2 Self induction

Three ml of the overnight culture was inoculated into 500 mL TB culture with antibiotic (according to plasmids). Cells were grown at 37°C and cells were cooling down to 22°C and FGF production induced at 22°C for 16 h.

### 2.5.3 Cell harvest

Flasks were chilled on ice. The cultures were transferred to pre-chilled, sterile 500 mL centrifuge tubes and centrifuged for 20 min, at 7,000 ×g, 4$^{o}$C.

Cell pellets were resuspended with 25 mL of pre-chilled sterile phosphate-buffered saline (PBS: 137 mM NaCl，2.7 mM KCl，10 mM $Na_2HPO_4$, 2 mM $KH_2PO_4$, pH 7.2) and transferred to 50 mL tubes, and centrifuged for 15 min, at 3,500 ×g, 4$^{o}$C. Pellets were

resuspended with 10 mL of Resuspension Buffer (50 mM Tris-HCl pH 6.8, 0.6 M NaCl, 1 mM DTT) and stored at -80$^{o}$C.

# 2.6 Chromotography

## 2.6.1 Chromatography columns

Three mL of Affi-Heparin agarose (Bio-Rad); 1 mL Heparin column (Hi Trap heparin HP, GE Healthcare Ltd, Buckinghamshire, UK); 1 mL Q HP column (Hi Trap heparin HP, GE Healthcare); Probond Ni; 1 mL HiTrap column (GE Healthcare)

## 2.6.2 Cell breakage

Bacterial cells were thawed on ice and transferred to a pre-chilled 100 ml glass beaker. Cells were sonicated for 30 s (Dawe Ultrasonic Generator 7533A, pulsed sonication, max power, 40 / 50 % duty cycle) and placed on ice for 1 min. The procedure was repeated 6 times. Samples were then centrifuged in pre-chilled sterile 50 mL centrifuge tubes at 17,000 ×g for 30 min.

## 2.6.3 Chromatography I

A column (depending on the FGF) was first connected to a Pharmacia LKB-P1 peristaltic pump and equilibrated with washing buffer (according to which FGF) at a flow rate of 1 mL/min. The supernatant from **Section 2.6.2** was loaded on to the column, then washed with washing buffer for 2 h at the same flow rate. Protein was eluted with elution buffer (depending on which FGF). Elution was monitored at 280 nm with a Bio-Rad ECONO UV monitor (Bio-Rad) connected to a Kipp and Zonnen (Netherlands) recorder.

## 2.6.4 TEV digestions

Proteins eluted from chromatography I (**Section 2.6.3**) were buffer-exchanged into 50 mM Tris.HCl, pH 7.5, 0.6 M NaCl using a centrifugal filter column (10 K MWCO, Millipore Ltd, Watford, UK). TEV protease was added 1:20 (w/w) into the buffer-exchanged protein

solution and digest was at 4$^{o}$C, overnight. The digested protein solution was loaded again into the nickel affinity column and the flow through was collected.

### 2.6.5 Chromatography II

The proteins eluted after chromatography I or after TEV digestion and Ni affinity chromatography was diluted or buffer-exchanged to a suitable concentration of electrolytes and then loaded onto a column (depending on the FGF) and eluted with a salt gradient using an AKTA TM HPLC system. Elutions were monitored at 214 and 280 nm and peaks collected in 1 mL fractions. Protein concentration was calculated by absorbance measurement at 280 nm (according to the calculated molar extinction coefficients)

## 2.7 Mammalian cell culture

### 2.7.1 Cell line

Normal Rat, fast sticking fraction, Rama (rat mammary) 27 fibroblast cells were used [101]

### 2.7.2 Tissue culture reagents

1. RM (Routine medium): DMEM (Dulbecco's modified Eagle medium) 1× (Gibco Life Technologies, Paisley, Scotland, UK), 10 % (v/v) FCS (foetal calf serum), 0.75 % sodium bicarbonate (w/v) (Invitrogen, Paisley, UK), 20 mM L-glucosamine (Gibco), 1,00 IU/mL, penicillin (Gibco), 100 µg/mL streptomycin (Gibco), 50 ng/mL insulin (Sigma-Aldrich), 50 ng/mL hydrocortisome (Sigma-Approach).

2. Trypsin/EDTA solution: 25 mL versene (0.5 mM EDTA in PBS, pH 7.2) containing 2.5 % trypsin (in PBS, w/v) (Gibco).

3. BSA (bovine serum, albumin) (Sigma-Aldrich).

4. SD medium (step down medium): DMEM, 250 µg/mL BSA.

5. Freezing medium: DMEM supplemented with 7.5 % (v/v) DMSO (dimethyl sulphoxide), 20 % (v/v) FCS.

6. Isoton II counting fluid.

7. PBS (phosphate buffered saline): 137 mM NaCl, 2.7 mM KCl, 8 mM $Na_2HPO_4$, 1.5 mM $KH_2PO_4$, pH7.2.

8. Tissue culture grade Petri dishes (Nunc, Roskilde, Denmark).

## 2.7.3 Routine fibroblasts cells

Rama 27 cells were incubated into 9 cm diameter dishes and grown in monolayer culture in RM at 37$^o$C in a humidified atmosphere of 10 % carbon dioxide: 90 % air (both v/v). When the cell monolayer reached 60 % confluence, the cells were subcultured at a ratio of 1:8. The cells were washed with 5-10 mL PBS, then incubated in 1 mL trypsin/EDTA at 37$^o$C 3-5 min. When all cells detached, 7 mL RM was added into each plate and resuspended, taking care to ensure there were no clumps of cells. One mL of resuspended cells was added into each new tissue culture dish (cells were split at a ratio of 1:8), and 9 mL medium was added per dish. Rama 27 cells were used within a narrow passage range between passages 30 and 45 to ensure that the cells retained their growth characteristics.

## 2.7.4 Determination of cell number

A cell suspension (0.5 mL), obtained by passaging (**Section 2.7.3**), was added to 19.5 mL of Isoton II. The number of cells in a suspension was counted using a Coulter Electronics particle counter. Two counts were collected on each suspension of cells and the mean was used to calculate the number of cells in the original suspension.

## 2.7.5 Freezing cells

Cells were collected by trypsinisation (**Section 2.7.3**), counted and collected by centrifugation in a universal tube at 700 ×g for 5 min. After removing the supernatant, the cell pellet was resuspended in an appropriate volume of freezing medium to achieve a final cell density of 1-1.5 x $10^6$ cells/mL and l mL aliquots were transferred into 1.5 mL cryotubes. The aliquots were placed on dry ice for at least 1 h and then stored at -140$^o$C.

### 2.7.6 Thawing

The cells were thawed at 37°C, then the cells were removed from the cryotube and put in a 25 mL universal tube. DMEM 20 % FCS was add slowly inside the tube to a total volume of 20 mL. Then the cells were spun down at 700 ×g for 5 min. After removing the supernatant, pellets were resuspended with 10 mL RM and placed into two 3 cm diameter culture dishes in appropriate culture medium pre-warmed and incubated at 37°C.

### 2.7.7 Cell fixing

The cells on the dish surface were first washed with PBS for several times and then incubated in 4 % paraformaldehyde (PFA) (w/v, dissolved in PBS at 60°C) for 20 min. The fixed cells were washed again with PBS, and stored in PBS with 0.02 % (w/v) azide at 4°C.

## 2. 8 DNA synthesis assay

### 2.8.1 Reagents

1. 40 µ Ci/mL [methyl-$^{3}$H]-thymidine. (ICN, Basingstoke, UK)
2. 5 % (w/v) TCA (trichloroacetic acid)
3. 95 % (v/v) ethanol.
4. 0.2 M NaOH.
5. Foetal Calf Serum (FCS)
6. BSA
7. 10 mg/mL heparin dissolved in PBS

### 2.8.2 Assay

Cells were plated out from near confluent 9 cm dishes into 24-well tissue culture plates (Gibco) at 10,000-20,000 cells per well and incubated at 37°C for 24 h. After washing wells twice with 500 µL PBS, 500 µL SDM was added to each well and incubated at 37°C. Different concentrations of FGFs were added at least 24 h after step down to make a concentration gradient and then incubated for 18 h. At maximal DNA synthesis (max S

phase, 18 h for Rama 27 cells), 20 µL 40 µ Ci/mL [$^3$H]-thymidine was added and incubated for 1 h. After washing cells with 2 x 500 µL PBS, 500 µL ice cold 5% (w/v) TCA (4$^o$C) was added into each well and left for at least 30 min at 4$^o$C. The wells were then washed with 1 x 500 µL ice cold 5 % (w/v) TCA and TCA was removed by two washes with 95 % (v/v) ethanol. Wells were left to dry and 500 µL 0.2 M NaOH was added to each well and left either overnight on the bench or at 37$^o$C for 1h. Then, 300 µL solubilised TCA precipitate was transferred to each scintillation vial followed by 1 ml scintillation cocktail. Radioactivity was determined by counting for 10 min in a Packard tri Carb 1900TR scintillation counter.

## 2.9 Differential scanning fluorimetry (DSF)

The method corresponds to that previously described [102]. In brief, FGF solutions (10 % v/v), sugars (10 % v/v), 50× diluted 5000× sypro orange (10 % v/v) and PBS were mixed together. Ten µL of the mixture were added into Fast Optical 96 well plates (Applied Biosystems, Warrington, Cheshire, U.K.), each experimental condition had 3 replicates, and the plates were sealed with Optical Adhesive Film (Applied Biosystems). The samples were analyzed by real time RT- PCR machine (7500 Fast) with a temperature gradient from 32$^o$C to 81$^o$C: containing 99 time readings, with 0.5$^o$C increase each reading. Data were collected by the installed software (7500 fast systems, Applied Biosystems) in the RT-PCR machine using the calibration setting for TAMRA dye detection (λex 560 nm; λem 582 nm). The original data were organized by Excel (Office 2007), and the first derivatives of the melting curves were calculated by Origin 7.

## 2.10 Protect and Label

This method was based on the previous publications [103]. Twenty µL slurry of AF-heparin beads (Tosoh Biosciences GmbH, Stuttgart, Germany) were packed into a micro column (made from a 50 µL tip, with a plastic air filter placed at its end to retain the heparin beads) with a 5 mL syringe. The column was equilibrated with 4× 50 µL Buffer P1 (17.9 mM $Na_2HPO_4$, 2.1 mM $NaH_2PO_4$, 150 mM NaCl, pH 7.8) and loaded with 20 µg proteins by the

syringe. The loading was repeated 2 times. Then, the column was washed with 4× 50 µL Buffer P1.

To block the amino groups, twenty µL Buffer P1 containing 50 mM sulfo-NHS-acetate (Pierce, Thermo Fisher Scientific p/a Perbio Science UK, Ltd., Northumberland) was first loaded into the column for equilibration, and then another 20 µL Buffer P1 containing 50 mM sulfo-NHS-acetate loaded into the column and the reaction was left for 5 min at room temperature. Excess sulfo-NHS-acetate was removed by washing the column with 4× 50 µL Buffer P1. Then, bound proteins were eluted in Buffer P2 (44.75 mM $Na_2HPO_4$, 5.25 mM $NaH_2PO_4$, pH 7.8) with 2 M NaCl.

Eluted proteins were diluted with 200 µL Buffer P2, and concentrated using a 5 kDa MWCO centrifugal filter (Sartorius Ltd, Epsom, UK) to a volume of 37 µL. After that, 2.8 µL 145 mM NHS-biotin (Pierce) in DMSO (final concentration 10 mM) was added to the concentrated proteins and incubated at room temperature for 30 min to label the amino group previously protected by heparin binding. Four µL 1 M Tris, pH 7.5 was added to the solution to stop the reaction. The sample was desalted on a 0.5 ml desalting column (Zeba TM Desalt Spin column, Thermo, UK) following the manufacturer's instruction and the desalted sample was then dried by centrifugal evaporation. The dried proteins were dissolved in 25 µL 8 M urea, 400 mM $NH_4HCO_3$ pH 7.8, 2.5 µL 45 mM DTT and incubated 15 min at 56$^{o}$C. Then, 2.5 µL freshly made 0.1 M iodoacetamide were added to carbamidomethylate SH groups for 15 min at room temperature. The solution was dissolved in 70 µL HPLC grade water, and digested overnight with 1.5 µg chymotrypsin (Sigma-Aldrich) at 37$^{o}$C.

Peptides were diluted with 400 µL HPLC grade water and applied to a mini column, which contained a 25 µL slurry of Step-TactinTM Sepharose beads (IBA GmbH), equilibrated with 4× 50 µL 500 mM urea, 25 mM $NH_4HCO_3$. The column was washed 3× 50 µL 500 mM urea, 25 mM $NH_4HCO_3$ and then 2×50 µL HPLC grade water. Finally, bound peptides were eluted with two times 20 µL 20 % (v/v) trifluoroacetic acid (TFA), 80 % (v/v) acetonitrile (ACN), 5

mM biotin. The elute was desalted using a C18 ZipTipTM (Millipore) according to manufacturer's instructions, and then analyzed by Tandem mass spectrometry (performed by Dr Ori, EMBL, Heidelberg).

Up to 1 µg of biotinylated peptides were injected into a LTQ-Orbitrap Velos instrument (Thermo) using a nanoAcquity UPLC system (Waters Corporation, Manchester, UK). Peptides were separated on a BEH300 C18 (75 µm × 250 mm, 1.7 µm) nanoAcquity UPLC column (Waters) using a 60 min linear gradient (5-35 % (v/v) ACN in 0.1 % (v/v) formic acid). Data acquisition was performed using a TOP-10 strategy where survey MS scans were acquired in the orbitrap (R = 30,000 at m/z 400) and up to 10 of the most abundant ions per full scan were fragmented by higher energy collision dissociation (HCD) and analyzed in the orbitrap (R = 7,500 at m/z 400).

Data analysis was performed using the Batch Tag tool of the Protein Prospector package v.5.9.2 (http://prospector2.ucsf.edu/) applying the following parameters: digest, chymotrypsin (FWYMEDLN); maximum missed cleavages, 5; possible modifications, acetyl (Lys), biotin (Lys), carbamidomethyl (Cys), oxidation (Met); parental ion tolerance, 10 ppm; fragment ion tolerance, 0.05 Da. The UniProt accession number of the protein analyzed was used as a research parameter (database, SwissProt 2011.01.11). Results were filtered using a peptide E-value < 0.001 and SLIP score threshold for site assignment was set to 6 (cite PMID: 21490164).

## 2.11 Biosensor binding assays

Steptavidin (Sigma-Aldrich) was immobilized on amino silane surfaces (Farfield Group, UK) using bissulfosuccinimidyl suberate ($BS_3$, Pierce) as the cross linker according to the manufacture's recommendation. Controls showed that FGFs in PBST (140 mM NaCl, 10 mM phosphate, pH 7.2, 0.02 % (w/v) $NaN_3$, 0.02 % (v/v) Tween 20) do not bind to this surface, or a streptavidin surface. DP8 oligosaccharides were biotinylated with NHS (LC)-biotin (Pierce) and then immobilized on to the streptavidin surface as described previously [57, 104]. The surface of the biosensor was inspected during every phase of the binding

reaction by examination of the resonance scans. The scans showed that the bound material was distributed on the curvette surface uniformly.

A single assay consisted of adding the 1-5 µL different concentration FGFs into a cuvette containing 49-45 µL PBST to a total volume of 50 µL. The association was followed until binding was at least 90 % of the calculated equilibrium value, usually between 60 s-240 s. The cuvette was washed using 3 times with 50 µL PBST and regenerated with 2 M NaCl. The dissociation was measured using a fixed concentration with all FGFs (5 µL, 100 µg/mL FGFs diluted into a cuvette containing 45 µL PBST. When binding was maximal the cuvette was washed quickly with 3x 50 µL PBST and dissociation was followed three times over 60 s.

Binding parameters of the association and dissociation were calculated using the non-linear curve fitting Fastfit. Each binding assay yields several parameters: the slope of the rate of the association, the on-rate constant ($k_{on}$) and the extent of binding, all calculated from the association phase and the off-rate constant, ($k_{off}$, equivalent to the dissociation rate constant, $k_d$), calculated from the dissociation phase [57, 105]. The association rate constant ($k_a$) was calculated from the values of $k_{on}$ determined at five to seven concentrations of FGFs. The equilibrium dissociation constant ($K_D$) was calculated from the ratio of the dissociation and association rate constant ($k_d$/ $k_a$).

## 2.12 SRCD

FGFs were buffer exchanged into CD buffer (15.3 mM $Na_2HPO_4$, 2.2 mM $NaH_2PO_4$, pH 7.5). FGFs (0.5 mg/mL – 1 mg/mL) and heparin were mixed in different ratios (1:5-5:1) and then were loaded into a quartz cuvette, pathlength 0.2 mm, and the spectrum was acquired from 178 nm to 260 nm on beamline 23 (Olis DSM 20, Diamond). The program SELCON3 and the database 3 were used to analyze the secondary structures (software from http://dichroweb.cryst.bbk.ac.uk/htmL/home.shtmL). Each set of data was based on the average of four scans.

# Chapter 3 Tools and Resources

## 3.1 Subcloning of FGF cDNAs

### 3.1.1 Materials

pETM-11 (a modified pET-24b vector, kind gift from Dr Paul Elliott, University of Liverpool), which provides the sequences of the 6×Histag and the TEV cleavage site.pET-14b-FGF-1 (UniProt Accession: P05230; residues: 16-155), pET-14b-FGF-2, (UniProt Accession: P09038-2; residues: 1-155), pET-14b-Histag-FGF-2 (from Dr Laurence Duchesne, which contains a sequence encoding a 6× Histag and a thrombin cleavage site: MGHHHHHHLVPRGS at the N-terminus [106]), pETM-11-FGF-9 (Uniprot Accession: P31371 residues: 1-208).

Plasmids containing human FGF-19, cDNAs pCMV-SPORT6-FGF-19 (UniProt Accession: O95750, residues: 25-216); human FGF-18 cDNA, pOTB7-FGF-18 (zFGF5) (UniProt Accession: O76093; residues: 28-207); human FGF-21 cDNA, pCMV-SPORT6-FGF-21 (Uniprot Accession: Q9NSA1; residues: 29-209); human FGF-23 cDNA, pCR-BluntII-TOPO-FGF-23 (UniProt Accession: Q9GZV9; residues: 25-251) were also acquired.

Plasmids pCR2.1 containing FGF-3 (Uniprot Accession: P11487, residues: 18-239), FGF-5 (Unipro Accession: P12034, residues: 18-268), FGF-7 (Uniprot Accession: P21781; residues: 32-194), FGF-16 (Unipro Accession: O43320**,** residues: 1-207), FGF-17 cDNA (Unipro Accession: O60258**,** residues: 23-216) were shipped from the company undertaking gene synthesis (Eurofins mwg, UK).

**Table 3.1 Restriction enzymes used for different FGFs**

| ***fgfs*** | **enzyme1** | **enzyme2** |
|---|---|---|
| *fgf-3* | Nco1 | Sal1 |
| *fgf-5* | Nco1 | Kpn1 |
| *fgf-7* | Nco1 | Sal1 |
| *fgf-16* | Nco1 | Kpn1 |
| *fgf-17* | Nco1 | Kpn1 |
| *fgf-18* | Nco1 | Kpn1 |
| *fgf-19* | Nco1 | Sal1 |
| *fgf-21* | Nco1 | Sal1 |
| *fgf-23* | Nco1 | Kpn1 |

**Table 3.2 Desalted PCR primers and cDNA.**

| **FGF** | | **Primer sequence** | **$T_M$ ($^oC$)** |
|---|---|---|---|
| FGF-5 | Forward: | 5'-ATTATCCATGGCATGGGCGCATGG -3' | 46 |
| | Reverse: | 5'-ATAATGGTACCTACCCAAACCGGAATTTCA-3' | 46 |
| FGF-16 | Forward: | 5'-TATAATCCATGGCGGAAGTTGGCGGT -3' | 48 |
| | Reverse: | 5'-TTATGGTACCTACCTATAGTGGAACAGATC -3' | 48 |
| FGF-18 | Forward: | 5'-ATTATCCATGGAGGAGAACGTGGACTTC -3' | 50 |
| | Reverse: | 5'- TAAATGGTACCCTAGGCAGGGTGT G -3' | 50 |
| FGF-21 | Forward: | 5'- TATTACCATGGCACACCCCATCCCTGA -3' | 51 |
| | Reverse: | 5'- TCGTAGTCGACTCAGGAAGCGTAG -3' | 51 |
| FGF-19 | Forward: | 5'-TAATCCATGGCTCTCGCCTTCTCGGAC -3' | 53 |
| | Reverse: | 5'-TAAGTCGACTTACTTCTCAAAGCTGGGACTCC -3' | 53 |
| FGF-23 | Forward: | 5'-ATTATCCATGGCATATCCCAATGCCTCC -3' | 50 |
| | Reverse: | 5'-TAG CTG GTA CCC TAG ATG AAC TTG GC -3' | 50 |
| FGF-19 | Forward: | 5'-ATGCTGCCTATGGTCCCAG -3' | 58 |
| (mutagenesis) | Reverse: | 5'-GGGACCATAGGCAGCATGGGCAGGAAATGAGA-3' | 58 |

FGF-5, FGF-16, FGF-18, FGF-19, FGF-21 and FGF-23 PCR primers sequences (Invitrogen). Stock solution was 100 μM, Working solution was 30 μM.

## 3.1.2 Methods

### 3.1.2.1 FGF-19 Mutagenesis (CCA→CCT)

For ligation, Nco1 (CCATGG) digestion was used, to allow the insertion of the FGF-19 cDNA into the pETM11 plasmid. However, the FGF-19 cDNA had an internal Nco1 restriction site, so mutagenesis was needed to change a codon (CCA →CCT) according to the general method (**Section 2.2**).

### 3.1.2.2 PCR and digestion

Full length human FGF-18, FGF-19, FGF-21, FGF-23 cDNAs were obtained from Imagenes (Imagenes, UK) and full length human FGF-5 and FGF-16 cDNA were obtained by gene synthesis. These were all amplified by PCR with forward primers which contained Nco1 restriction sites at their 5' terminus and reverse primers which contained a Kpn1/Sal1 (**Table 3.1**) restriction site at their 3'terminus (primer sequence: **Table 3.2**) (**Section 2.3.1**).

### 3.1.2.3 Ligation

FGF-5, FGF-9, FGF-16, FGF-18, FGF-19, FGF-21 and FGF-23 PCR products were digested withdouble enzymes according to Table 3.1 and ligated to digested pETM-11 (**Section 2.3.3**).

## 3.1.3 Results

### 3.1.3.1 Strategy for subcloning FGF cDNAs into pETM-11

Full length human FGF cDNAs were amplified with forward primers, which contained Nco1 restriction sites at their 5' terminus and reverse primers, which contained Sal1 or Kpn1 restriction site at their 3'terminus (**Section 3.1.2.2**). The PCR products were digested with Nco1 and Kpn1/Sal1, as appropriate, whilst the pETM-11 vector was digested with Nco1 and Kpn1 (**Section 3.1.2.2**). The cDNAs were then ligated into the expression vector (**Section 3.1.2.3**).

### 3.1.3.2 Mutagenesis

Internal restriction sites will cause the cloning strategy to fail. For example, in FGF-19 there is an Nco1 site at bases 510-512. Therefore, mutagenesis, performed by PCR on the whole plasmid was used to change the corresponding codon CCA→CCT, which eliminated the internal restriction site, but did not change the corresponding amino sequence of the cDNA (**Section 3.1.2.1**).

### 3.1.3.3 PCR of cDNAs

Six FGF cDNAs (*fgf-5, fgf-16, fgf-18, fgf-19, fgf-21 and fgf-23*) were amplified by PCR (**Section 3.1.2.2**), and the products were analyzed by agarose gel electrophoresis. The bands above 500 bp corresponded to a size expected of the FGF cDNAs.

### 3.1.3.4 Ligation

FGF cDNAs were ligated into the pETM-11 vector (**Section 3.1.2.3**). The expected products of the ligation were analyzed by transformation of the products into DH5α cells (**Section 2.4.3**) and sequencing in both directions of the insert. Analysis of the returned sequences showed that they were identical to those of the corresponding FGF and the predicted amino acid sequences were also correct (result not shown). Quantification of the plasmids by their absorbance at 260 nm showed there was sufficient for transformation (FGF-18: 126.0 ng/µL, FGF-19: 91 ng/ µL, FGF-21: 110.8 ng/ µL, FGF-23: 124.0 ng/ µL).

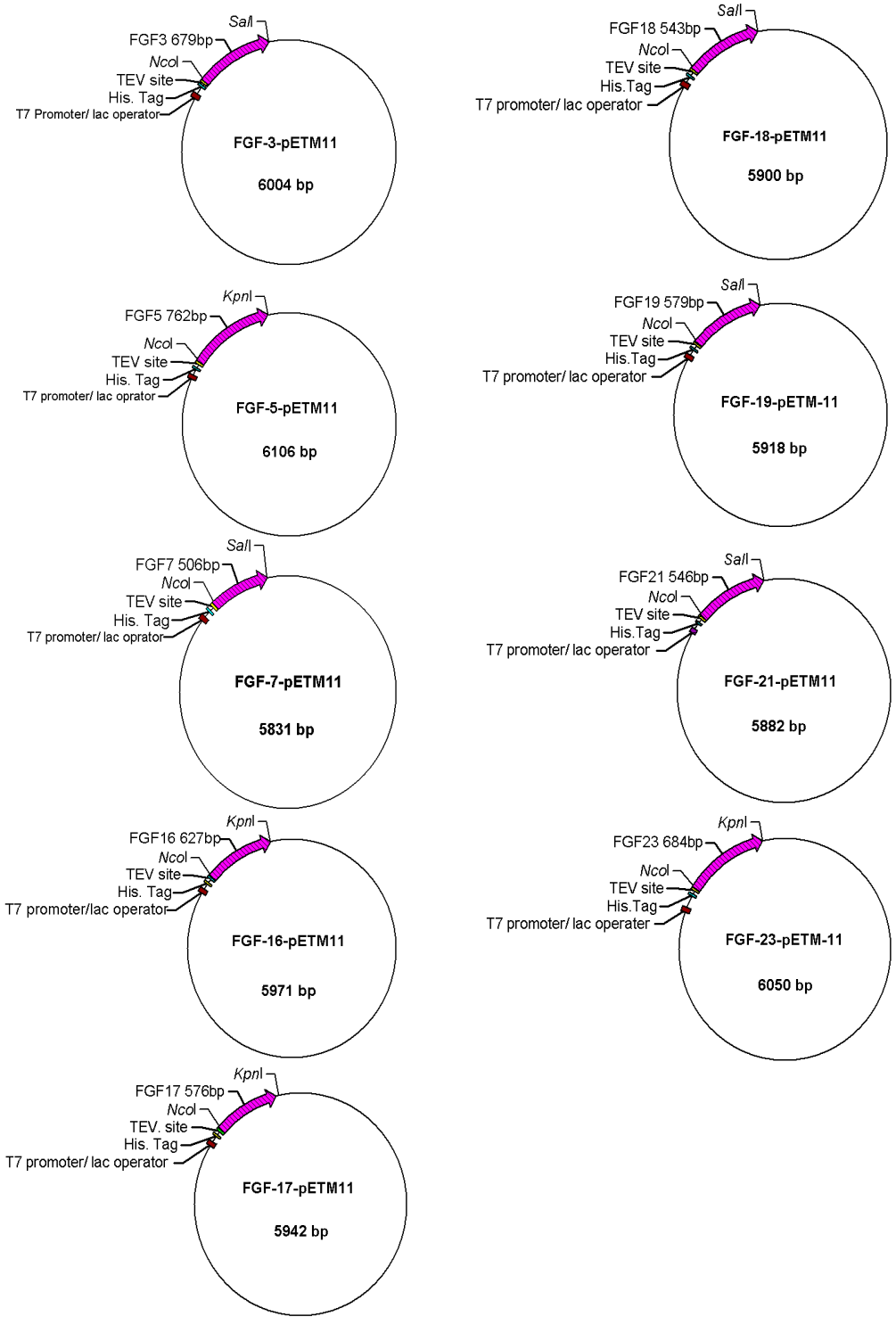


**Figure 3.1 Maps of expression plasmids.**

FGF-3, FGF-5, FGF-7, FGF-16, FGF-17, FGF-18, FGF-19, FGF-21 and FGF-23 cDNAs (purple) were ligated into the pETM-11 vectors (which contain a 6× his-tag and a TEV-site).

# 3.2 FGF expression and purification

## 3.2.1 Methods

### 3.2.1.1 Bacteria transformation

One hundred ng pET-14-FGF-1, pET-14-FGF-2, pET-14b-Histag-FGF-2, pETM-11-FGF-9, pETM-11-FGF-18, pETM-11-FGF-21 were transformed into CL41 (DE3) cells separately, while 100 ng pETM-11-FGF-7 was transformed into BL21 (DE3) plysS cells, following the transformation protocol (**Section 2.4.3**).

### 3.2.1.2 Bacterial cultures

#### *3.2.1.2.1 FGF-1, FGF-2 and His-tagged FGF-2*

Two liters (4× 500 mL) LB-ampicillin culture of C 41 cells contain pET-14b-FGF-1, pET-14-FGF-2 or pET-14b-Histag-FGF-2 was induced with IPTG at a final concentration of 1 mM for 3 h at 37°C (**Section 2.5.1**).

#### *3.2.1.2.2 FGF-7*

Two liters (4× 500 mL) LB- LB-Kan and chloramphenicol (Sigma-Aldrich) culture of C 41 cells containing pETM-11-FGF-7 was induced with IPTG at a final concentration of 1 mM for 3 h at 37°C (**Section 2.5.1**).

#### *3.2.1.2.3 FGF-9*

Two liters (4× 500 mL) LB-kanamycin culture of C 41 cells containing pETM11-FGF-9 was induced with a self induction system (**Section 2.5.2**).

*3.2.1.2.4 FGF-18 and FGF-21*

Two liters (4× 500 mL) LB-kanamycin culture of C 41 cells contain pETM11-FGF-18 or pETM11-FGF-21 was induced with IPTG at a final concentration of 1 mM for 16 h at 16°C (**Section 2.5.1**).

### 3.2.1.3 Cell breakage

Cell breakage was achieved in the resuspension buffer (20 mM phosphate buffer, 0.6 M NaCl, 1 mM DTT, pH 6.5), except FGF-9 where Buffer A9 (0.3 M NaCl, 50 mM Tris, 1 mM DTT, pH 7.4) was used, supplemented with 0.2 mg/ml lysozyme (lysozyme, chicken egg white, Calbiochem, Nottingham, UK), 10 µg/ml DNase I (deoxyribonuclease I, from bovine pancreas, Sigma-Aldrich), 1 tablet of protease inhibitor (complete EDTA-Free, Protease Inhibitor Cocktail Tablets, Roche, West Sussex, UK), 0.2 % (v/v) Tween-20 and 5 % (v/v) glycerol (**Section 2.6.2**).

### 3.2.1.4 Chromatography I

FGF-1, FGF-2 and Histag-FGF-2 were loaded separately onto a three mL Affi-heparin agarose (Bio-Rad) column, which was equilibrated with washing buffer F11 (20 mM phosphate buffer, 0.6 M NaCl, 1 mM DTT, pH 6.5), and the proteins eluted with elution buffer F12 (20 mM phosphate buffer, 2 M NaCl, 1 mM DTT, pH 6.5) (**Section 2.6.3**).

The FGF-9 was loaded onto a 5 mL heparin agarose column, which was washed with Buffer A9 until the absorbance returned to baseline. FGF-9 was eluted in Buffer B9 (50 mM Tris, 2 M NaCl, 1 mM DTT, pH 7.5) (**Section 2.6.3**).

FGF-7, FGF-18 and FGF-21 were loaded separately onto a three mL Ni Resin (Probond Lot: 1202530 Invitrogen) column, equilibrated with washing buffer F71 (50 mM imidazole, 0.5 M NaCl, 50 mM Tris.HCl, pH 7.9), and the proteins were eluted with elution buffer F72 (500 mM imidazole, 0.5 M NaCl, 50 mM Tris-Cl, pH 7.9) (**Section 2.6.3**).

### 3.2.1.5 TEV digestions

FGF-7 and FGF-18 eluted from the Probond resin were buffer exchanged and digested with TEV protease, then loaded again to Ni Probond resin (**Section 2.6.4**).

### 3.2.1.6 Chromatography II

The FGF-1, FGF-2 and Histag-FGF-2 previously eluted from the affinity heparin agarose were separately diluted 3 fold with Buffer 13 (20 mM phosphate buffer, 1 mM DTT, pH 6.5) to a final NaCl concentration of 0.5 M, then applied to a 1 mL Hi-Trap heparin column using the same buffer and eluted with a NaCl gradient 0.5-2 M using an AKTA system (**Section 2.6.5**).

Eluted FGF-9 was diluted 4-fold with 50 mM Tris-Cl and applied to a 1 mL HiTrap Ni column, and eluted with an imidazole gradient (50 mM to 500 mM imidazole) in 0.5 M NaCl, 1 mM DTT, 50 mM Tris-Cl, pH 7.5 (**Section 2.6.5**). Eluted protein was dialyzed against 10 mM phosphate, 1 mM DTT, pH 7.5.

The flow through of second Ni Probond of FGF-7 and FGF-18 were then applied separately to a 1 ml heparin column using the same buffer and eluted with a NaCl gradient 0.6-2 M (**Section 2.6.5**).

The FGF-21 elute peak was dialyzed against Buffer F21 (10 mM Tris-Cl, 1 mM DTT, 50 mM NaCl, pH 8.0) at 4$^{o}$C and and then applied to a 1 mL Q column using the same buffer and eluted with a NaCl gradient 0.05-1 M using an AKTA system (**Section 2.6.5**).

Protein concentration was calculated by absorbance measurement at 280 nm (extinction coefficient: FGF-1: 17545 $M^{-1}$ $cm^{-1}$, FGF-2: 16180 $M^{-1}$ $cm^{-1}$, his-tagged FGF-2: 16180 $M^{-1}$ $cm^{-1}$, FGF-7: 35785$M^{-1}$ $cm^{-1}$, FGF-9: 20525 $M^{-1}$ $cm^{-1}$, FGF-18: 20775 and FGF-21: 14565 $M^{-1}$ $cm^{-1}$).

## 3.2.2 Results of expression and purification

### 3.2.2.1 Introduction

Except for FGF-1 and FGF-2, all the other expressed FGFs possess an N-terminal hexhistidine tag and a TEV cleavage site (26 amino acids, MKHHHHHHPMSDYDIPTTENLYFQGA), which derived from the vector pETM-11 sequence and provides one method for purification. The high affinity of all FGFs, except for the endocrine FGFs (FGF-19, FGF-21 and FGF-23), for heparin, provides an affinity method for purification. The plasmid also encodes a TEV protease site between the 6×his tag and the FGF protein. So, following TEV cleavage, reverse $Ni^{2+}$ chelation chromatography can be used to remove the 6×his tag, the TEV protease (this has a non-cleavable 6×his tag) and unwanted contaminants that bind the $Ni^{2+}$ column. Generally, heparin affinity chromatography is the method of choice, but if it is only partly successful, or in the case of the endocrine FGFs, $Ni^{2+}$ chelation chromatography provides a route to producing very pure protein.

### 3.2.2.2 Expression and Purification of FGF-1 and FGF-2

#### *3.2.2.2.1 Purification of FGF-1*

FGF-1 was produced using an existing plasmid from a culture of 2 L (**Section 3.2.1.2**) and the protein eluting from the Affi-Heparin agarose with 2 M NaCl (**Section 3.2.1.4**) was diluted and loaded on to a HPLC heparin affinity column (**Section 3.2.1.6**). Four fractions were collected (A10-A13), corresponding to the protein peak (**Figure 3.2**). These, along with samples corresponding to the starting material and unbound protein were analyzed by SDS-PAGE. The results show that a single band, of ~17 kDa was present in fractions A10 to A13 (**Fig. 3.3**). Measurement of the protein concentration by absorbance indicated that there was 0.17 mg protein in A10, 1.4 mg in A11, 1.8 mg in A12 and 0.17 mg in A13. These fractions were stored as 100 µl aliquots in elution buffer at -80°C.

*3.2.2.2.2 Purification of FGF-2*

FGF-2 was produced using the plasmid from a culture of 2 L (**Section 3.2.1.2**) and the protein eluting from the Affi-Heparin agarose column (**Section 3.2.1.4**) was diluted and loaded on to a HiTrap heparin affinity column (**Section 3.2.1.6**). The protein peak (A13-B1) eluted just after that for FGF-1 (**Figs 3.4**) in agreement with the known requirement for higher concentrations of NaCl to elute FGF-2 from heparin (**Section 3.2.1.6**). These, along with samples corresponding to the starting material and unbound protein were analyzed by SDS-PAGE. The results show that a single band, of ~18 kDa was present in fractions A13 to B1 (**Fig. 3.4**). Measurement of the protein concentration by absorbance indicated that there was 1.2 mg protein in A13, 1.5 mg in A14, 1.1 mg in A15 and 0.1 mg in B1. These fractions were stored as 100 µL aliquots in elution buffer at -80$^{o}$C.

*3.2.2.2.3 Purification of His-tagged FGF-2*

His-tagged FGF-2 was produced using a 2 L culture (**Section 3.2.1.2**) and the protein eluting from the Affi-Heparin agarose column (**Section 3.2.1.4**) was diluted and loaded on to a HPLC heparin affinity column (**Section 3.2.1.6**). The protein peak (A12-B13) eluted similar to FGF-2 from heparin. These, along with samples corresponding to the starting material and unbound protein were analyzed by SDS-PAGE. The result shows that a single band, of ~17 kDa was present in fractions A13 to B14 (**Fig. 3.5**). Measurement of the protein concentration by absorbance indicated that there was 2.1 mg protein in A13, 3.1 mg in A14, 3.2 mg in A15 and 1.1 mg in B1. These fractions were stored as 100 µl aliquots in elution buffer at -80$^{o}$C.

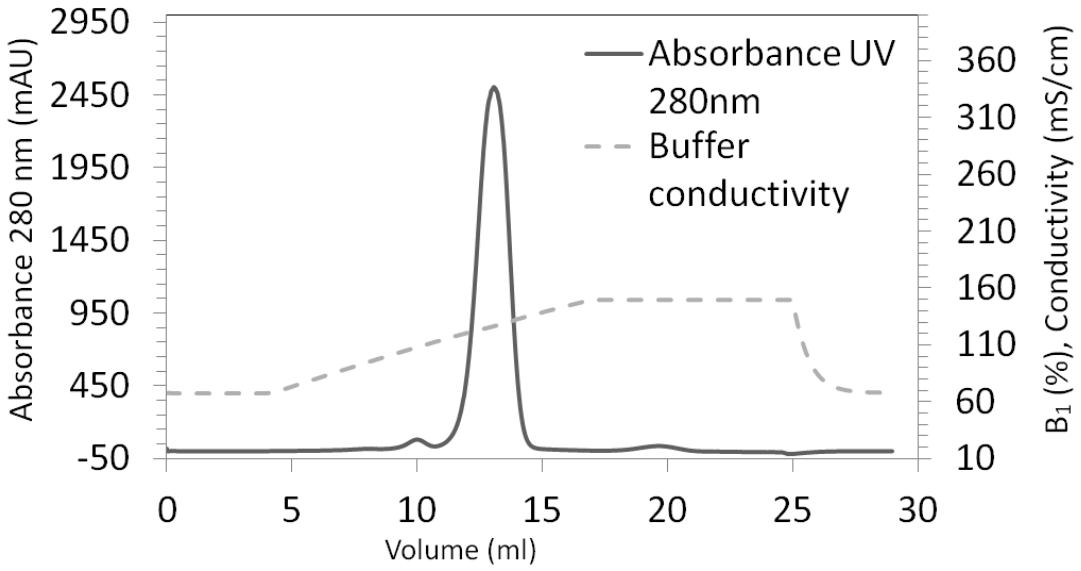


**Figure 3.2 Chromatography of FGF-1 on HiTrap heparin.**

Single-step purification of FGF-1 protein from heparin elution (**Section 2.6.3**) using 1 mL HiTrap heparin column (loading buffer B1: 50 mM phosphate, 0.6 M NaCl, 1 mM DTT, pH 6.5; elution buffer E1: 50 mM phosphate, 2 M NaCl, 1 mM DTT, pH 6.5; flow rate: 1 mL/min; sample load volume: 30 mL). Solid line represents the absorbance at 280 nm. Dashed line represents conductivity. The peak was collected and analyzed by SDS-PAGE.

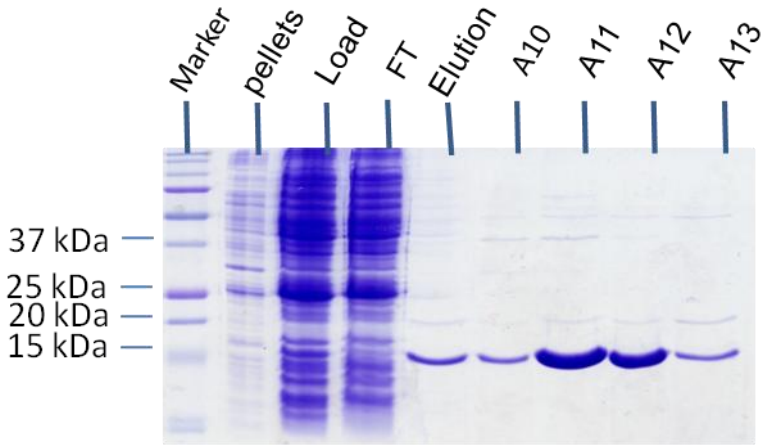


**Figure 3.3 Analysis of fractions containing FGF-1 by SDS-PAGE.**

Bacteria from a 2 L culture were broken by sonication and the clarified supernatant loaded on a 3 mL column of heparin agarose. The 2 M NaCl eluate from this column was diluted 4 fold and applied to a 1 mL heparin HiTrap column on an AKTA HPLC system (**Section 3.2.1**). Elution was monitored at 280 nm (**Fig. 3.2**) and peaks collected in 1 mL fractions and were analyzed by SDS-PAGE followed by coomassie staining. The molecular weight of FGF-1 is ~17 kDa. Pellets = insoluble material following cell breakage; Load = sample applied to 3 mL heparin column; FT = flow through fraction; elution = 2 M NaCl eluate; A10-A13 = fractions from HiTrap heparin column.

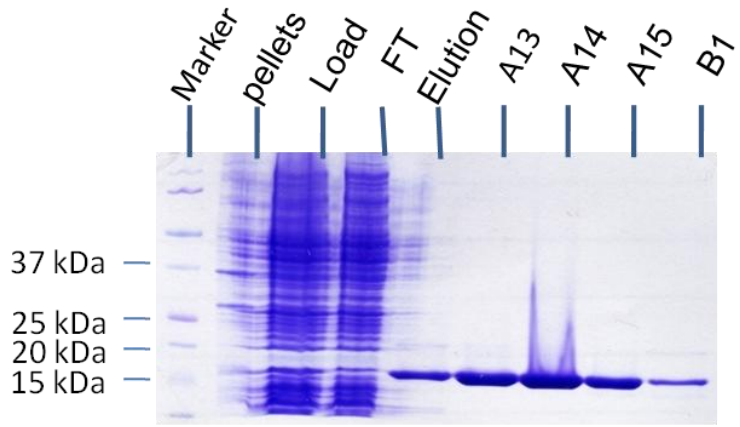


**Figure 3.4 Analysis of fractions containing FGF-2 by SDS-PAGE.**

Bacteria from a 2 L culture were broken by sonication and loaded on a 3 mL column of heparin agarose. The 2 M NaCl eluate from this column was diluted 4 fold and applied to a 1 mL heparin column on an AKTA HPLC systems (**Section 3.2.1**). Elution was monitored at 280 nm and peaks collected in 1 mL fractions and were analyzed by SDS-PAGE followed by Coomassie Staining. The molecular weight of FGF-2 is ~17 kDa. Pellets = insoluble material following cell breakage; Load = sample applied to 3 mL heparin column; FT = flow through fraction; elution = 2 M NaCl eluate; A10-B1, fractions from HiTrap heparin column.

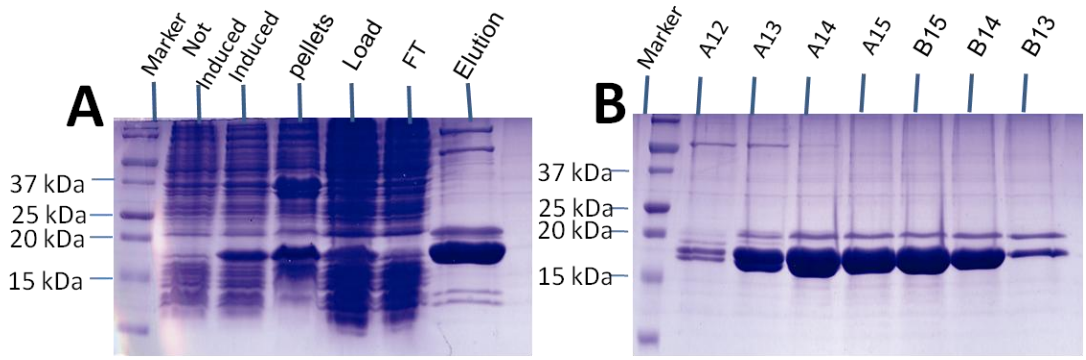


**Figure 3.5 Analysis of fractions containing his-tagged FGF-2 by SDS-PAGE.**

Bacteria from a 2 L culture were broken by sonication and loaded on a 3 mL column of heparin agarose. The 2 M NaCl eluate from this column was diluted 4 fold and applied to a 1 mL HiTrap heparin column on an AKTA HPLC systems (**Section 3.2.1**). Elution was monitored at 280 nm and peaks collected in 1 mL fractions and were analyzed by SDS-PAGE followed by coomassie staining. The molecular weight of His-tagged FGF-2 is ~18 kD. Non-induced bacteria cultured in the absence of IPTG; induced, bacteria induced with IPTG; Pellets = insoluble material following cell breakage; Load = sample applied to 3 mL heparin column; FT = flow through fraction; elution = 2 M NaCl eluate; A12-B15, fractions from HiTrap heparin column.

## 3.2.2.3 Expression and Purification of FGF-7

*3.2.2.3.1 Expression*

FGF-7 was indicated to be toxic to *E. coli* cells according to a previous study [107]. BL21 (DE3) plsS cells were used to fully repress the FGF-7 gene by producing T7 lysozyme (a special T7 polymerase-inhibitor), to avoid the expression of the toxic FGF-7 while the cells were grown to the appropriate density for protein production.

*3.2.2.3.2 Purification*

FGF-7 was produced using the plasmid described in **Section 3.1.3.4** from a culture of 2 L (**Section 3.2.1.2**). The proteins from lysis were loaded onto a Ni column and the elution was then digested by TEV protease (**Section 2.6.4**). The second flow through (after overnight digestion) from the Probond $Ni^{2+}$ resin column (**Section 3.2.1.4**) was diluted and loaded on to a HPLC heparin affinity column (**Section 3.2.1.6**). Three fractions were collected (A14-B15) corresponding to the protein peak. These eluted before FGF-2, suggesting that similar amount of NaCl is needed to break the FGF7-heparin interaction (**Figure 3.6**). These fractions, along with samples corresponding to the starting material and unbound protein were analyzed by SDS-PAGE. The most obvious band, of ~17 kDa, was present in fractions A14 to B15 (**Figure 3.6 B**). Measurement of the protein concentration by absorbance indicated that there was 0.5 mg protein in A14, which was stored as 100 µL aliquots in elution buffer at -80°C.

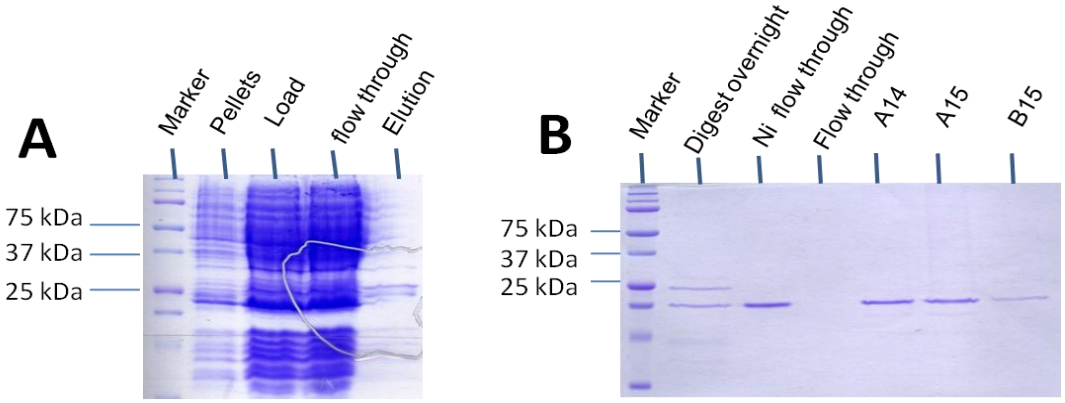


**Figure 3.6 Purification of FGF-7.**

A.Bacteria from a 2 L culture were broken by sonication and loaded on a 3 ml column of $Ni^{2+}$ agarose. B. The 0.5 M imidazole eluate from $Ni^{2+}$ column was buffer-exchanged and digested with TEV protease (**Section 2.6.4**). The digested proteins were applied again to the $Ni^{2+}$ column, and the $Ni^{2+}$ flow through was loaded to a 1 mL heparin column on an AKTA HPLC system (**Section 3.2.1**). Elution was monitored at 214 and 280 nm and peaks collected in 1 ml fractions. Fractions were analyzed by SDS-PAGE followed by comassie staining. The molecular weight FGF-7 with his tag is ~17 kDa. Pellets = insoluble material following cell breakage; Load = sample applied to Ni column; FT = flow through fraction; elution = imidazole eluate; digest overnight, product of TEV protease digest; Ni flow though = material not binding to Ni column after TEV digest; flow through = flow through after loading on heparin column; A14-B15, fractions eluted from HiTrap heparin column.

## 3.2.2.4 Expression and purification of FGF-9

*3.2.2.4.1 Expression*

FGF-9 was found to be largely present (> 90 %) as insoluble proteins after IPTG induction, which suggests that most of the protein is in inclusion bodies. As an alternative, a self induction system, which uses medium containing sucrose to induce expression was employed (**Section 2.5.2**), to increase the proportion of soluble FGF-9.

*3.2.2.4.2 Purification*

FGF-9 was produced using the plasmid described in **Section 3.1.3.4** from a culture of 2 L (**Section 3.2.1.2**). To help protect the structure of FGF-9 and avoid unexpected degradation, a small amount of glycerol (5 %) and Tween 20 (0.2 %) and a tablet of protease inhibitor cocktail were added into the lysis buffer prior to the sonication step (**Section 3.2.1.3**). Lysozyme and DNase I were also added to increase cell breakage.

The elute from the heparin affinity resin column (**Section 3.2.1.4**) was diluted and purified on a HiTrap 1 mL Ni column (**Section 3.2.1.6**). Twenty-two fractions were collected (A5-B5) corresponding to the protein peak. These fractions, along with samples corresponding to the starting material and unbound protein were analyzed by SDS-PAGE. The most obvious band, of ~26 kDa, was present pure in fractions A12 to B15 (**Figure 3.7 B, C**). Measurement of the protein concentration by absorbance indicated that there was 0.1-0.2 mg/mL protein in A12 to B5, which was concentrated by spin column (5,000 MWCO, GE, Healthcare) to 1 mg/mL, and stored as 100 µL aliquots in elution buffer at -80°C.

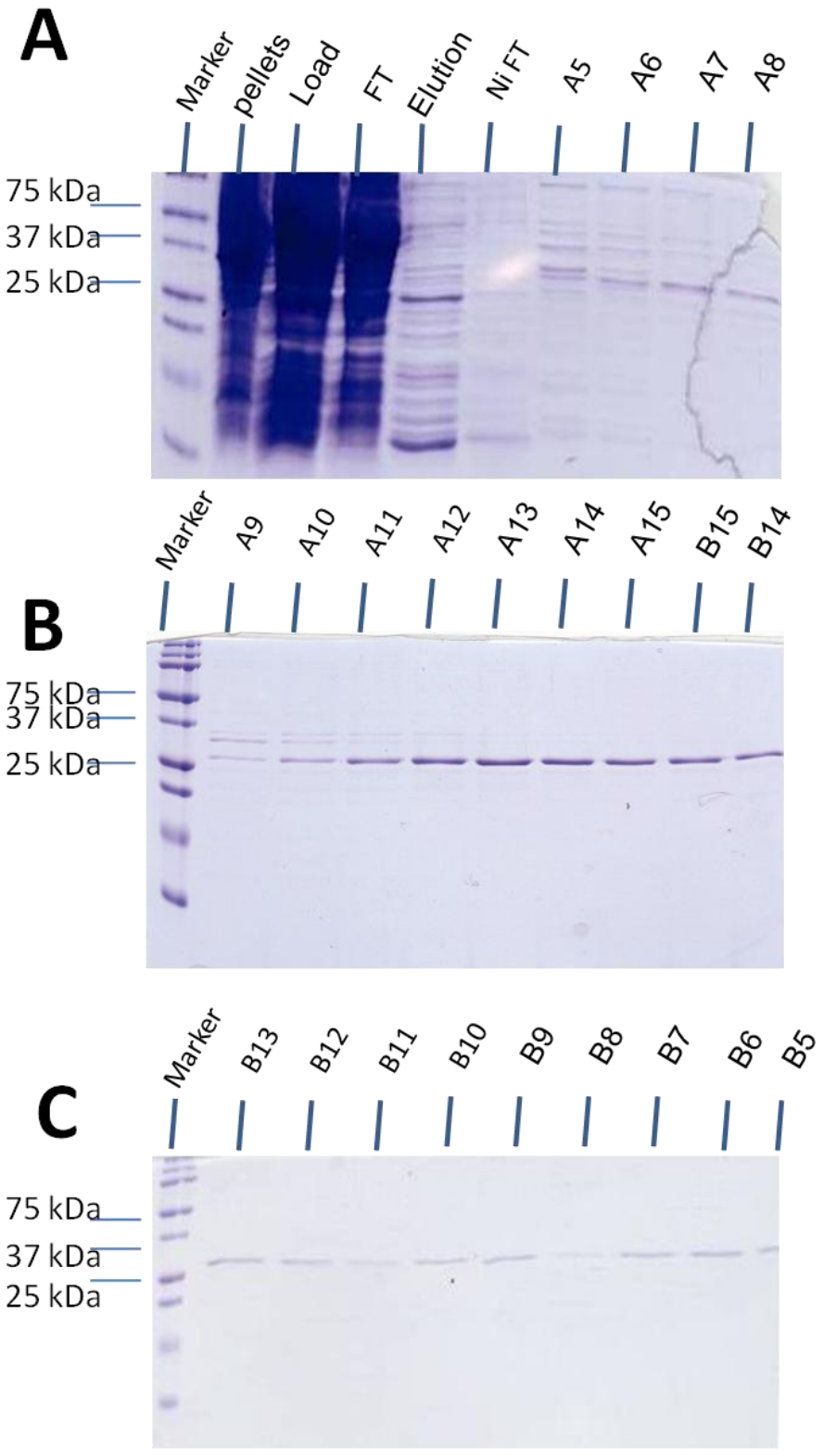
A
Marker
pellets
Load
FT
Elution
Ni FT
A5
A6
A7
A8
75 kDa
37 kDa
25 kDa
B
Marker
A9
A10
A11
A12
A13
A14
A15
B15
B14
75 kDa
37 kDa
25 kDa
C
Marker
B13
B12
B11
B10
B9
B8
B7
B6
B5
75 kDa
37 kDa
25 kDa

**Figure 3.7 Purification of FGF-9.**

A.Bacteria from a 2 L culture were broken by sonication and loaded on a 5 mL column of heparin agarose. B. The 2 M NaCl eluate from this column was diluted 4 times by 50 mM Tris.HCl, pH 7.5 and applied to a 1 mL HiTrap Ni column on an AKTA HPLC system (**Section 3.2.1**). Elution was monitored at 280 nm and peaks collected in 1 mL fractions. Fractions were analyzed by SDS-PAGE followed by Coomassie staining. The molecular weight of FGF-9 with its his tag is ~26 kDa. Pellets = insoluble material following cell breakage; Load = sample applied to heparin column; FT = flow through fraction; elution = NaCl elute; Ni flow though = flow through after loading on Ni column; A5-B5, fractions eluted from HiTrap Ni column. Fractions without other visible bands were concentrated and stored in -80$^{o}$C.

## 3.2.2.5 Expression and purification of FGF-18

FGF-18 was produced using the plasmid described in **Section 3.1.3.4** from a culture of 0.5 L (**Section 3.2.1.2**). The second flow through (after overnight digestion with TEV) from the Probond $Ni^{2+}$ resin column (**Section 3.2.1.5**) was diluted and loaded on to a HPLC HiTrap heparin affinity column (**Section 3.2.1.6**). Four fractions were collected (B11-B8) corresponding to the major protein peak (**Figure 3.8A**). FGF-18 clearly requires far higher concentrations of NaCl for elution from heparin than FGF-1, FGF-2 or FGF-9. SDS-PAGE shows that the most obvious band, of ~21 kDa was present in fractions B11-B8 (**Figure 3.8 B**). Measurement of the protein concentration by absorbance indicated that there was 0.3 mg protein in B10 and 0.2 mg in B9. These two fractions were stored as 100 µL aliquots in elution buffer at -80$^{o}$C.

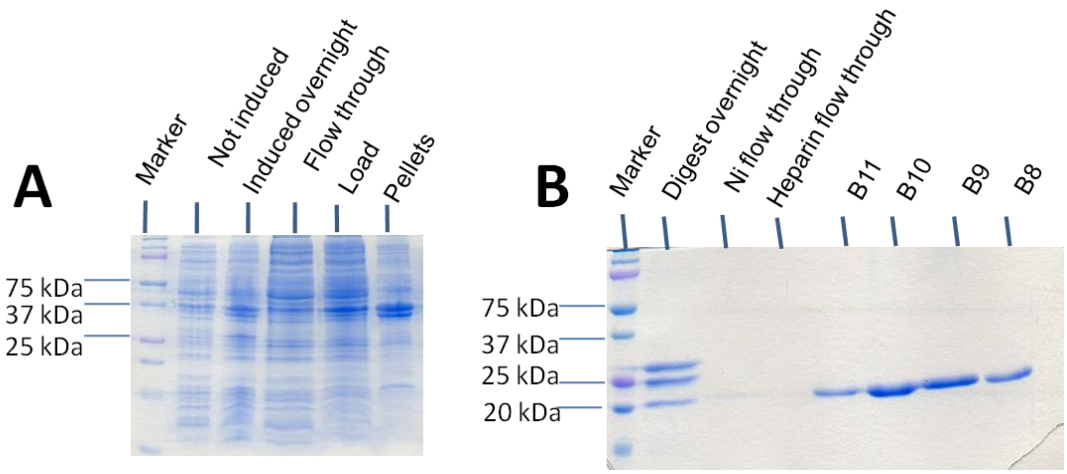


**Figure 3.8 Purification of FGF-18.**

A.Bacteria from a 2 L culture were broken by sonication and loaded on a 3 mL column of $Ni^{2+}$ agarose. B. The 0.5 M imidazole eluate from the $Ni^{2+}$ column was buffer-exchanged into 50 mM Tris-Cl, pH 7.5, 0.6 M NaCl and digested with TEV protease (**Section 2.6.4**). The digested proteins were applied again to the $Ni^{2+}$ column and the flow through was loaded to a 1 mL heparin column on an AKTA HPLC system (**Section 3.2.1**). Elution was monitored at 280 nm and peaks collected in 1 mL fractions. Fractions were analyzed by SDS-PAGE followed by comassie staining. The molecular weight of FGF-18 is ~21 kDa. Pellets = insoluble material following cell breakage; Load = sample applied to heparin column; FT = flow through fraction; elution = NaCl elute; digest overnight = product of TEV protease digest;Ni flow though = material not binding to Ni column after TEV digest; Heparin flow through = flow through after loading on heparin column; B11-B8, fractions eluted from HiTrap heparin column.

## 3.2.2.6 Expression and purification of FGF-21

### *3.2.2.6.1 Introduction*

The protein sample from cell breakage was purified on the $Ni^{2+}$ Resin and Q column, because this endocrine FGF does not bind strongly to heparin, and according to FGF-21's theoretical pI (5.78), it is acidic. So anion-ion exchange chromatography was used after Ni chelation to further purify FGF-21.

### *3.2.2.6.2 Purification*

FGF-21 was produced using an existing plasmid described in **Section 3.1.3.4** from a culture of 0.5 L (**Section 3.2.1.2**) The elute from the Probond $Ni^{2+}$ resin column (**Section 3.2.1.5**) was diluted and loaded on to a HPLC Q column 1 mL column (**Section 3.2.1.6)**. Eight fractions were collected (A10-B14) corresponding to the major protein peak. These fractions were analyzed by SDS-PAGE (**Figure 3.9B**). The result shows that the most obvious band, of ~25 kDa, was present in the fractions. Measurement of the protein concentration by absorbance indicated that there were 0.6 mg protein in A12, 1.06 mg in A13 and 0.91 mg in A14. These three fractions were stored in buffer B at -80$^{o}$C.

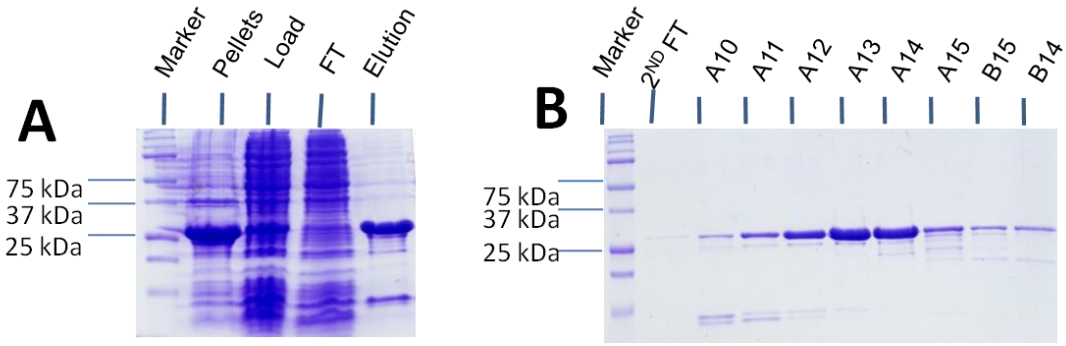


**Figure 3.9 Purification of FGF-21.**

A.Bacteria from a 0.5 L culture were broken by sonication and loaded on a 3 mL column of $Ni^{2+}$ agarose. B. The 0.5 M imidazole eluate from this column was buffer- exchanged into 50 mM Tris-Cl, pH 7.5 and applied to a 1 mL Q column on an AKTA HPLC system (**Section 3.2.1**). Elution was monitored at 280 nm and peaks collected in 1 mL fractions. Fractions were analyzed by SDS-PAGE followed by Comassie staining. The molecular weight FGF-21 with a his tag is ~25 kDa. Pellets = insoluble material following cell breakage; Load = sample applied to heparin column; FT = flow through fraction; Elution = NaCl elute; $2^{ND}$ FT = flow through after loading on Q column; A10-B14, fractions eluted from HiTrap heparin column.

### 3.2.3 Expression of other FGFs (FGF-3, FGF-5, FGF-16, FGF-17, FGF-19 & FGF-23)

FGF-19 and FGF-23 plasmids were transformed into different *E.coli* cells (C41, T1, RG (blue) and Rosetta) using different antibiotics, according to the requirement of the different cells] and protein was expressed from a culture of 0.1 L following the protocol used for FGF-1 (**Section 3.2.1.2**). Induction was at 37$^{o}$C for 3 h as for FGF-1 (**Section 3.2.1.2**). The products from 100 mL culture were then subjected to purification on $Ni^{2+}$ chelation columns. There was no evidence for elution of a protein corresponding to these FGFs. SDS-PAGE showed that there was a band of the correct size, but it was in the cell pellets, so these proteins are not soluble.

## 3.3 Different FGF stimulations of DNA synthesis on Rama 27 cells

### 3.3.1 Introduction

As growth factors, FGFs have been found to induce the stimulation of a number of intracellular signaling pathways that lead to cell division. In these experiments, cells were treated with 10 % (v/v) FCS as a positive control for the stimulation of DNA synthesis. The stimulation of DNA synthesis by six different FGFs (FGF-1, FGF-2, FGF-7, FGF-9, FGF-18 and FGF-21) with and without heparin was tested in Rama 27 fibroblast cells.

### 3.3.2 Results

Different concentrations of six FGFs were added to quiescent Rama 27 cells to determine and compare the dependence of DNA synthesis on the growth factors (**Section 2.8**).

In the case of FGF-1, an increase of DNA synthesis occurred between concentrations 1 to 30 ng/mL (**Fig. 3.10A**). When 5 µg/mL heparin was present, the FGF-1 starts stimulation at a lower concentration (0.1 ng/ml), since a stimulation of DNA synthesis reached a maximum

at 3 ng/mL (**Figs 3.10A**). This is in accord with previous results, which showed that heparin can stabilize FGF-1 and increase its activity in such assays [108-110].

For FGF-2, an increase of the stimulation started at 0.1 ng/mL, so similar to FGF-1 in the presence of heparin (**Fig. 3.10B**) and reached a maximum at 1 ng/mL.

For FGF-9, an increase of the stimulation was apparent from 15.4 ng/mL (**Fig.3.11A**) and continued increase up to 15,400 ng/mL. Heparin (5 μg/mL) had no effect on the stimulation of DNA synthesis by FGF-9 in these cells (**Figs 3.11A**).

FGF-18 has an effect on DNA synthesis only between the concentrations of 140 ng/mL to 1,400 ng/mL (**Fig.3.11B**). In contrast, when heparin was present, the stimulation of DNA synthesis started from a lower concentration, 14 ng/mL, and reached a maximum at 1,400 ng/mL (**Figs 3.11B**).

For FGF-7 and FGF-21, there was no measurable change induced by these FGFs (FGF-7: 27300 ng/mL, FGF-21: 12000 ng/mL) (**Fig.3.12**) and no effect of heparin.

Taken together, different FGFs have different stimulation on Roma 27 cells. FGF-2 starts to have signal at lower levels compared to other FGFs. Heparin (5 μg/mL) increases the potency of FGF-1 to stimulate DNA synthesis from a lower level than FGF-1 itself, and heparin also help with FGF-18 to stimulate the cells from a lower level, but heparin had no such effect on FGF-18.

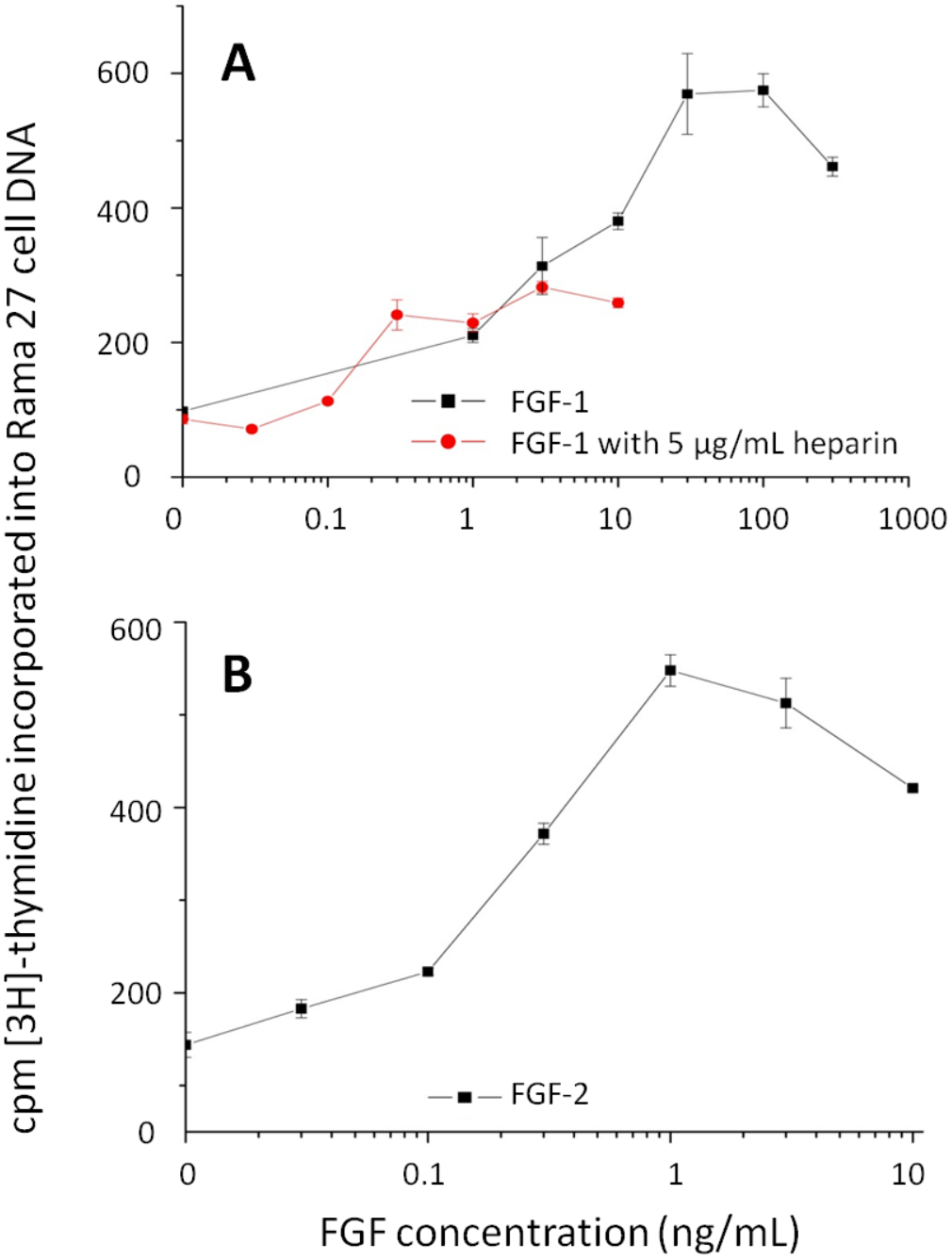


**Figure 3.10 Concentration dependence of the stimulation of DNA synthesis in Rama 27 cells by FGF-1 and FGF-2.**

The experiment was carried out as described in Method 2.8. A. FGF-1 with and without 5 µg/mL heparin. B. FGF-2. Results are expressed as the mean cmp±SD of triplicate samples.

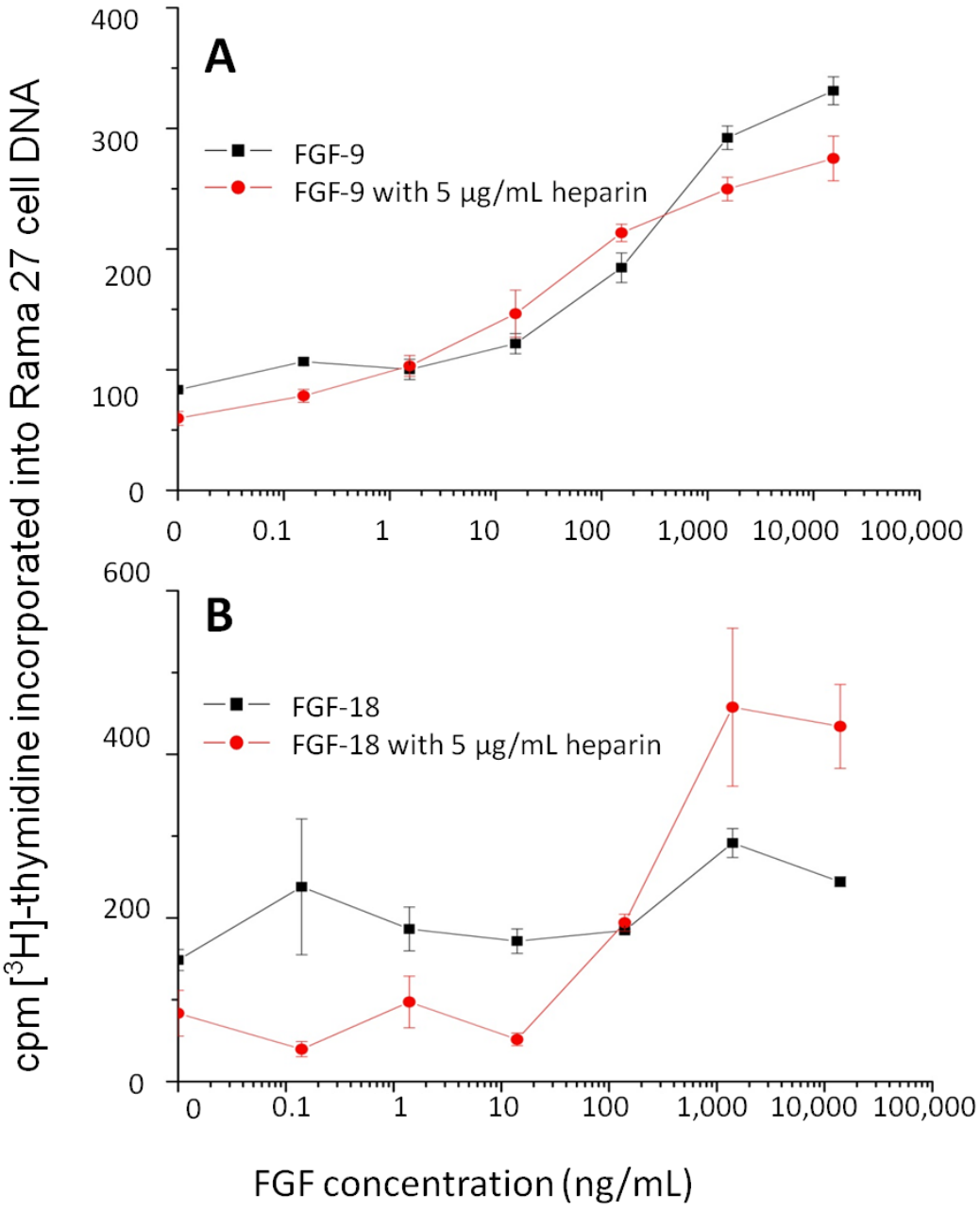


**Figure 3.11 Concentration dependence of the stimulation of DNA synthesis in Rama 27 cells by FGF-9 and FGF-18.**

The experiment was carried out as described in **Section 2.8**. A. FGF-1 with and without 5 µg/mL heparin. B. FGF-2. Results are expressed as the mean cmp±SD of triplicate samples.

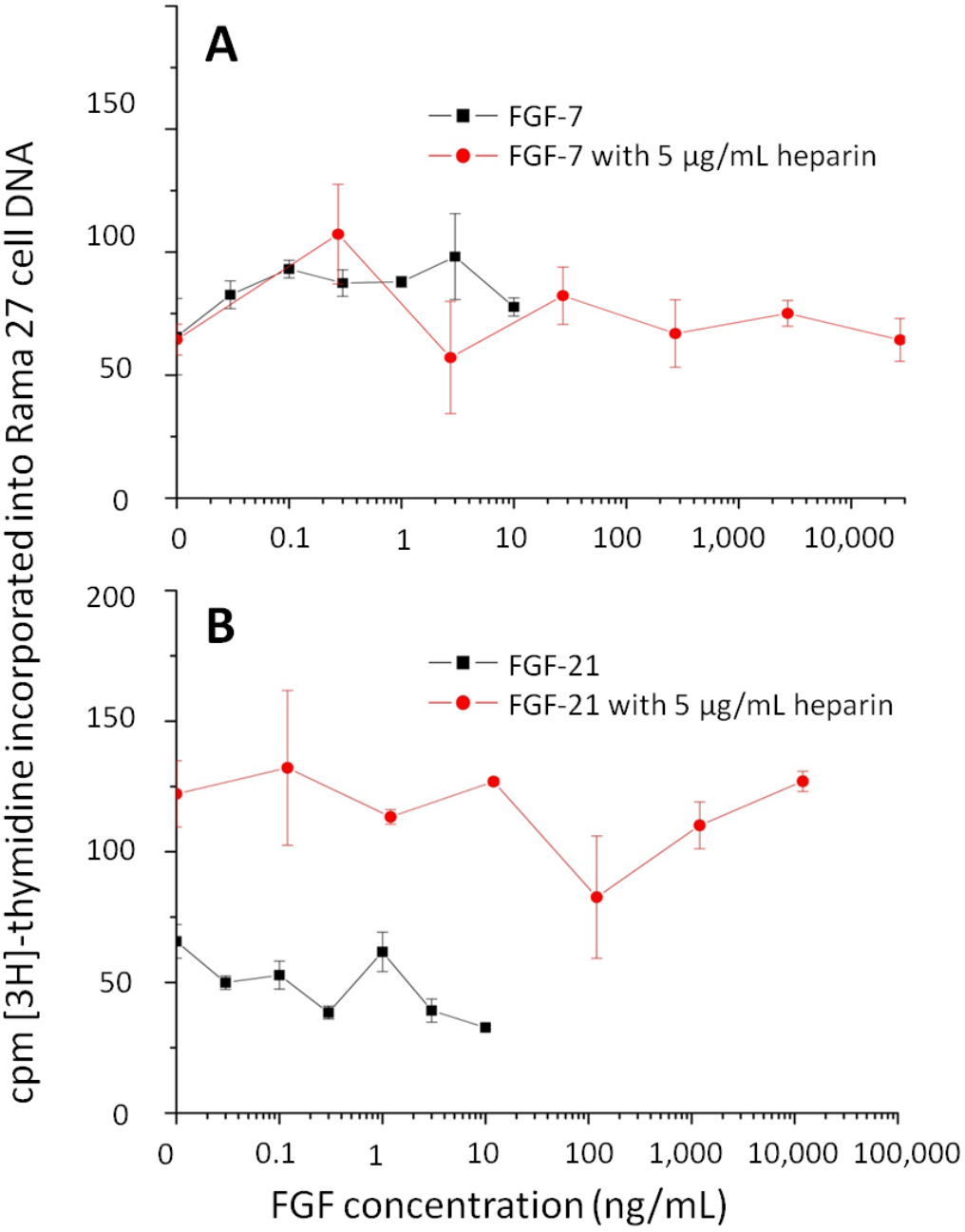


**Figure 3.12 The stimulation of DNA synthesis in Rama 27 cells by FGF-7 and FGF-21.** The experiment was carried out as described in **Section 2.8**. A. FGF-1 with and without 5 µg/mL heparin. B. FGF-2. Results are expressed as the mean cmp±SD of triplicate samples.

## 3.3.3 Discussion

The DNA synthesis experiment was used to test the activity of six recombinant FGFs (FGF-1, FGF-2, FGF-7, FGF-18 and FGF-21) in Rama 27 cells. Rama 27 cells are fibroblasts and

have been shown by PCR to express FGFR1c as the two and three Ig loop isoforms [96]; (Chen and Fernig, unpublished). They are, therefore, typical of a stromal cell in this respect. The dose-dependence of FGF-2, which started to stimulate the cells' DNA synthesis at 0.1 ng/mL and reached the maximal level at 1 ng/mL, is in agreement with previous results on these cells obtained with natural FGF-2, purified from cow pituitary [111]. The lower potency of FGF-1 is also in agreement with previous results with these cells [108]. Moreover, the increased potency of FGF-1 observed in the presence of heparin has been noted for many years [108-110]. Though both FGF-9 and FGF-18 stimulated DNA synthesis in these cells, they were far less potent compared to FGF-1 and FGF-2. At a concentration of 3 ng/mL, stimulation of incorporation of [$^3$H] thymidine into DNA synthesis of FGF-1 reached its 50 % effective dose (ED50), which is 12 times higher than that needed by FGF-2 (ED50: 0.25 ng/mL). FGF-18 reached a half maximum (ED50) at a concentration of 220 ng/mL, which is about 70-fold above that of FGF-1. In contrast, the stimulation of DNA synthesis by FGF-9 was still increasing at 15.4 µg/mL, which is 500-fold more than the concentration of FGF-1 required for maximal DNA synthesis. The reason for the considerable lower potency of FGF-9 and of FGF-18 may be related to the weak activity of these two FGFs with FGFR1c compared to the FGF-1 sub-family [46], because the R27 cells only have the FGFR1c.

The lack of activity of FGF-7 is not surprising, since this FGF is uniquely specific for epithelial cells, which express the FGFR2c splice variant. mRNA encoding FGFR2c is not detected in stromal cells such as Rama 27 fibroblasts (Chen and Fernig, unpublished). For FGF-21, a previous study showed that FGF-21 only has weak FGFR stimulatory activity [46] and it is a hormone, regulating glucose metabolism, so that it is not surprising that it does not detectably stimulate DNA synthesis.

## 3.4 Discussion

Recombinant FGFs (FGF-1, FGF-2, FGF-7, FGF-9, FGF-18 and FGF-21) were expressed using *E. coli* system, and purified by affinity chromatography and ion-exchange chromatography, ~ 1 to 10 mg pure proteins (no substantial contaminants or SDS-PAGE) were achieved (according to concentration measurement) for each FGF. That these FGFs are correctly folded is indicated by the observation that they bind heparin (all except FGF-21) and that all the FGFs were able to activate FGFR1c in DNA synthesis assays. Thus, good coverage of the FGF sub-families that are extracellular (**Figure 1.1**) was achieved, with at least one FGF ligand produced from FGF sub-families 1, 7, 8, 9 and 19, and only a representative from sub-family FGF-4 missing

# Chapter 4 Diversification of the structural determinants of FGF-heparin interactions

## 4.1 Introduction

It is a major question whether there are specificities in the interactions between HS/heparin and FGFs. It is accepted that HS/heparin are essential for FGF ligands to engage the FGFR and generate signals that lead to cell division. *In vivo* it is also clear that the polysaccharide is critical for FGF signaling activity in development (**Section 1.8**). There is evidence that shows that the FGF:HS:FGFR interactions require specific structures in the sugar [91, 112]. However, the details of such specificity are not clear. Thus, DP8 has been shown to be the minimal length of heparin sugars to allow FGF-1 and FGF-2 to bind FGFR1 or FGFR2 and 6-O-sulfate was similarly shown to be essential to allow receptor dimerization [93]. However, other studies have shown that smaller oligosaccharides are effective for FGF-2 [57]. Finally, a series of studies suggest that the binary FGF:heparin interactions are very promiscuous and failed to identify any real specificities [97-99]. According to this view different FGFs bind to HS-derived oligosaccharides with similar relative affinities and low selectivity, such that the strength of these interactions increases largely due to the overall level of sulfation rather than other characteristics [97] and that different members of the FGF family share the same binding sites on the HS chains [98, 99]. One weakness of this previous body of work is that it is piecemeal; interactions are often measured qualitatively and, in many instances, in a format in which ionic bonding will predominate. The problems associated with measuring protein-heparin interactions were reviewed some eight years ago [27].

To try to resolve the question of specificity, this study has focused on using several complementary methods to study the interactions of FGFs with heparin and allied molecules. In addition, by using a panel of FGFs from different sub-families, any constraints on specificity related to the evolution of the FGF family should also become apparent.

Consequently, several methods were applied to characterize the interaction of the panel of FGFs with heparin.

***MST and optical biosensor***-: two methods which were used to quantify the binding kinetics and/or affinity of FGFs to an octasaccharide derived from heparin. These techniques, by measuring fundamental physical parameters, are not prone to biases of interpretation associated with qualitative methods used in some other studies.

***Protect & Label***-: a strategy used to identify the binding sites in FGFs of heparin. This would provide a "mirror" to the work on sugars; differences in binding sites in the proteins might be reflected in some way in differences in binding specificity and/or affinity.

***SRCD***-: a method which measures the secondary structure of FGFs and their sugar complexes, to test whether there are conformational changes in FGF ligands after binding to heparin.

***DSF***-: measures the thermal stabilizing effect on FGF ligands when they bind to heparin. Since DSF is a solution technique of high throughput, the interactions of FGFs with a library of sugars could be determined. This allowed questions of specificity relating to the length of sugar binding site, sulfation patterns and cation forms of heparin to be measured.

The results of this work have been submitted for publication at the Journal of Biological Chemistry and the manuscript is appended below.

## 4.2 Paper

This text box is where the unabridged thesis included the following third party copyrighted material:

**Xu, R.**, Ori, A., Rudd, T.R., Uniewicz, K.A.,Ahmed, Y.A., Guimond, S.E., Skidmore, M.A., Siligardi, G., Yates, E.A. and Fernig, D.G. (2012) Diversification of the structural determinants of fibroblast growth factor-heparin interactions; implications for binding specificity. J. Biol. Chem. 287:40061-40073.

http://www.jbc.org/content/287/47/40061.long

Contributions of the authors

Xu, R.: Production of FGF proteins, DSF, Protect and Label, SRCD and biosensor measurements. co-wrote the paper.

Ori, A.: Mass spectrometry of biotinylated peptides. Edited paper.

Rudd, T.R.: PCA. Edited paper.

Uniewicz, K.A.: Some DSF experiments (repeated by RX) and help with cloning of FGF-18 and protect and label experments. Edited paper.

Ahmed, Y.A.: Oligosaccharides of DP2 to DP12. Edited paper.

Guimond, S.E.: Assisted with SRCD experiments. Edited paper.

Skidmore, M.A.: Assisted with SRCD experiments. Edited paper.

Siligardi, G.: SRCD beamline manager, assisted with SRCD experiments and their interpretation. Edited paper.

Yates, E.A.: Provided heparin derivatives, conceived study and co-wrote the paper.

Fernig, D.G.: Conceived study and co-wrote the paper.

# 4.3 DSF

## 4.3.1 DSF and heparin-dependent thermostabilizing effects on FGFs

DSF was used to determine the melting temperature of six different FGFs (FGF-1, FGF-2, FGF-7, FGF-9, FGF-18 and FGF-21) and their sugar complexes. The FGF-1, FGF-2 and FGF-18 data shown below are repeat experiments of the previous publication [102], and the FGF-7, FGF-9 and FGF-21 data are from the paper above. The ligand melting temperatures were sharp, indicating that these FGFs were properly folded and spanned 12$^{o}$C (**Figures 4.1-4.3; Figure 7 and Figures S11-13 in Section 4.2**), suggesting that the different FGFs have different rigidities and thermal stabilities. A concentration range from 0.05 µM to 500 µM of heparin with these six FGFs was also measured by DSF. The addition of heparin caused an increase in melting temperature in all the FGFs, except for FGF-21 (**Figures 4.1-4.3; Figure 7 and Figures S11-13 in Section 4.2**).

The effect of heparin on FGF-1, FGF-2 and FGF-18 agreed with a previous study [102], in which heparin has a concentration dependent effect on the melting temperature of these FGFs. FGF-1 $T_M$ increased about 7 degrees in the presence of 1.25 µM heparin, which then increased another 14 degrees as the concentration of heparin increased to 500 µM (**Figure 4.1**). When heparin was added to 5 µM FGF-2, the melting temperature of FGF-2 increased in a dose–dependent manner (**Figure 4.2**). The $T_M$ of FGF-2 also started increasing from 1.25 µM heparin, and reached the highest level at 25 µM heparin, to 80$^{o}$C. Like FGF-1, the $T_M$ of FGF-7 also started increasing with 1.25 µM heparin and quickly reached a maximum at 5 µM heparin. In contrast, FGF-7 was stabilized to a lower extent than FGF-1 and FGF-2, since when it bound heparin there was only a 7$^{o}$C increase in melting temperature. Maximum stabilization was achieved at relatively low concentrations of heparin (5 µM). In contrast, the $T_M$ of FGF-9 started increasing at a lower heparin concentration (0.05 µM), and continued to increase until 2.5 µM (**Figure S11 in Section 4.2**). FGF-18 was progressively stabilized

from the lowest concentration of heparin and maximum stabilization had not been reached at 500 µM heparin (**Figure 4.3**).

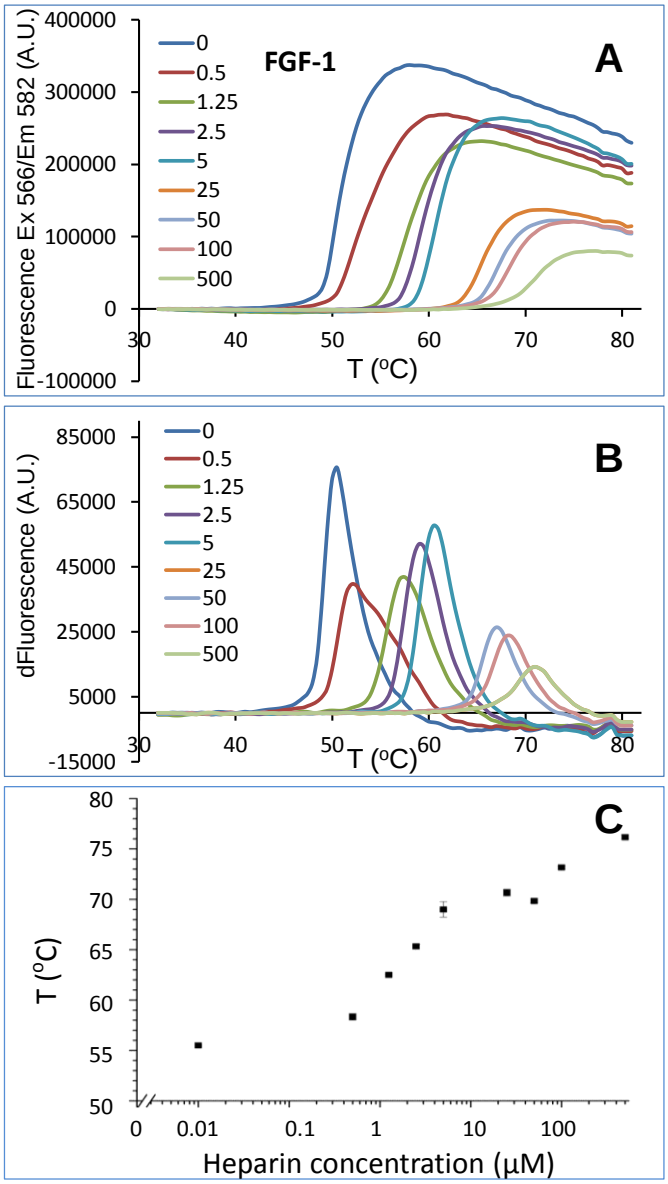


**Figure 4.1 Stabilization effect of heparin on FGF-1.**

Differential scanning fluorimetry of 5 µM FGF-1 in the presence of different concentrations of heparin (**Section 2.9**): A, Melting curve profiles of FGF-1 (5 µM) with a range of heparin concentrations (0 µM-500 µM). B, The first derivative of the melting curves in (A). C, Peak of the first derivative of the melting curves from (B), which is the melting temperature, $T_M$ (mean of triplicates +/- SE).

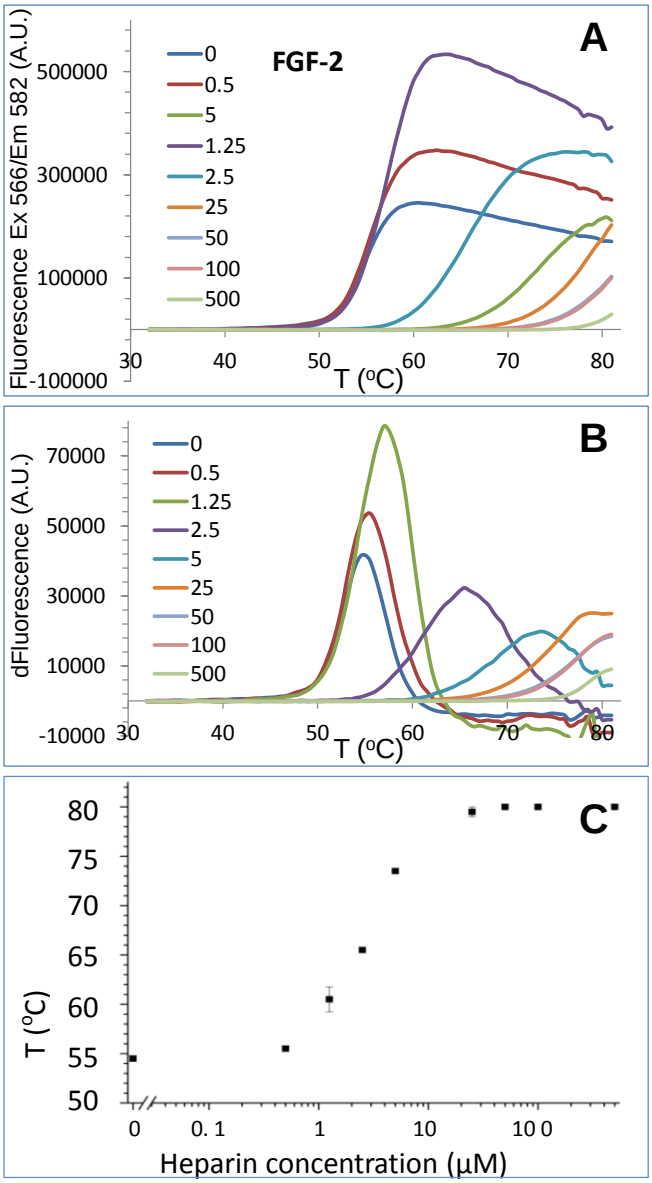


**Figure 4.2 Stabilization effect of heparin on FGF-2.**

Differential scanning fluorimetry of 5 µM FGF-2 in the presence of different concentrations of heparin (**Section 2.9**): A, Melting curve profiles of FGF-2 (5 µM) with a range of heparin concentrations (0 µM-500 µM). B, The first derivative of the melting curves in (A). C, Peak of the first derivative of the melting curves from (B), which is the melting temperature, $T_M$ (mean of triplicates +/- SE).

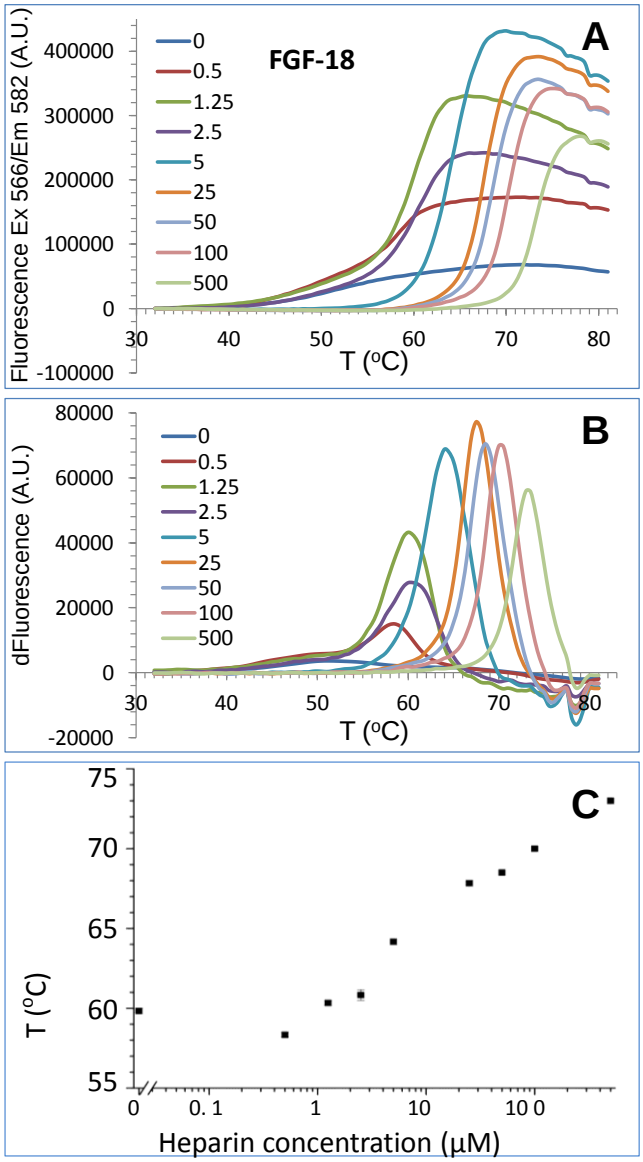


**Figure 4.3 Stabilization effect of heparin on FGF-18.**

Differential scanning fluorimetry of 10 µM FGF-18 in the presence of different concentrations of heparin (**Section 2.9**): A, Melting curve profiles of FGF-18 (10 µM) with a range of heparin concentrations (0 µM-500 µM). B, The first derivative of the melting curves in (A). C, Peak of the first derivative of the melting curves from (B), which is the melting temperature, $T_M$ (mean of triplicates +/- SE).

## 4.3.2 Characterization of the thermo stabilizing effect of different polysaccharides on FGFs

A heparin library of sugars was tested against a fixed concentration (5 µM or 10 µM) of 5 FGFs (FGF-1, FGF-2, FGF-7, FGF-9 and FGF-18), which belong to 4 different sub-families (FGF-1 sub-family, FGF-7 sub-family, FGF-9 sub-family and FGF-8 sub-family) to identity the variety of the sugars binding to FGFs (**Fig. 4.4**).

To understand the different binding effect of different sulfation pattern of heparin, D1-D9 were tested against these 5 different FGFs (**Fig. 4.4A**). FGF-1 was sensitive to the loss of any sulfate group, though it appeared to have a preference for 2S over the two O-sulfates. Loss of two or more sulfates caused a loss of interaction. With singly desulfated heparins, FGF-2 clearly required 2S and NS, but not 6S for strong binding. Loss of two or more sulfates abrogated binding. This is quite similar to FGF-1. FGF-7 appeared to bind derivatives equally well with any pair of sulfates, losing about 20-30 % of heparin binding affinity, but less than two sulfates reduced binding appreciably. With loss of any one sulfate, FGF-9 lost about 50 % binding affinity compared to intact to heparin. Loss of 2 or more sulfates reduced binding to just 10-20 % of the original level. For FGF-18, somewhat lower binding was achieved with any two sulfates. Losing two sulfates decreased heparin binding further and 2S alone was less effective than either 6S or NS.

To understand the different binding effect of length heparin, oligosaccharides from DP2 to DP12 were tested against these 5 different FGFs (**Fig. 4.4B**). FGF-1 had a weak interaction with DP2 and this progressively increased to reach a maximum with DP8. Analysis of data acquired with heparin oligosaccharides of different lengths showed that DP2 did not bind FGF-2, whereas DP4 bound and further increasing the oligosaccharide length to DP12 resulted in a progressive increase in the thermal stability of FGF-2. FGF-7 bound DP4 and it was maximally stabilized by DP8, which had about 50 % of the stabilization effect of

heparin. In contrast, FGF-9 started binding from DP4, but required longer oligosaccharides, DP10 achieving the maximum effect. FGF-18 bound DP2, but its thermal stability was enhanced by larger structures up to DP12. Other GAGs (HS, HA, CS and DS were also tested (**Fig. 4.4C**). HS has a similar effect on FGF-1, FGF-2 and FGF-7, which is only half of the binding affinity compared to heparin. FGF-9 and FGF-18 are similar, only about 30 % of heparin binding. Only FGF-18 had 20 % binding to HA, others did not bind. FGF-2 failed to interact with CS or DS, whereas the other FGFs showed possible weak interaction with CS and a weak, but significant, interaction with DS.

Cation modified heparins ($Na^+$, $K^+$, $Ca^{2+}$, $Cu^{2+}$ and $Zn^{2+}$) were also tested with these five FGFs (**Fig. 3.19D**). Different cationic forms bind FGF-1 differently, $Na^+$, $K^+$ and $Ca^{2+}$ had similar effects on binding, which reduced binding slightly, to ~ 80 % of the level observed with heparin. In contrast, FGF-1 bound very poorly to the $Zn^{2+}$ form of heparin. In the presence of $Cu^{2+}$ heparin, no melting curve was apparent, suggesting that FGF-1 cannot interact with this form of heparin. In contrast, these five cationic forms of heparin all bound FGF-2 similarly, causing a small (10 %) increase in stabilization compared to native heparin. FGF-7 binding was reduced by all the cationic forms of heparin compared to that observed with native heparin; by ~30 % with $Na^+$, $K^+$, $Ca^{2+}$ and $Zn^{2+}$ heparin and by 80 % with $Cu^{2+}$ heparin. In contrast, the different cationic forms of heparin all bound FGF-9 equally, causing a 30 % reduction in thermal stabilization. FGF-18 binds better to the $Zn^{2+}$ form of heparin than to heparin itself. However, the $Na^+$ form heparin only has half the affinity when bound to FGF-18 compared to heparin, and the other three cationic forms of heparin have similar effects on FGF-18 binding, causing a 10-20 % decrease in thermal stabilization.

Most of the data here for FGF-1, FGF-2 and FGF-18 are in agreement with a previous study, except that FGF-18 was previously observed to start binding from DP6 [102]. However, the data in previous publication are quite noisy for DP2 and DP4, and it is possible that weak binding to these smaller oligosaccharides may have been obscured.

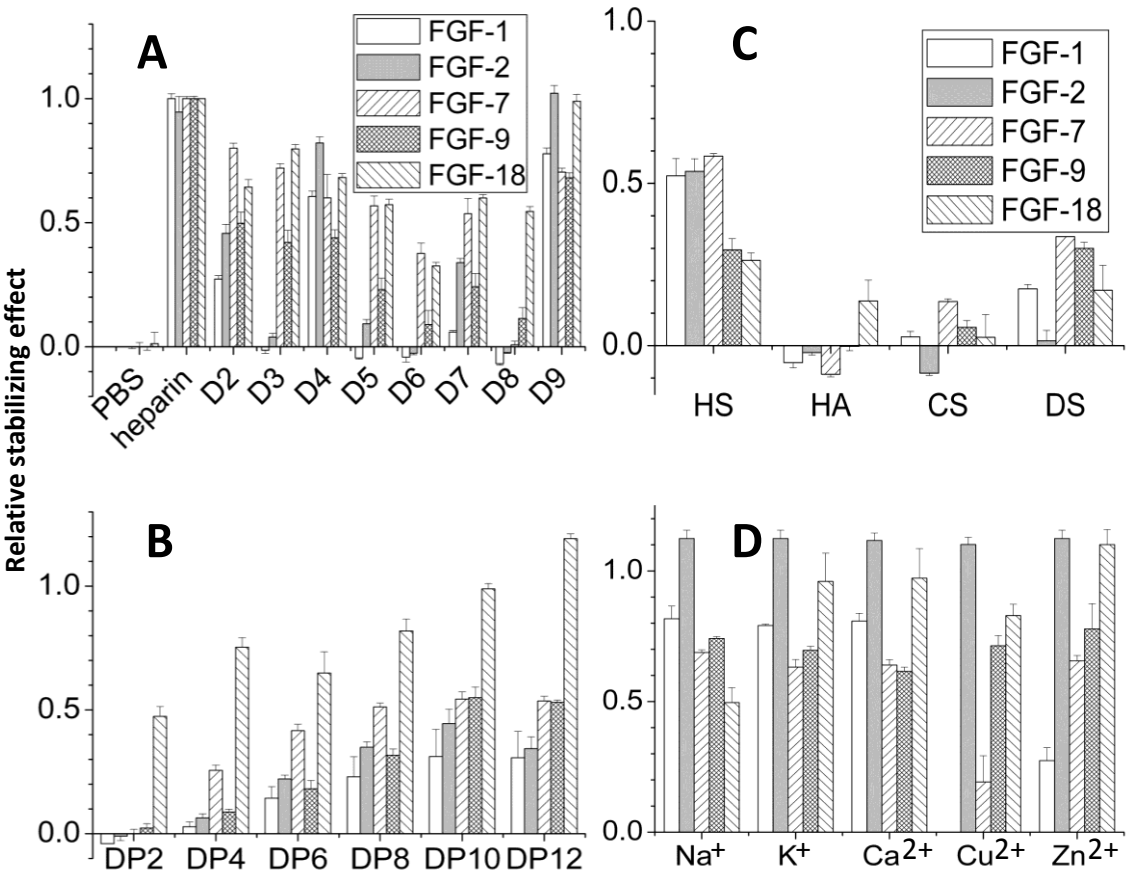


**Figure 4.4 Differential scanning fluorimetry analysis of heparin derivatives on FGF-7 and FGF-9 reveals distinct dependency on substitution pattern.**

Differential scanning fluorimetry was performed with a range of heparin-based poly- and oligosaccharides with 5 µM protein and 175 µg/mL sugar. The relative thermal stabilization effect of: A. Controls (PBS and heparin), chemically modified heparins (D2-D9). B. Heparin-derived oligosaccharides, ranging from DP2-12. C. Other GAGs (HS, HA, CS and DS). D. Cation modified heparin forms [113]. Results are the mean of triplicates after normalisation +/- SE, an apparent absence of error bar is due to a small SE).

## 4.4 Discussion

The specificities of FGF-heparin interactions are clearly revealed by all these methods: kinetic parameters and affinity measurements clearly showed differences in binding; Protect and Label showed that the binding for the polysaccharide in the FGFs employs different combinations of amino acids at the different positions on the surfaces of the FGFs; SRCD data showed that FGFs have different conformational changes when bound to heparin; DSF screening against sugar libraries results showed that they have different binding selectivity to the sugar chains and sulfation patterns. However, the specificity does not correspond to a high fidelity 1:1 binding. Instead, FGFs have preferences, but can recognize a wide range of sites in the sugar.

### 4.4.1 Multiple specificities

***DSF and principle component analysis (PCA)***:- The PCA was carried out by Dr Tim Rudd, DSF analysis of binding of the six FGFs (FGF-1, FGF-2, FGF-7, FGF-9, FGF-18 and FGF-21) to the sugar library clearly showed that there are binding preferences between FGFs and heparin. However, the relationships were complex, so a PCA was used to identify the main components contributing to the specificity of interaction. The PCA clearly shows that the FGFs are different, but does not identify a single component, e.g., N-sulfation. This highlights that specificity of interaction is due to the interaction of a number of contributing elements, e.g., sulfation pattern, length, which are not necessarily separable.

Thus, the binding specificities of FGFs to heparin/HS exhibit multiple specificities, which means the binding does not only rely on one structure pattern, but instead is much more reliant on the whole structure. The current analysis can only report on the sequence of saccharides, rather than their conformation, but the two are interdependent. Thus, though not tested here, this points to specificity relying on the solution conformation of the sugar chains.

### 4.4.2 Heparin binding sites overlapped with FGFR binding sites

FGF mediate their bioactivities by binding to their cell surface receptors FGFR and HS to form a signaling complex. It seems likely that *in vivo* FGF binds first to HS first then to the FGFR, since HS binding sites are several orders of magnitude more abundant in the pericellular matrix and cell surface (Duchesne *et al.* 2012) [114]. According to the present results there are different numbers of HBSs found in these 4 FGF sub-families. A question is of interest is whether there is any overlap between these and the FGFR binding sites.

FGF-2 has 3 heparin binding sites [49, 75, 88, 115, 116], and the residues interacting with the FGFR have been identified by site-directed mutagenesis [50] and by X-ray crystallography (FGF-2-FGFR1, PDB: 1CVS) [51]. A comparison of these binding sites indicates that HBS-3 at the N-terminus overlaps with the FGFR binding site at position K30.

As well as FGF-2, others FGFs also have residues involved in both interactions. According to the Protect and Label results and crystal structures of heparin-FGF-1-FGFR2 (PDB: 1E0O) [53], in FGF-1, K24 in HBS-3 overlaps with the FGFR binding site. K24 in FGF-1, which is located at N-terminus of the protein, is at the equivalent position as K30 of FGF-2 when the secondary structures of these proteins are aligned (**Figure 2A in Section 4.2**).

According to the sequence alignment of FGF-7 (**Figure 2B in Section 4.2**), there might be a HBS-3 at the N-terminus, but because this only contains arginines, which cannot be identified by Protect and Label it was not identified here. Interestingly, R65 in the putative FGF-7 HBS-3 is also a part of its FGFR [117]. Moreover, by using the sequence alignment of the FGF-7 subfamily and the FGF-10-FGFR2b crystal structure (PDB: 1NUN) [23], R78 of FGF-10, which is at the equivalent position as R65 in FGF-7 might be part of a HBS-3 (**Figure 2C in Section 4.2**) and is involved in binding to FGFR.

The HBSs of FGF-8 were predicted by the sequence alignment of the FGF-8 subfamily (**Figure 2D in Section 4.2**), while the FGFR binding sites for this FGF was reported in the FGF-8b-FGFR2c crystal structure (PDB: 2FDB) [24]. There are two positions of HBS-2

that overlap with the FGFR binding site, one is between beta strand 12 and the C-terminus ($^{196-}$KRLPR$^{-200}$), the other one is R27, which is at the same position as the HBS-3 of FGF-2 (**Figure  in Section 4.2**).

HBS-1 is of higher affinity that HBS-3, in the only instance where this has been measured [115]. However, on a cell, the concentration of HS binding sites is high. Moreover, at least for FGF-2, though it may dissociate locally from cellular HS, it rebinds very rapidly, such that it does not, in a cell culture, dissociate in the bulk culture medium. Thus, all the HBS of and FGF are likely, at some point, to interact with HS on the cells surface. Given that the HBSs seem to be conserved within FGF subfamilies, they seem likely to have a collective role that has been selected for in the course of evolution. This points to a role for the overlap of the HBS-3 of these five FGFs with their FGFR binding site. HBS-3 may have a role in transferring the binding in the FGF signaling complex: in which HS engaged to the HBS-3 of the FGF, guides the HBS-3 of the FGF binding to FGFR. Due to the weaker binding of HBS-3, this may help the transfer. The part of HBS-2 of FGF-8, which is located between beta 12 and C-terminal is merged together with HBS-3 in the 3-D structure of the protein and so may also have a similar effect as HBS-3.

# Chapter 5 SRCD: Circular dichroism spectroscopy reveals distinct secondary structures among FGF sub-family members.

## 5.1 Introduction

To determine the secondary structural changes of six different FGFs when binding to heparin, the purpose built SRCD beamline B-23 at the Diamond Synchrotron was used. Circular dichroism (CD) is a method which is widely used for examining protein secondary structure characteristics and protein-protein interactions [115-117]. CD is a spectroscopic method that measures the differential absorption of left and right circularly polarized light by chiral molecules. In the case of proteins, CD is very sensitive method for the detection of secondary structures [118, 119].

Owing to characteristic geometry, each protein secondary structure type has a characteristic CD spectrum, e.g., the typical α-helix spectrum contains a large positive peak at ~192 nm, another positive peak of roughly half of the magnitude at around 208 nm, and a negative peak at ~222 nm. For β-sheet, there is a negative peak at ~198, which is about half of the helix magnitude, and a small negative peak at ~215 nm. Turns and disorders structure do not have specific spectral features.

The dextrorotary and levorotary components within protein structures will give different absorptions. The amide group of the peptide chain is the most consequential chromophore of proteins [118]. The far UV region of a CD spectrum (180-260 nm) is related to the peptide backbone chromophore transitions ($n \rightarrow \pi^*$ and $\pi \rightarrow \pi^*$).

Because of the position and intensity of all these transitions, it causes different secondary structures of proteins giving rise to different far-UV spectra, e.g. the negative peak at ~222 nm of α-helix and the one of β-sheet at ~215 are the $n \rightarrow \pi^*$ transition; the positive peaks of

α-helix at ~192 nm and ~208 nm and the negative peak of β-sheet at ~198 are caused by $\pi \rightarrow \pi^*$ transitions [118, 119].

Then, by analyzing the CD spectra, it is possible to estimate the secondary structures (α-helices, β-sheets, turns and disorders) for each protein. SRCD provides intense synchrotron light, with $10^3$-$10^4$ fold greater photon flux than normal CD. Also, the heparin itself were measured by SRCD, it only have a very little signals, which is because of heparin chains are loose helix structure [120], which would not give a strong signal.

## 5.2 Methods

Six different FGFs (FGF-1, FGF-2, FGF-7, FGF-9, FGF-18 and FGF-21) at concentration of 0.5 mg/ml (FGF-1, FGF-2, FGF-7, FGF-18 and FGF-21) or 1 mg/mL (FGF-9) and their heparin complexes at different molar ratios at 1:5, 1:1 and 5:1 (heparin: FGF, w/w) were measured by SRCD (**Section 2.12**). Also, different FGFs were tested with several different chemically modified heparins at 1:1 molar ratio: FGF-1 with D8, FGF-2 with D4 or D6, FGF-7 with D2 or D8, FGF-9 with D7 and FGF-18 with D6.

## 5.3 Results

SRCD was used explore the structural changes of FGFs and their sugar complexes. The SRCD spectra of the protein constructs of six FGFs and their heparin complexes were collected under the same conditions (**Figure 5.1**) (**Section 2.12**) and the spectra were analysed using SELCON3 and Database 3 (**Section 2.12**). FGFs and their 5:1 (heparin: FGF) complexes were used for the work in the publication (**Chapter 4**). The spectrum of FGF-18 exhibited significant changes when heparin was introduced, while FGF-1, FGF-2 and FGF-7 also showed some visible changes (**Figure 5.1 A-D and Table 5.1-5.4**). The spectra of FGF-1 showed that, as more heparin was introduced, the signals of FGF-1 became more linear, however, the FGF-9 spectra became less flat. In contrast, the spectra of other FGF heparin

complexes were not concentration dependent **(Figure 5.1)**. According to analysis using SELCON 3, when 1:5 or 5:1 (F:H) molar ratios of heparin were added to FGF-1, the spectrum exhibited more α-helix, while, for a 1:1 (F:H) molar ratio of heparin, the spectra were more disordered (**Table 5.1**). As more heparin was added to FGF-2 and FGF-18, the signal progressively increased until a protein sugar ratio of 1:1, where the spectra are quite similar to those of the protein alone (**Figure 5.1B and E, Table 5.1 and 5.5**). With a 5:1 (F:H) molar ratio, FGF-7 started to exhibit more helix, whereas, when the molar ratio changed to 1:1 (F:H), the FGF-7 spectrum changed from α-helix to β, and when heparin levels continued to increase to a 1:5 (F:H) ratio, the structure returned to resemble as FGF-7 itself (**Figure 5.1 C, Table 5.3**). Taken together, there was not a simple trend of structural changes when the heparin concentration increased in the system. However, the spectrum of FGF-9 was only partly affected; the changes only started with higher concentrations at molar ratio 1:5 (F:H) (**Figure 5.1 D and Table 5.4**) and FGF-21 was largely unaffected (**Figure 5.1 F and Table 5.6**). The small change seen with FGF-21 agrees with previous studies, confirming that FGF-21 binds to heparin only weakly, and is further corroborated by the lack of change in the DSF data (**Figure 5.1F**).

Almost no change in the FGF-21 spectrum before or after the addition of heparin showed that heparin had almost no effect on the absorbance, indicating that this method is suitable for measuring the effect of heparin on FGFs structure.

Several chemically modified heparins were also tested by this method. Chemically modified heparins have less effect on FGFs than heparin. There are no major changes between FGFs alone and when bound to these modified heparins for FGF-1, FGF-2 and FGF-7 (FGF-1 with D8, FGF-2 with D4 and D6 and FGF-7 with D8) (**Figure 5.1**). In contrast, FGF-9 with D7 and FGF-18 with D6 showed considerable changes. However, they provide only limited information; confirming that modified heparins can also induce conformational changes

when binding to FGF, and indicating that the sulfation pattern is important for FGF-heparin interactions.

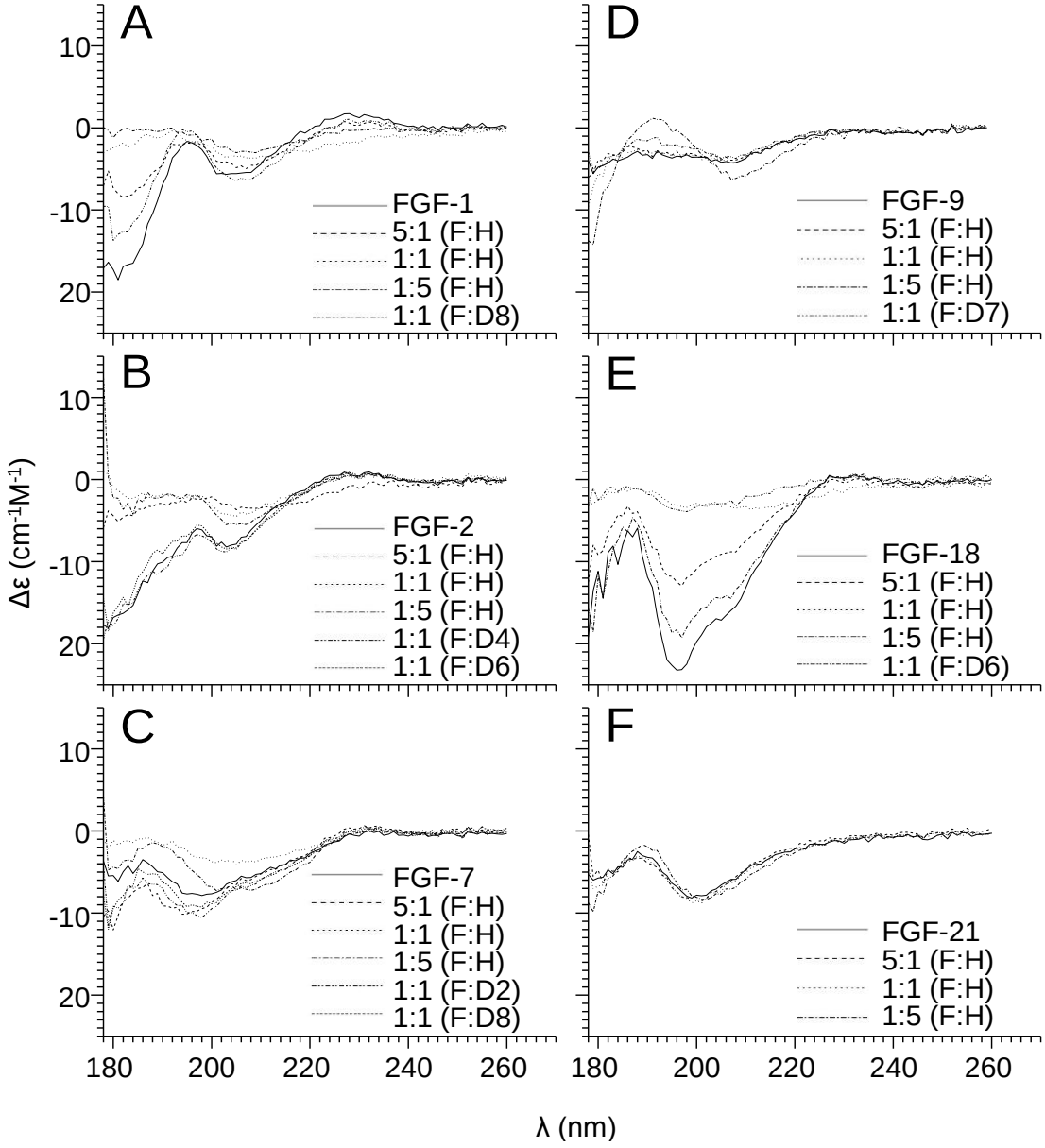


**Figure 5.1 SRCD spectra of FGFs with different concentrations of heparin at molar ratios 1:5, 1:1 and 5:1, and with selected chemically modified heparins.**

A, FGF-1 with heparin and D8. B, FGF-2 with heparin, D4 and D6. C, FGF-7 with heparin, D2 and D8. D, FGF-9 with heparin and D7. E, FGF-18 with heparin and D6. F, FGF-21 with heparin.

**Table 5.1 Secondary structure analysis of SRCD spectra of FGF-1 and heparin.**

| Sample | Helix1 | Helix2 | Strand1 | Strand2 | Turns | Unordered | Total |
|---|---|---|---|---|---|---|---|
| FGF-1 | -0.001 | 0.027 | 0.293 | 0.195 | 0.228 | 0.250 | 0.993 |
| 1:5 (H:F) | 0.053 | 0.082 | 0.211 | 0.111 | 0.211 | 0.337 | 1.006 |
| 1:1(H:F) | 0.000 | 0.001 | 0.016 | 0.096 | 0.285 | 0.611 | 1.009 |
| 5:1 (H:F) | 0.053 | 0.083 | 0.211 | 0.111 | 0.211 | 0.339 | 1.009 |
| 1:1 (F:D8) | 0.053 | 0.082 | 0.211 | 0.111 | 0.211 | 0.336 | 1.003 |

SRCD spectra of the FGF-1 alone, in the presence of molar ratios of heparin or with molar ratio 1:1 D8 were analyzed using SELCON 3 (**Section 2.12 and 5.2**).

**Table 5.2 Secondary structure analysis of SRCD spectra of FGF-2 and heparin.**

| Sample | Helix1 | Helix2 | Strand1 | Strand2 | Turns | Unordered | Total |
|---|---|---|---|---|---|---|---|
| FGF-2 | 0.000 | 0.018 | 0.247 | 0.118 | 0.297 | 0.314 | 0.994 |
| 1:5 (H:F) | 0.421 | 0.245 | 0.051 | 0.038 | 0.117 | 0.136 | 1.009 |
| 1:1 (H:F) | -0.001 | -0.001 | 0.014 | 0.096 | 0.285 | 0.610 | 1.003 |
| 5:1 (H:F) | 0.000 | 0.000 | 0.015 | 0.096 | 0.285 | 0.610 | 1.006 |
| 1:1 (F:D4) | 0.000 | 0.028 | 0.294 | 0.196 | 0.229 | 0.252 | 0.998 |
| 1:1 (F:D6) | 0.000 | 0.028 | 0.294 | 0.197 | 0.230 | 0.253 | 1.003 |

SRCD spectra of the FGF-2 alone, in the presence of molar ratios of heparin or with molar ratio 1:1 D4 and D6 were analyzed using SELCON 3 (**Section 2.12 and 5.2**).

**Table 5.3 Secondary structure analysis of SRCD spectra of FGF-7 and heparin.**

| Sample | Helix1 | Helix2 | Strand1 | Strand2 | Turns | Unordered | Total |
|---|---|---|---|---|---|---|---|
| FGF-7 | 0.211 | 0.136 | 0.043 | 0.067 | 0.231 | 0.314 | 1.001 |
| 1:5 (H:F) | 0.582 | 0.222 | -0.001 | -0.001 | 0.050 | 0.143 | 0.995 |
| 1:1(H:F) | 0.007 | 0.087 | 0.298 | 0.161 | 0.109 | 0.340 | 1.001 |
| 5:1 (H:F) | 0.001 | 0.000 | 0.012 | 0.094 | 0.284 | 0.608 | 0.999 |
| 1:1 (F:D2) | 0.214 | 0.194 | 0.000 | 0.000 | 0.234 | 0.361 | 1.004 |
| 1:1 (F:D8) | 0.215 | 0.195 | 0.001 | 0.000 | 0.234 | 0.362 | 1.006 |

SRCD spectra of the FGF-7 alone, in the presence of molar ratios of heparin or with molar ratio 1:1 D8 were analyzed using SELCON 3 (**Section 2.12 and 5.2**).

**Table 5.4 Secondary structure analysis of SRCD spectra of FGF-9 and heparin.**

| Sample | Helix1 | Helix2 | Strand1 | Strand2 | Turns | Unordered | Total |
|---|---|---|---|---|---|---|---|
| FGF-9 | 0.536 | 0.223 | 0.000 | 0.000 | 0.107 | 0.138 | 1.005 |
| 1:5 (H:F) | 0.536 | 0.224 | 0.002 | 0.001 | 0.107 | 0.139 | 1.010 |
| 1:1 (H:F) | 0.536 | 0.223 | 0.001 | 0.001 | 0.107 | 0.139 | 1.006 |
| 5:1 (H:F) | 0.210 | 0.136 | 0.044 | 0.068 | 0.233 | 0.316 | 1.006 |
| 1:1 (F:D7) | 0.000 | 0.000 | 0.016 | 0.097 | 0.286 | 0.611 | 1.011 |

SRCD spectra of the FGF-9 alone, in the presence of molar ratios of heparin or with molar ratio 1:1 D7 were analyzed using SELCON 3 (**Section 2.12 and 5.2**).

**Table 5.5 Secondary structure analysis of SRCD spectra of FGF-18 and heparin.**

| Sample | Helix1 | Helix2 | Strand1 | Strand2 | Turns | Unordered | Total |
|---|---|---|---|---|---|---|---|
| FGF-18 | 0.000 | 0.000 | 0.015 | 0.095 | 0.285 | 0.609 | 1.004 |
| 1:5 (H:F) | 0.215 | 0.195 | 0.001 | 0.001 | 0.233 | 0.361 | 1.005 |
| 1:1 (H:F) | 0.006 | 0.087 | 0.299 | 0.161 | 0.110 | 0.340 | 1.003 |
| 5:1 (H:F) | 0.054 | 0.083 | 0.211 | 0.110 | 0.212 | 0.335 | 1.004 |
| 1:1 (F:D6) | 0.215 | 0.195 | 0.001 | 0.001 | 0.233 | 0.361 | 1.005 |

SRCD spectra of the FGF-18 alone, in the presence of molar ratios of heparin or with molar ratio 1:1 D6 were analyzed using SELCON 3 (**Section 2.12 and 5.2**).

**Table 5.6 Secondary structure analysis of SRCD spectra of FGF-21 and heparin.**

| Sample | Helix1 | Helix2 | Strand1 | Strand2 | Turns | Unordered | Total |
|---|---|---|---|---|---|---|---|
| FGF-21 | 0.421 | 0.245 | 0.051 | 0.038 | 0.117 | 0.136 | 1.008 |
| 1:5 (H:F) | 0.422 | 0.246 | 0.050 | 0.038 | 0.117 | 0.136 | 1.007 |
| 1:1(H:F) | 0.421 | 0.245 | 0.051 | 0.038 | 0.117 | 0.136 | 1.008 |
| 5:1 (H:F) | 0.421 | 0.245 | 0.051 | 0.038 | 0.117 | 0.136 | 1.009 |

SRCD spectra of the FGF-21 alone and in the presence of molar ratios of heparin were analyzed using SELCON 3 (**Section 2.12 and 5.2**).

## 5.4 Discussion

CD spectra are averaged and deconvoluted into the spectra of the contributing protein secondary structures, alpha helixes, beta strands and random coils. The analysis of CD spectra is based on the comparison of protein structures against protein databases using different analysis methods. Thus, the selection of methods and databases is important for understanding the CD spectra. Several methods (SELCON 3, CDSSTR, CONTIN and K2D) and databases (1, 3 and 6) were used for the spectra of FGF-1 and FGF-2, and the results were compared with available 3-D structures of these two proteins. SELCON 3 and database 3 were chosen, because combinations of all the other methods and databases provided a poor match for their crystal and NMR structures. Through SELCON 3 and database 3 worked well in this respect, it is still not completely certain if the deconvolution is correct for FGFs for which there are no crystal/NMR structures or when FGFs bind heparin.

A relevant issue is that of solution versus crystal structure (**Section 1.5.2**). Thus, conflicts between the SRCD data and crystal structures may also simply reflect the difference between a crystal and a solution structure, which will always be more dynamic. This highlights the value of NMR spectra, which should be closer to the CD spectra.

A final issue is the contribution from the polysaccharide. Heparin and its analogues have a CD signal and this is clearly sensitive to the conformation of the sugar chain [121]. However, the chromophores in heparin are weaker than those of proteins (c.f., **Fig 6A in Section 4.1** and Fig. 1 in Rudd, *et al.* 2008 [121]). Therefore, although the present spectra contain contributions from both sugar and protein, the latter will account for over 80 %-90 % of the signal.

Though the SRCD data are complex, very clear relationships are apparent where these data are considered with those in Chapter 3. Thus, the SRCD results demonstrated that there was not a simple trend in the structural changes when more heparin was added to the FGFs (not

one direction of change). It is likely that the structural changes depend on the concentration of heparin, but the higher concentrations do not necessarily give larger changes in secondary structure. The structural changes may be related to the number of binding sites established in Chapter 3. When a small amount of heparin is present, most of the heparin will bind to the canonical heparin binding sites (HBS-1) since it is of highest affinity, and this might initiate a particular set of conformational changes in the FGF ligands. As more heparin is added, the canonical heparin binding sites became saturated, then the heparin will start binding the lower affinity HBS-2 and HBS-3, producing additional conformational changes. This could explain why at different molar ratios of heparin FGFs present different secondary structures, and that there was not a single direction for conformational changes linked to heparin concentration. For example, FGF-1 (HBS-1, HBS-2 and HBS-3) has very different secondary structures at different molar ratios of heparin, while in contrast, FGF-9, which has only an enlarged HBS-1, but no independent HBS-2, HBS-3 or HBS-4, has only one trend of conformational change: when heparin concentration increases, the protein structure changes from α to β. The sulfation patterns of heparin seem also to have an effect on the protein conformational change. For example, FGF-7 binding to D2 and D8 showed that different sulfation patterns affect the binding differently (**Figure 5.1 B**). However, at this point there is too little information to tell which sulfation played important part in and whether this is identified to that found to be primarily responsible for binding, determined by DSF. It is possible that not all sulfate groups involved in binding cause substantial conformational change in the FGF. Taken together, the SRCD data also showed that there are multiple specificities between FGFs and heparin to effect the FGFs' conformational changes when forming the binding complexes.

# Chapter 6 Analysis of individual FGF-2 molecules bound to heparan sulfate in the pericellular matrix

## 6.1 Introduction

FGF-2 mediates its bioactivity by binding to the matricellular and cell surface HS. In the pericellular matrix, FGF-2 may interact with HS or bind to FGFR above the plasma membrane to form a complex. It is well established that most of the cell bound FGF-2 is associated with HS. At any time, only a small proportion of the FGF-2 is associated with a ternary signaling complex, with HS and FGFR [48, 122-124]. Until recently there was no evidence for how the binding sites of FGF-2 are distributed in the pericellular matrix. Immunocytochemical and immunofluorescence measurements just do not have the spatial resolution [125]. However, in a recent paper [114] high resolution techniques show that these binding sites are not uniformly distributed in the pericellular matrix of Rama 27 fibroblasts. Moreover, in the same paper it is suggested that this non-uniform distribution is the reason why FGF-2 undergoes different types of motion in the matrix. One question that this work poses is whether the non-random distribution of the binding sites for FGF-2 in the pericellular matrix arises, in part, from the "space" taken up by non-FGF binding glycosaminoglycans, namely CS and DS.

To address this question, and as a means of starting to determine what might be the specificity and selectivity of the interaction of FGF-2 with endogenous cellular HS, a series of experiments were carried out with gold nanoparticle labeled FGF-2 (FGF-2-NP). Using this method, FGF-2 was conjugated with Tris-NTA-nanoparticles (Tris-NTA-NPs) at a stoichiometry of 1 FGF: 1 nanoparticle, according to a recent published method [106]. Such FGF-2-nanoparticles possess similar activity to free FGF-2 [114]. The distribution of FGF-2-NPs was measured at 2 concentrations (0.55 nM, 2.8 nM) with or without 0.5 mg/mL DP12.

Chondroitinase and hyaluronidase were used to remove the CS and HA from the cell surfaces.

# 6.2 Methods

## 6.2.1 Preparation of Tris-NTA gold nanoparticles and FGF2-NP.

### 6.2.1.1 Materials:

1. Modified peptides CVVVT-ol (T-ol is for threoninol) (Anaspec Inc., San Jose, CA): working solution: 4 mM in DMSO.

2. PeGylated alkanethiol SH-C11-$EG_4$-OH (Prochimia Surfaces Sp. Zo.o., Sopot, Poland): 360 μL methanol was added to the100 mM SH-C11-$EG_4$-OH stock solution (in methanol) to make a 10 mM working solution.

3. Colloidal Gold Nanoparticles (NP) (BritishBiocell (BBInternational Ltd., UK)): diameter 8.6 nm: stabilized in citrate buffer.

4. Tris-NTA powder: 10 mM in methanol.

5. Nanosep centrifugal ultra filtration devices: PALL (PALL Corp., Portsmouth, Hants, UK).

6. G25 Sephadex superfine (Sigma-Aldrich): 10 mL column.

7. Tween 20 (Sigma-Aldrich).

8. 200 ml NaCl.

9. 250 mM $NiSO_4$.

10. 10×PBS (a ten-fold concentrated solution of PBS): 8.1 mM $NaHPO_4$, 1.2 mM $KH_2PO_4$, 140 mM NaCl, and 2.7 mM KCl, pH7.4.

11. Peptide Biotin-GAAHHHHHH: at 10 mg/mL in PBS (7.24 mM, MW 1380, Sigma-Aldrich).

12. Strep-Tactin Sepharose. Binding capacity for biotin> 300 nmoles/mL.

### 6.2.1.2 Preparation of 1 mL of mix matrixed NPs

One hundred µL of ligand mix contained: 35 µL 4 mM CVVVT-ol, 6 µL 10 mM SH-C11-$EG_4$-OH, 52 µL $H_2O$, 6 µL methanol, 1 µL Tris-NTA were all added together and vortexed. The ligand solution was titrated into 900 µL gold nanoparticles and mixed by vortex. Then 100 µL 10 × PBS was added, mixed by vortexing and left to react on a rotating wheel overnight at room temperature. The NPs concentration was calculated using the epsilon value of 10 nm gold NP, $\varepsilon_{520nm}$ ($9.5 \times 10^8$) [106].

### 6.2.1.3 Preparation of hexa-histidine-Sepharose beads

Four mL of Strep-Tactin Sepharose was washed with 3×10 ml PBS. Biotinylated 6×His peptide (200 µL, 7.4 mM) was added to the Strep-Tactin Sepharose to a final concentration of 300 µM. Then 8 mL of PBS with 0.01 % (v/v) Tween was also added and the gel slurry incubated on a rotating wheel overnight. After incubation, the resin was loaded into a 10 mL plastic column, which was then washed with 5× 10 mL PBS and 2× 10 mL $H_2O$ with 0.01 % (v/v) Tween. Any free biotin binding sites on the Strep-Tactin Sepharose were blocked by adding 5 mL of 1 mM biotin. After that, the resin was washed by 10×10 mL $H_2O$ with 0.01 % (v/v) Tween and 5×10 mL PBS and then stored in PBS with 0.02 % (w/v) azide at 4°C.

### 6.2.1.4 Preparation of Tris-NiNTA–Capped NPs

Mixed matrix NPs were concentrated with nanosep filters by centrifugation at 7,700 ×g for 7 min and were then loaded onto a 10 mL Sephadex G25 column, equilibrated in 200 mM NaCl. The column was washed with 200 mM NaCl, and the sample of the concentrated NPs

applied. Fractions (3 mL) were collected and those corresponding to the excluded volume (coloured red due to the absorbance of the nanoparticles) were collected. The excess ligands (<1000 Da) eluted at the end of the included volume and so were well separated from the nanoparticles. The Tris-NTA groups were loaded with $Ni^{2+}$ by adding 250 mM $NiSO_4$ to the nanoparticle containing fractions and incubating for at least 2 h on a rotating wheel. The (v/v) ratio of $NiSO_4$: NP was 1:3.

The nanoparticles were concentrated again using Nanosep filters, which also removed some unbounded $NiSO_4$. Then the nanoparticles were applied again to a 10 mL G25 column as before and the excluded fraction was collected and buffer exchanged to 1×PBS.

NPs bearing at least one Tris-Ni-NTA were then purified using His Sepharose. Ten percent volume of the hexa-histidine Strep-Tactin Sepharose was added to the nanoparticles and placed on a rotating wheel overnight. The Sepharose was then placed in a column and washed with 10 volumes of PBS, then the nanoparticles were eluted with 200 mM imidazole in PBS and buffer exchanged into $H_2O$ using Nanosep filters.

### 6.2.1.5 Coupling Histag-FGF to the Tris-Ni-NTA-Capped NPs

NP with just one Tris-Ni-NTA were concentrated to 178 mM, and mixed with 197 µM His-tag FGF-2 and left to react on a rotating wheel at 4°C overnight. The reaction mixture was then concentrated and buffer exchanged to PBS using Nanosep filters. Excess FGF-2 was removed by centrifugation at 10,000 ×g for 7 min. The nanoparticle pellets were resuspended in PBS. FGF-2-NP concentration was calculated using the epsilon value of 10 nm NPs, $\varepsilon_{520\ nm}$ ($9.5\times10^8$) [106].

## 6.2.2 Transmission electron microscopy (TEM)

### 6.2.2.1 Production of coated TEM grids

#### *6.2.2.1.1 Materials:*

Pioloform: 0.3 % (w/v) Pioloform diluted in chloroform

Grids: 200 mesh (TAAB Laboratories Equipment Ltd., Berks, UK)

Glass Slides: 1.0 mm × 1.2 mm thick (Agar Scientific, Essex, UK)

#### *6.2.2.1.2 Pioloform coating grids*

The grids were first washed in ethanol and dried in a dry oven at 40$^{o}$C. The 3 % Pioloform (w/v) was placed in a glass dip-mister, which had been first washed with chloroform. The cleaned glass slide was dipped into 3 % Pioloform (w/v) and slowly pulled out and dried in air Excess film on the dried slide was trimmed to the edge of the glass with a razor blade and was then moisturized by breathing on both sides. Then, the coverslip was slowly dipped into water so that the film separated from the glass and floated on the water. The dried grids were placed onto the floating film and the film full of grids was picked up from the water and placed onto a glass slide with a white label on it. The grids were dried for 1-5 days.

#### *6.2.2.1.3 Carbon coating grids*

The dried grids were carbon coated with a carbon coating machine.

### 6.2.2.2 Chondroitinase and Hyaluronidase digestion

#### *6.2.2.2.1 Chondroitinase digestion*

Chondroitinase (Sigma-Aldrich) (20 mU/40 µL dissolved in water) were diluted 100 fold and Chondroitinase buffer (500 mM Tris acetate, pH 8.0) were diluted 5 fold with RM

medium and 500 µL of the dilution were added into each well and incubated at 37°C for overnight.

*6.2.2.2.2 Hyaluronidase digestion*

Hyaluronidase (Sigma-Aldrich) (20 mU/60 µL dissolved in water) was diluted 100-fold into cell culture medium and 500 µL of the dilution was added into each well and incubated at 37°C overnight.

## 6.2.2.3 Preparation of plasma membrane sheets

*6.2.2.3.1 Materials:*

1. PBS: 8.1 mM $Na_2HPO_4$, 1.2 mM $KH_2PO_4$, 140 mM NaCl and 2.7 mM KCl, pH 7.4

2. 10 mg/mL BSA in PBS

3. Ringer: 140 mM NaCl, 5 mM KCl, 2 mM $CaCl_2$, 2 mM $MgCl_2$, 11 mM glucose, 10 mM Hepes, pH 7.4

4. Reaction buffer: Ringer: 10 mg/ml BSA in PBS (1:9/2:8).

5. Cells: Rama27 passages 30 to 40

6. Gold nanoparticles: 10 nm from BBI with a mix matrix ligand shell containing with n=0, n=1 or n=1-2 Tris-Ni-NTA per nanoparticle.

7. KOAc (Potassium acetate buffer): 25 mM Hepes, 115 mM potassium acetate, 2.5 mM $MgCl_2$, pH 7.4.

8. 4 % (w/v) PFA, 0.1 % (v/v) glutaraldehyde.

9. 2 % (w/v) methylcellulose and 3% (w/v) uranyl acetate were mixed at a ratio of 9:1 (v/v).

*6.2.2.3.2 Method:*

Cells were grown on 13 $mm^2$ coverslips (**Section 2.7**) until they were 50% confluent and then were subjected to digestion with chondroitinase, hyaluronidase or both overnight (**Section 6.2.2.2**). Cells were then incubated in SDM (**Section 2.7**) for 4 h at 37℃. The coverslips with cells were then washed twice with PBS. Samples (200 µL for each) (Tris-NTA-NPs, 2.8 nM with 0.5 mg/mL DP12, 0.55 nM or 2.8 nM FGF-2-NPs, concentrations were calculated as described in **Section 6.2.1.5** were added to different wells for 3 min at room temperature and then left to incubate for 3 h on ice to prevent receptor-mediated endocytosis of the FGF-2. Previous work [122] has shown that on ice FGF-2 binding to cells reaches a maximum by 90 min.

After incubation the cover slips were washed twice with PBS, and then the cells on the coverslips were pressed lightly onto two grids, which were placed on a clean filter paper to avoid contamination.

The coverslip was turned over, and KOAc buffer (200 µL) was quickly added around the grids to separate them from the coverslip. Then, the grids with membranes were fixed by adding 4 % PFA (w/v) and 0.1 % (v/v) glutaraldehyde in KOAc for 10 min. The reaction was stopped with 3 × 3 min incubation in 50 mM glycine in PBS. The grids were then washed with 5×1 min $H_2O$. The grids were first washed twice by methylcellulose 2 % (w/v) and uranyl acetate 3 % (w/v) solution and incubated in this solution for 10 min.

Grids were picked up separately with loops and the excess solution was dried slowly with a piece of filter paper and then they were left dry on the loop for 10 min. Grids were carefully removed with tweezers from the loop and placed in an FEI Tecnai $G^2$ 120 kV transmission electron microscope (TEM).

### 6.2.2.4 TEM imaging and data analysis

At least 24 images were acquired at 26,500 × or 43,000 × magnification. At least 24 imagines were accounted for each sample (except negative controls).

The number of NPs was counted manually in each image and used to calculate the number of NPs per $\mu m^2$. The mean and SD for each sample were determined and the non-parametric Kplmogorov-Smirnov test was used to determine the significance of any differences.

The backgrounds of single images (750×750 $nm^2$) were changed to white with Adobe Photoshop and the co-ordinates of dots corresponding to NPs were then calculated by Image J and exported. The spatial data were analyzed by an Excel Macro, which implemented Ripley's K-function analysis of clustering [114, 126]. The analyzed data were then combined and mean values calculated and plotted.

## 6.3 Results and discussion:

To examine the distribution of FGF-2 in the pericellular matrix of Rama 27 cells at the single molecule level the growth factor was labeled with a 8.6 nm diameter gold nanoparticle probe at a stoichiometry of 1:1 [106, 114] (**Section 6.2**). The hexa-histidine tag of FGF-2 is on its N-terminus, so the Tris-NTA-NP is on the opposite side of the protein to the canonical heparin binding site [18] and the FGFR binding sites of FGF-2 [52, 116]. In addition, there are natural N-terminal extensions of FGF-2, which do not affect its ability to bind to HS or FGFR [48]. Such FGF-2-NPs have been shown to stimulate DNA synthesis and the phosphorylation of the adaptor protein FRS2 and p42/44MAPK to the same extent as unlabelled FGF-2 [114]. Taken together, these data mean that the FGF-NP will be able to interact with its HS co-receptors and FGFR similarly to unlabelled FGF-2.

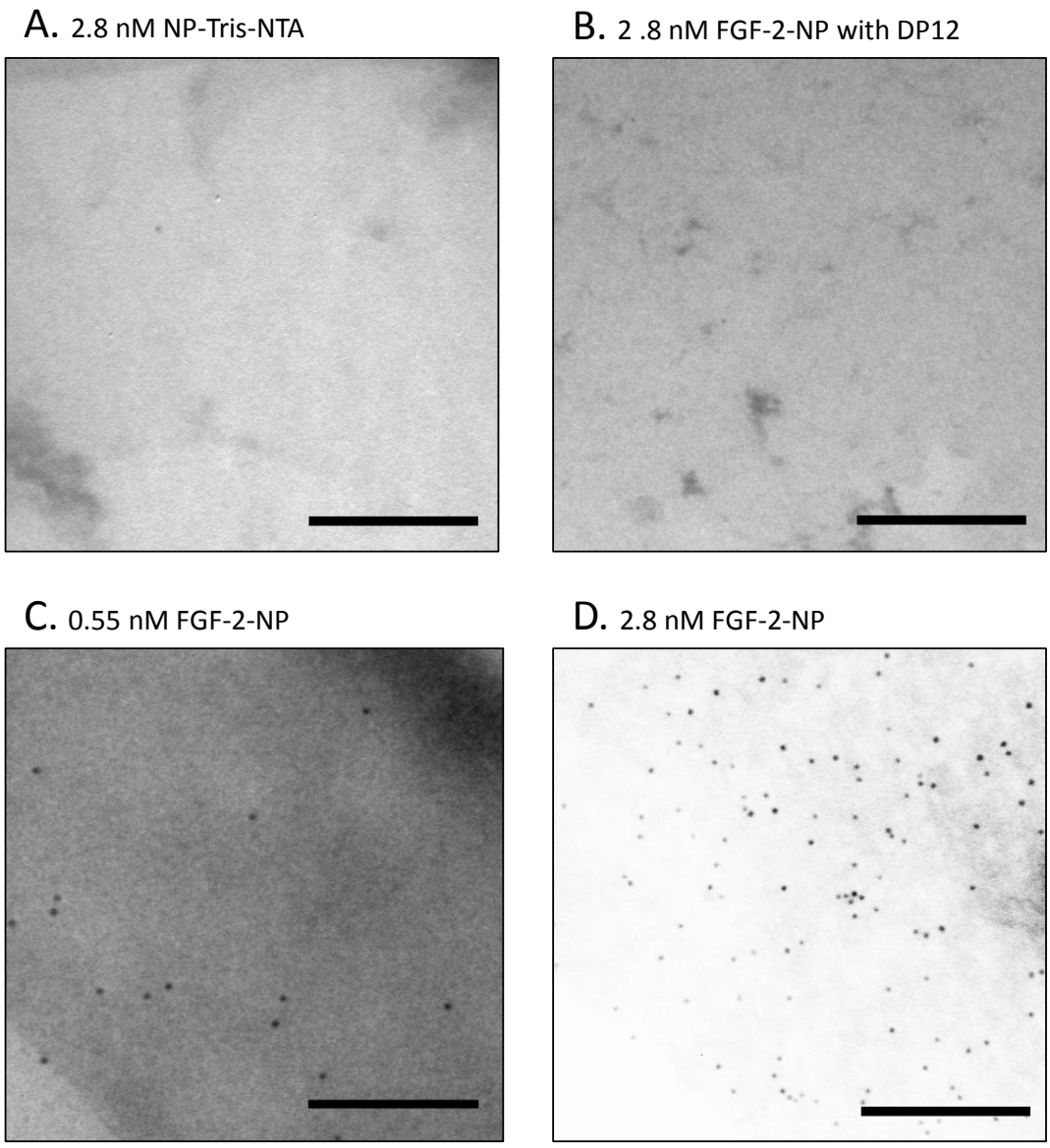


**Figure 6.1 Distribution of FGF-2-NP in the pericellular matrix of Rama 27 fibroblasts.**

Two concentrations of FGF-2-NP (0.55 nM and 2.8 nM) were added to living cells and incubated for 3 h on ice, then washed and plasma membrane sheets were prepared for TEM (**Section 6.2.2**). Cells incubated with A, 2.8 nM NP-Tris-NTA; B, 2.8 nM FGF-2-NP with 0.5 mg/ml DP12; C, 550 pM FGF-2-NP; D, 2.8 nM FGF-2-NP.Scale bar is 250 nm.

A 0.55 nM FGF-2-NP, chondroitinase

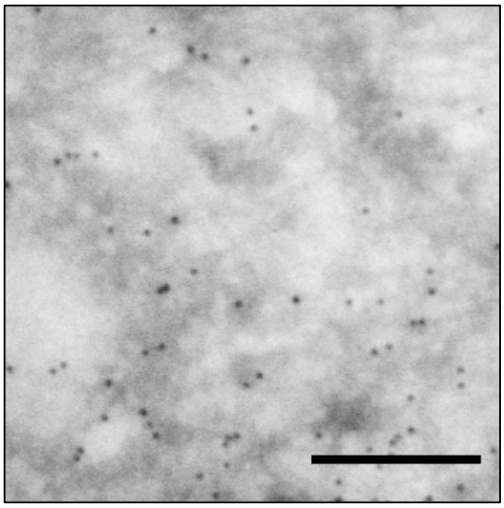

B 2.8 nM FGF-2-NP, chondroitinase

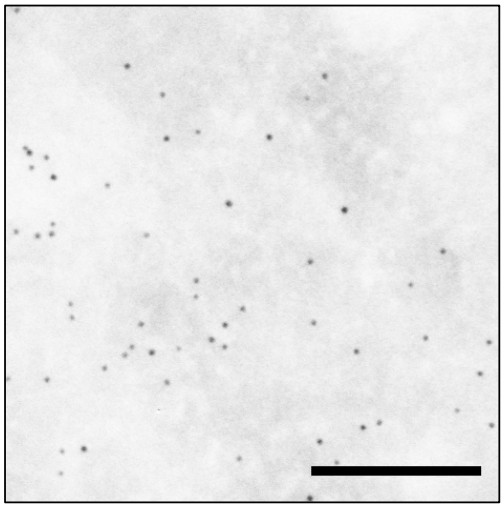

C 0.55 nM FGF-2-NP, hyaluronidase

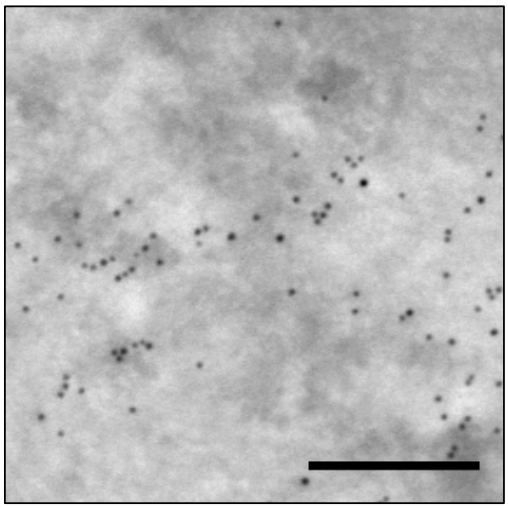

D 2.8 nM FGF-2-NP, hyaluronidase

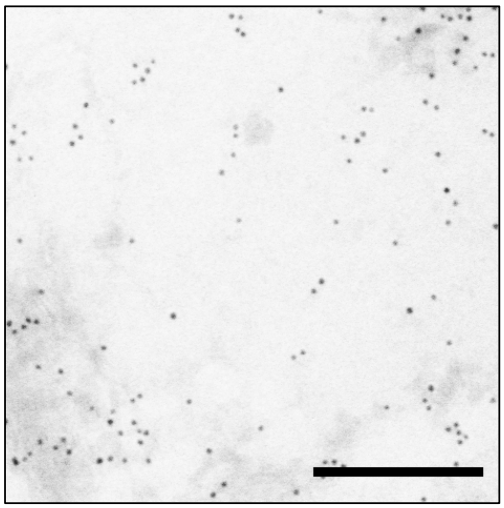

E 0.55 nM FGF-2-NP, C+H

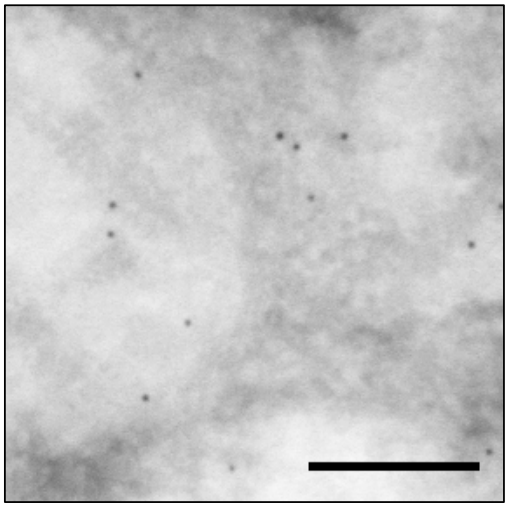

F 2.8 nM FGF-2-NP, C+H

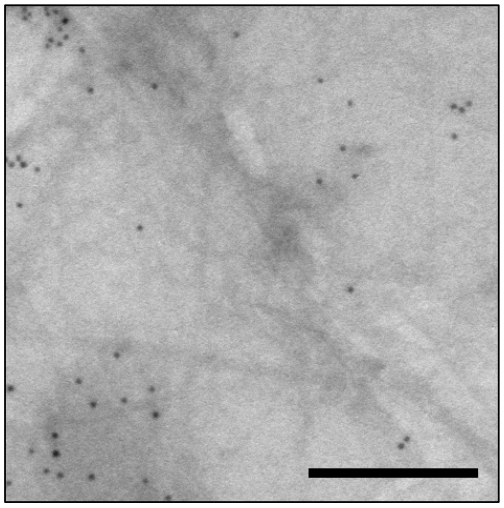

**Figure 6.2 Effect of enzyme digestion on the distribution of FGF-2-NP in the pericellular matrix of Rama 27 fibroblasts.**

Cells were treated with chondroitinase ABC (C), hyaluronidase (H) or both (C+H) (**Section 6.2.2.2**), after which FGF-2-NP (0.55 nM or 2.8 nM) was added and incubated for 3 h on ice and then the cells were washed and plasma membrane sheets were prepared for TEM (**Section 6.2.2**). A-C, 0.55 nMFGF-2-NP; C-E, 2.8 nM FGF-2-NP; A, D, Chondroitinase digested; B, E Hyaluronidase digested; C, F, cells digested with both chondroitinase ABC and hyaluronidase (C+H). Scale bar is 250 nm.

**A**

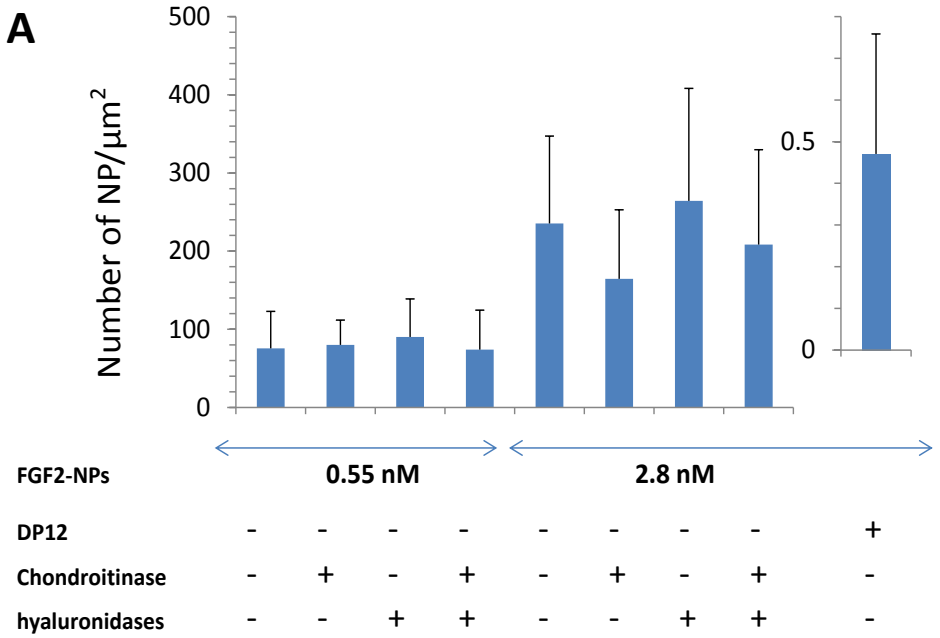


**B**

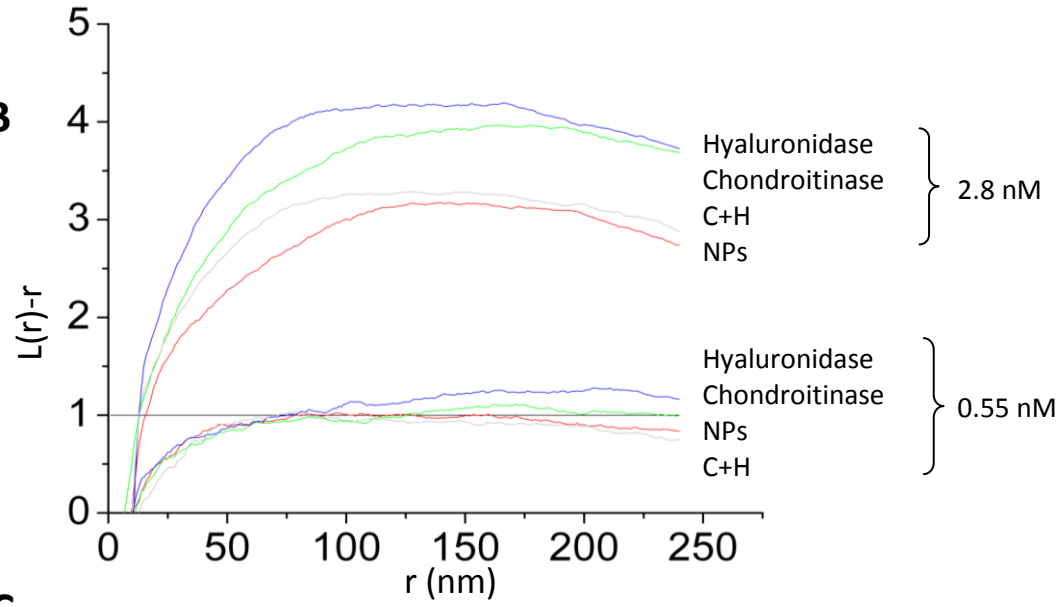


**C**

| | FGF-2-NP | Chondroitinase | hyaluronidase | Double digest | DP12 |
|---|---|---|---|---|---|
| 0.55 nM (number) | 75 | 80 | 90 | 74 | - |
| 2.8 nM (number) | 235 | 164 | 264 | 208 | 0.47 |
| 0.55 nM (P value) | 1.87e-5 | 0.421 | 0.478 | 0.94 | - |
| 2.8 nM (P value) | 1.87e-5 | 0.097 | 0.965 | 0.562 | 0 |

**Figure 6.3 Analysis of FGF-2 NP in the pericellular matrix**

Rama 27 cells were grown on glass coverslips, and treated with or without overnight enzyme digestions (chondroitinase, hyaluronidase or both), incubated with FGF-2-NPs or FGF-2-NPs in the presence of 0.5 mg/mL DP12 at two different concentrations (0.55 nM and 2.8 nM). The coverslips were washed and, after fixing the cells, sheets of plasma membrane and associated pericellular matrix were prepared for TEM (**Section 6.2.2**). Analysis of images of TEM of plasma membrane. A, Average number of NPs per $\mu m^2$measured from at least 20 images ($725\times725$ $nm^2$) at two different concentrations with or without digestions or with 0.5 mg/mL DP12 (mean ± SD).The number of NP/$\mu m^2$ when cells were incubated with 2.8 nM FGF-2-NP was 235, 164 following chondroitinase ABC digestion, 264 after hyaluronidase digestion, 208 for chondroitinase ABC and hyaluronidase digestion, and 0.47 in the presence of DP12. The number of NP/µm2 when cells were incubated with 0.55 nM FGF-2-NP was 75, 80 for chondroitinase digestion, 90 for hyaluronidase digestion, and 74 for digestion with both enzymes. B, the clustering of FGF-2-NP at two different concentrations (2.8 nM and 0.55 nM) in the pericellular matrix of cells with or without digestion (chondroitinase, hyaluronidase or double digested) was analysed by Ripley's K function (**Section 6.2.2.4**). A value of L(r)-r above the 99 % confidence interval (CI) (black line) indicates significant clustering within the defined x-axis radius values (r). C, The non-parametric Kolmogorov-Smirnov test gave the following P-values: 0.55 nM FGF-2-NP against 2.8 nM, P=1.87 e-5; 0.55 nM FGF-2-NP against chondroitinase digested, P=0.421; 0.55 nM FGF-2-NP against hyaluronidase digested, P=0.478; 0.55 nM FGF-2-NP against double digested, P=0.94; 2.8 nM FGF-2-NP against chondroitinase digested, P=0.097; 2.8 nM FGF-2-NP against hyaluronidase digested, P=0.965; 2.8 nM FGF-2-NP against double digested, P=0.562, 2.8 nM FGF-2-NP against 2.8 nM FGF-2-NP in present of DP12, P=0.

In the pericellular matrix, FGF-2 may interact with HS or bind to the FGFR to form a signalling complex. As with most cells, the number of HS binding sites on Rama 27 fibroblasts has been shown to be ~100- to ~1000-fold greater than the number of FGFR binding sites [114, 122]. To highlight that FGF-2-NP is indeed primarily engaged with the HS co-receptor on these cells, 0.5 mg/mL DP12 was included in some of the incubations. DP12 will compete for binding to endogenous cellular HS, but it will also enable the formation of ternary signalling complexes with the FGFR [57, 114]. The results showed that only a small number of FGF-2-NP (at the higher concentration 2.8 nM) remained bound to the cell in the presence of DP12 (**Figures 6.1 and 6.3)**. By counting the number of NPs on the cell membrane, it was found that DP12 caused a~400 fold reduction in the binding of FGF-2-NP (**Figure 6.3**), which agrees with previous studies [114, 122]. The digestions with chondroitinase ABC and hyaluronidase also served as controls for the specificity of binding. Though hyaluronidase digested cells had a slightly higher number of FGF-2-NP and chondroitinase ABC digested cells a slightly lower (for 2.8 nM) number of FGF-2-NP than undigested cells, the non-parametric Kolmogorov-Smirnov test demonstrated that these differences were not significant (P-values for all digestions> 0.05). Thus, these differences are likely to be due to experimental noise. However, there may also be a contribution from the cells adjusting to the effect of the digestions, since these were performed on live cells. Together with the DP12 competition data, these data indicate that the FGF-2-NPs are indeed bound to HS in the pericellular matrix of Rama 27 cells and that other glycosaminoglycans did not significantly contribute to this binding.

The distribution of FGF-2-NPs bound to HS in the pericellular matrix was analyzed by Ripley's K-function, which showed that the FGF-2-NP were clustered; that is, their spatial distribution was not random (**Figure 6.3**). At the lower concentration of 0.55 nM FGF-2-NP they were found to be clustered at ~100 nm (out of 99 % confidence). This is slightly different to that observed previously [114]. However, the line is only just above the 99 %

confidence interval, so there is perhaps more uncertainty in the present results and more data would have to be acquired to determine if this is a real difference. In cells digested with chondroitinase, clustering was more evident and occurred from ~150 nm to 200 nm, whereas in hyaluronidase treated cells, FGF-2-NP were clustered at all lengths above 100 nm. Surprisingly, digestion of both chondroitinase sulfate and hyaluronic acid resulted in only marginal clustering at ~ 80 nm. At the higher concentration of 2.8 nm FGF-2-NP, all samples were showed clustering at lengths from ~20 nm (**Figure 6.2**).

These results demonstrate that the conjugation of gold nanoparticles to FGF-2 provides a highly specific probe to analyze its interactions with HS in the pericellular matrix of cells, since most of the FGF-2-NP is bound to HS rather than some other glycosaminoglycan or the FGFR. Although FGF-2-NP did not interact with chondroitinase sulfate or hyaluronic acid, digestion of these glycoaminoglycans did, under some circumstances, affect the clustering of the FGF-2. Thus, at 0.55 nM FGF-2-NP, digestion of these sugars increased the clustering of the FGF-2. Though no such effect was observed at 2.8 nM FGF-2-NP, it should be noted that at this higher concentration clustering was evident at all lengths above 20 nm for the undigested control cells, so differences were unlikely to be observed by this analysis. However, the different L(r)-r values found with control and enzyme digested cells indicates that there was an effect of enzyme digestion. Clearly some other analysis of clustering and/or a different experimental design might reveal more. For example, the digestions were performed on live cells. This would allow the cells to adapt their pericellular matrix. Digestion on fixed cells may have provided more clear-cut differences. In any event, it would seem that the non-FGF-2 binding glycosaminoglycans CS and HA either through their interactions with other proteins or simply because they take up a substantial amount of space in the pericellular matrix affect the distribution of the binding sites of FGF-2 in HS. These binding sites, as has been shown previously [114] are not distributed randomly. The present results, therefore, raise the possibility that the distribution of the free binding sites for FGF-2

in the pericellular matrix might be controlled, at least to an extent, by the level and structures of glycosaminoglycans that do not bind FGF-2.

# Chapter 7 General discussion and conclusion

## 7.1 Discussion

The necessity for HS to bind FGFs to form the FGF-receptor complexes led us to study the binding of the HS to FGFs. The interaction of FGFs with HS is far from unique; at least 435 heparin binding proteins are encoded in the human genome and they are clearly key regulators of cell communication [89, 90]. Thus, the question of the binding specificities between HS and these proteins becomes important. There are two positions regarding specificity. One is that there are clear specificities for the heparin-proteins interactions, whereas the other is that there is little specificity beyond the size of oligosaccharide and that the binding is entirely charge-driven (**Section 1.11**). With 22 FGFs members, the evolutionary relationships between the different members and the association of heparin selectivity of these FGFs is an interesting platform to tackle the question of specificity. Thus, in this thesis, FGFs from different subfamilies were used so that the evolutionary relationships of this protein family could be exploited in the interpretation of the results. Six FGFs (FGF-1, FGF-2, FGF-7, FGF-9, FGF-18 and FGF-21) from 5 different sub-families were produced as recombinant proteins and their interactions with a library of heparin sugars and cellular HS were measured by several different methods.

In Chapter 4, four different approaches were used to determine what level of binding specificity might exist. First, the differences of binding kinetics of four FGFs (FGF-1, FGF-7, FGF-9 and FGF-18) to a model, heparin octasaccharide (DP8) showed there are binding specificities with respect to the binding parameters, which supports the idea that the HBS-1 of different FGFs possess different kinetics and affinities for

heparin, e.g., FGF-7 has very different $K_D$ when binding to DP8 compared to FGF-1 and FGF-2. Ionic bonding dominates kinetics, just as it does the qualitative measurements that use the concentration of NaCl required to dissociate sugar-protein complex as a proxy for affinity. However, DSF and SRCD, which are not necessarily dominated by ionic interactions, demonstrated that there was a lot of conformational change in FGFs when they bound to heparin (**Section 4.2**). Presumably, this is why ionic binding was found to only account for 30 % of ΔG of the FGF-2: heparin interaction and other 70 % was from nonionic interactions, such as hydrogen bonding and van der Waals packing [88].

The HBSs of the FGFs were found to differ. By comparing biosensor, Protect and Label and the DSF data, we can clearly see the relationships of binding activities of different HBSs. In a previous study that used peptides, FGF-2 HBS-1 (peptide 127-140) and HBS-2 (peptide 117-126) binding to heparin was measured in an optical biosensor; the $K_D$ of the peptide corresponding to HBS-1 was 30±4 μM, and that of the peptide corresponding to HBS-2 was 120±50 μM. In contrast the $K_D$ FGF-2 binding to heparin, which can only measure the highest affinity site (HBS-1) was 84±55 nM [115]. However, peptides do not have restricted conformations, so the peptide HBS-1 $K_D$ (30±4 μM), which is of the order of 1000-fold lower affinity than when in the context of the protein is reasonable. Thus, the binding affinity of HBS-2 may also be 100- to 1000-fold higher than when determined with a peptide: 1.0 to 0.1 μM in the FGF-2 protein. The ITC determination of the $K_D$ of FGF-2 for heparin in 0.1 M NaCl found a value of 0.47 μM [88]. ITC requires saturation of all binding sites and the experiment was conducted at a lower concentration of electrolytes than PBS. Thus, this is consistent with an average of HBS-1, HBS-2 and HBS-3.

Moreover the DSF data showed that the thermostabilizing effect of FGF-2 binding to heparin reached the highest level at 25 µM heparin (**Figure 4.3**). Assuming that thermostabilization of FGF-2 is contributed to by all three HBSs, together these data suggest that FGF-2 can indeed bind to heparin via all three sites.

The FGF-1 biosensor data showed that the affinity of FGF-1 for DP8 ($K_D$=60±6.2 nM) was similar to that of FGF-2. Interestingly, the FGF-1 DSF data showed that the thermostabilization of FGF-1 by heparin had not reached at a maximum at 500 µM, the highest concentration of heparin used (**Figure 4.2**). This is consistent with the FGF-1 binding to heparin by all three of its HBSs. Similarly FGF-18's thermostabilization by heparin was still rising at 500 µM, while the $K_D$ of FGF-18 for DP8 (reflecting binding by HBS-1) was 38±12 nM, which also indicated that the binding between FGF-18 and heparin relates to both of its HBSs.

Although the thermostabilizing effect of heparin binding on FGF-7 reached a maximum at 5 µM, the $K_D$ of FGF-7 for DP8 measured in the biosensor was $K_D$=290±49 nM (**Table 3 in Section 4.2**). The 17-fold difference may be due to FGF-7 binding to heparin through HBS-1, HBS-2, and maybe also HBS-4, and/or the protein accommodating the sugar in different orientations across its 'T' shaped binding site at different concentrations. In contrast, there was no large difference between the affinity of FGF-9 for DP8 measured in a biosensor, $K_D$=620±340, and the concentration of heparin required to elicit maximal thermostabilization (1.25 µM). Since at $K_D$ half the binding sites are occupied, these data are consistent with FGF-9 possessing a single HBS. The above highlights the value of using different approaches to analyze a molecular interaction. Consistencies and apparent

discrepancies appear, which, when considered with what a particulate technique actually measures, allows important conclusions to be drawn.

The DSF experiments gave a view of different sugars binding to these FGFs. The concentration of sugars used here (5 μM) would probably not be too sensitive to multiple HBSs, though there might be some contribution from HBS-2. The better binding of heparin/HS compared to HA, CS and DS and selective binding of heparins of different lengths and sulfation patterns demonstrates that the interactions are not simply based on ion-exchange. The selectivity of sugar structures was separable by PCA, with the results clearly showing that there were specificities when different proteins bound to heparin. However, there is clearly no simple and absolute specificity. This is reasonable, since such specificity is the exception rather than the rule. For example, FGF ligands have clear selectivity for different FGFRs, but except for FGF-7 this is never one to one (**Table 1.1**). Thus, more useful is the idea of a consensus site used to describe the DNA sequences bound by transcription factors. Departures from consensus often reflect the occunence of a higher degree of regulation rather than binding that is not functionally significant.

An analysis of the HBS and FGFR binding sites reveals some interesting features. The HBS-3 of FGF-1, FGF-2, FGF-7 (predicted) overlapped with the FGFR binding sites, and in FGF-1 and FGF-2 part of HBS-2 also overlapped with their FGFR binding sites. Thus, the HBS-3 and part of HBS-2 in some instances may be involved in the transport of the FGF on the cell surfaces, but not in the formation of the FGFR complex. Indeed their secondary HBS may negatively regulate this, which may

account for the previous identification of HS structures that bind FGF-2, but do not allow the activation of mitogenic signaling [85, 96, 127].

However, the above is all with model sugars and purified molecules. In reality the S and SAS domains of HS (**Section 1.6.3**, [32]) are less sulfated than heparin and *in vivo* already associated with endogenous proteins. So what FGF will bind in a cell may be rather different. Some S and SAS will not be free and/or require a displacement reaction, others may be forced into favorable or unfavorable conformations due to the binding of endogenous proteins to the opposing face of the sugar. The preliminary work in Chapter 6 demonstrates that it will be possible to gain some insights into the interactions of FGFs will real HS *in vivo*.

## 7.2 Future work

It is clear from this study that there are binding specificities between heparin and FGFs, alongside subfamily similarities, which are related to the evolution of FGFs, however, the overall picture is far from complete. First, only one representative ligand in the FGF-7, FGF-8 and FGF-9 sub-families, and no member of the FGF-4 sub-family was investigated. The hypothesis that HBS and specificity are conserved within subfamilies and varies more between these (**Section 4.2**) needs formal evidence. Ideally the entire set of heparin binding FGF ligands needs to be produced and by using similar methods to those in this study understand the differences and similarities of the sub-family members in their binding to heparin.

Despite differences between HS or a cell and pure sugar, the intrinsic specificities and preferences of a FGF-sugar interaction *in vitro* should be reflected *in vivo* and so

determine FGF function. Duchesne *et al.* 2012 [114] used FGF-2 to predict that the transport of heparin binding proteins in extracellular matrix is simply due to cycles of association and dissociation from cellular HS. If this is true, then for HS on a given cell, two FGFs with different heparin specificities and binding kinetics should exhibit different distributions and transport parameters. The original work was done with FGF-2, which has a $K_D$ ~$10^{-8}$ M and a preference for sulfation patterns of 2S and NS [92-95, 102] (**Section 4.3**). The most different FGFs of the four available compared to FGF-2 are FGF-7 and FGF-9; the binding affinity of DP8 to FGF-7 ($K_D$= 290±49 nM) is about 10-fold lower and for FGF-9 ($K_D$= 620±340 nM) around 50-fold lower than FGF-2 ($K_D$= 11±2 nM) (**Table 3 in Section 4.2**) [57]. Moreover, their sulfation patterns preferences are different, both FGF-7 and FGF-9 need 6S and NS more than 2S (**Figure 8 in Section 4.2**). Therefore, NP conjugated FGF-7 and FGF-9 would provide well characterized tools to test this hypothesis. Such work would also pave the way for the deployment of nanoparticle probes as a means to analyze the binding of FGFs to HS in cells, rather than to purified sugars.

# Supplemental data

# Papers and manuscripts

## Contributions to work

Paper1

Uniewicz, K.A., Ori, A., **Xu, R.**, Ahmed, Y., Fernig, D.G. and Yates, E.A. (2010). Differential Scanning Fluorimetry measurement of protein stability changes upon binding to glycosaminoglycans: a rapid screening test for binding specificity. Anal. Chem. **82**: 3796-3802.

Produced FGF-18 protein and contributed to the development of the DSF assay.

Paper 2

Rudd, T.R., Uniewicz, K.A., Ori, A., Guimond, S.E., Skidmore, M.A., Gaudesi, D., **Xu, R.**, Turnbull, J.E., Guerrini, M., Torri, G., Siligardi, G., Wilkinson, M.C., Fernig, D.G. and Yates, E.A. (2010). Comparable stabilisation, structural changes and activities can be induced in FGF by a variety of HS and non-GAG analogues: Implications for sequence-activity relationships. Org. Biomol. Chem. **8**: 5390-5397

Produced FGF proteins and contributed to data acquisition at synchrotron.

Paper 3

Thompson, S.M., Connell, M.G., van Kuppevelt,,T.H., **Xu, R.**, Turnbull, J.E., Losty, P.D., Fernig, D.G. and Jesudason, E.C. (2011). Structure and epitope distribution of heparan sulfate is disrupted in experimental lung hypoplasia: a glycobiological epigenetic cause for malformation? BMC Dev. Biol. **11**:38.

Produced FGF-9 protein used to demonstrate specificity and biological significance of epitopes recognized by HS antibodies.

Paper 4

**Xu, R.**, Ori, A., Rudd, T.R., Uniewicz, K.A.,Ahmed, Y.A., Guimond, S.E., Skidmore, M.A., Siligardi, G., Yates, E.A. and Fernig, D.G. (2012). Diversification of the structural determinants of fibroblast growth factor-heparin interactions; implications for binding specificity. J. Biol. Chem. 287(47):40061-40073.

Made FGF proteins, performed the experiments and drafted the entire manuscript. other co-authors supplied sugars, led the development of DSF, helped with PCA and with acquisition of spectra on the SRCD beamline.

Paper 5

**Ruoyan Xu**, Timothy R. Rudd, Ashley J Hughes, Giuliano Siligardi, David G. Fernig and Edwin A. Yates. (2012). Analysis of the FGFR Signalling Network with Heparin as Co-Receptor: Evidence for the expansion of the core FGFR signalling network. Submitted to FEBJ, December 2012.

Made FGF proteins, acquired spectra, interpreted these and drafted manuscript.

# Bibliography


1. Itoh, N. and D. M. Ornitz (2004) *Evolution of the Fgf and Fgfr gene families.* Trends in Genetics **20**: 563-569.
2. Crabb, J. W., L. G. Armes, S. A. Carr, C. M. Johnson, G. D. Roberts, R. S. Bordoli and W. L. McKeehan (1986) *Complete primary structure of prostatropin, a prostate epithelial cell growth factor.* Biochemistry **25**: 4988-4993.
3. Esch, F., A. Baird, N. Ling, N. Ueno, F. Hill, L. Denoroy, R. Klepper, D. Gospodarowicz, P. Bohlen and R. Guillemin (1985) *Primary structure of bovine pituitary basic fibroblast growth factor (FGF) and comparison with the amino-terminal sequence of bovine brain acidic FGF.* Proc. Natl. Acad. Sci. U. S. A. **82**: 6507-6511.
4. Gospodarowicz, D. (1974) *Localisation of a fibroblast growth factor and its effect alone and with hydrocortisone on 3T3 cell growth.* Nature **249**: 123-127.
5. Jaye, M., R. Howk, W. Burgess, G. A. Ricca, I. M. Chiu, M. W. Ravera, S. J. O'Brien, W. S. Modi, T. Maciag and W. N. Drohan (1986) *Human endothelial cell growth factor: cloning, nucleotide sequence, and chromosome localization.* Science **233**: 541-545.
6. Smith, J. A., D. P. Winslow, M. J. O'Hare and P. S. Rudland (1984) *Brain and pituitary fibroblast growth factor activities behave identically on three independent high performance liquid chromatography systems.* Biochem. Biophys. Res. Commun. **119**: 311-318.
7. Itoh, N. (2007) *The Fgf families in humans, mice, and zebrafish: Their evolutional processes and roles in development, metabolism, and disease.* Biological & Pharmaceutical Bulletin **30**: 1819-1825.
8. Itoh, N. and D. M. Ornitz (2008) *Functional evolutionary history of the mouse Fgf gene family.* Developmental Dynamics **237**: 18-27.
9. Itoh, N. and D. M. Ornitz (2011) *Fibroblast growth factors: from molecular evolution to roles in development, metabolism and disease.* J. Biochem. **149**: 121-130.
10. Mergia, A., R. Eddy, J. A. Abraham, J. C. Fiddes and T. B. Shows (1986) *The genes for basic and acidic fibroblast growth factors are on different human chromosomes.* Biochem. Biophys. Res. Commun. **138**: 644-651.
11. Abraham, J. A., J. L. Whang, A. Tumolo, A. Mergia, J. Friedman, D. Gospodarowicz and J. C. Fiddes (1986) *Human basic fibroblast growth factor: nucleotide sequence and genomic organization.* EMBO. J. **5**: 2523-2528.
12. Ornitz, D. M. and N. Itoh (2001) *Fibroblast growth factors.* Genome Biol. **2**: REVIEWS3005.
13. Mignatti, P., T. Morimoto and D. B. Rifkin (1992) *Basic fibroblast growth factor, a protein devoid of secretory signal sequence, is released by cells via a pathway independent of the endoplasmic reticulum-Golgi complex.* J. Cell Physiol. **151**: 81-93.
14. Abraham, J. A., J. L. Whang, A. Tumolo, A. Mergia and J. C. Fiddes (1986) *Human basic fibroblast growth factor: nucleotide sequence, genomic organization, and expression in mammalian cells.* Cold Spring Harb. Symp. Quant. Biol. **51 Pt 1**: 657-668.
15. Kiefer, P., P. Acland, D. Pappin, G. Peters and C. Dickson (1994) *Competition between nuclear localization and secretory signals determines the subcellular fate of a single CUG-initiated form of FGF3.* EMBO J. **13**: 4126-4136.
16. Arnaud, E., C. Touriol, C. Boutonnet, M. C. Gensac, S. Vagner, H. Prats and A. C. Prats (1999) *A new 34-kilodalton isoform of human fibroblast growth factor 2 is cap dependently synthesized by using a non-AUG start codon and behaves as a survival factor.* Mol. Cell Biol. **19**: 505-514.

17. Eriksson, A. E., L. S. Cousens, L. H. Weaver and B. W. Matthews (1991) *Three-dimensional structure of human basic fibroblast growth factor.* Proc Natl Acad Sci U S A **88**: 3441-3445.
18. Zhu, X., H. Komiya, A. Chirino, S. Faham, G. M. Fox, T. Arakawa, B. T. Hsu and D. C. Rees (1991) *Three-dimensional structures of acidic and basic fibroblast growth factors.* Science **251**: 90-93.
19. Plotnikov, A. N., A. V. Eliseenkova, O. A. Ibrahimi, Z. Shriver, R. Sasisekharan, M. A. Lemmon and M. Mohammadi (2001) *Crystal structure of fibroblast growth factor 9 reveals regions implicated in dimerization and autoinhibition.* J. Biol. Chem. **276**: 4322-4329.
20. Plotnikov, A. N., S. R. Hubbard, J. Schlessinger and M. Mohammadi (2000) *Crystal structures of two FGF-FGFR complexes reveal the determinants of ligand-receptor specificity*. Cell **101**: 413-424.
21. Osslund, T. D., R. Syed, E. Singer, E. W. Hsu, R. Nybo, B. L. Chen, T. Harvey, T. Arakawa, L. O. Narhi, A. Chirino and C. F. Morris (1998) *Correlation between the 1.6 A crystal structure and mutational analysis of keratinocyte growth factor.* Protein Sci. **7**: 1681-1690.
22. Ye, S., Y. Luo, W. Lu, R. B. Jones, R. J. Linhardt, I. Capila, T. Toida, M. Kan, H. Pelletier and W. L. McKeehan (2001) *Structural basis for interaction of FGF-1, FGF-2, and FGF-7 with different heparan sulfate motifs.* Biochemistry **40**: 14429-14439.
23. Yeh, B. K., M. Igarashi, A. V. Eliseenkova, A. N. Plotnikov, I. Sher, D. Ron, S. A. Aaronson and M. Mohammadi (2003) *Structural basis by which alternative splicing confers specificity in fibroblast growth factor receptors.* Proc. Natl. Acad. Sci. U. S. A. **100**: 2266-2271.
24. Olsen, S. K., J. Y. Li, C. Bromleigh, A. V. Eliseenkova, O. A. Ibrahimi, Z. Lao, F. Zhang, R. J. Linhardt, A. L. Joyner and M. Mohammadi (2006) *Structural basis by which alternative splicing modulates the organizer activity of FGF8 in the brain.* Genes Dev. **20**: 185-198.
25. Blaber, M., J. DiSalvo and K. A. Thomas (1996) *X-ray crystal structure of human acidic fibroblast growth factor.* Biochemistry **35**: 2086-2094.
26. Canales, A., R. Lozano, B. Lopez-Mendez, J. Angulo, R. Ojeda, P. M. Nieto, M. Martin-Lomas, G. Gimenez-Gallego and J. Jimenez-Barbero (2006) *Solution NMR structure of a human FGF-1 monomer, activated by a hexasaccharide heparin-analogue.* FEBS. J. **273**: 4716-4727.
27. Powell, A. K., E. A. Yates, D. G. Fernig and J. E. Turnbull (2004) *Interactions of heparin/heparan sulfate with proteins: appraisal of structural factors and experimental approaches.* Glycobiology **14**: 17R-30R.
28. Conrad., H. E. Structures of Heparinoids, in *Heparin-binding proteins*. 1998 San Diego ; London : Academic Press, 7-61.
29. Esko, J. D. and S. B. Selleck (2002) *Order out of chaos: assembly of ligand binding sites in heparan sulfate.* Annu Rev Biochem **71**: 435-471.
30. Rabenstein, D. L. (2002) *Heparin and heparan sulfate: structure and function.* Nat Prod Rep **19**: 312-331.
31. Bashkin, P., S. Doctrow, M. Klagsbrun, C. M. Svahn, J. Folkman and I. Vlodavsky (1989) *Basic fibroblast growth factor binds to subendothelial extracellular matrix and is released by heparitinase and heparin-like molecules.* Biochemistry **28**: 1737-1743.
32. Fromm, J. R., R. E. Hileman, J. M. Weiler and R. J. Linhardt (1997) *Interaction of fibroblast growth factor-1 and related peptides with heparan sulfate and its oligosaccharides.* Arch. Biochem. Biophys. **346**: 252-262.
33. Lindahl, U., M. Kusche-Gullberg and L. Kjellen (1998) *Regulated diversity of heparan sulfate*. J. Biol. Chem. **273**: 24979-24982.

34. Szebenyi, G. and J. F. Fallon (1999) *Fibroblast growth factors as multifunctional signaling factors.* Int. Rev. Cytol. **185**: 45-106.
35. Burke, D., D. Wilkes, T. L. Blundell and S. Malcolm (1998) *Fibroblast growth factor receptors: lessons from the genes.* Trends Biochem. Sci. **23**: 59-62.
36. Johnson, D. E. and L. T. Williams (1993) *Structural and functional diversity in the FGF receptor multigene family.* Adv. Cancer Res. **60**: 1-41.
37. Duchesne, L., B. Tissot, T. R. Rudd, A. Dell and D. G. Fernig (2006) *N-glycosylation of fibroblast growth factor receptor 1 regulates ligand and heparan sulfate co-receptor binding.* J Biol Chem **281**: 27178-27189.
38. Polanska, U. M., L. Duchesne, J. C. Harries, D. G. Fernig and T. K. Kinnunen (2009) *N-Glycosylation regulates fibroblast growth factor receptor/EGL-15 activity in Caenorhabditis elegans in vivo.* J. Biol. Chem. **284**: 33030-33039.
39. Pellegrini, L., D. F. Burke, F. von Delft, B. Mulloy and T. L. Blundell (2000) *Crystal structure of fibroblast growth factor receptor ectodomain bound to ligand and heparin.* Nature **407**: 1029-1034.
40. Sleeman, M., J. Fraser, M. McDonald, S. Yuan, D. White, P. Grandison, K. Kumble, J. D. Watson and J. G. Murison (2001) *Identification of a new fibroblast growth factor receptor, FGFR5.* Gene **271**: 171-182.
41. Givol, D. and A. Yayon (1992) *Complexity of FGF receptors: genetic basis for structural diversity and functional specificity.* FASEB J. **6**: 3362-3369.
42. Green, P. J., F. S. Walsh and P. Doherty (1996) *Promiscuity of fibroblast growth factor receptors.* Bioessays **18**: 639-646.
43. Shimizu, A., K. Tada, C. Shukunami, Y. Hiraki, T. Kurokawa, N. Magane and M. Kurokawa-Seo (2001) *A novel alternatively spliced fibroblast growth factor receptor 3 isoform lacking the acid box domain is expressed during chondrogenic differentiation of ATDC5 cells.* J. Biol. Chem. **276**: 11031-11040.
44. Gasteiger E., Hoogland C., Gattiker A., Duvaud S., Wilkins M.R., Appel R.D. and B. A. Protein Identification and Analysis Tools on the ExPASy Server, in *The Proteomics Protocols Handbook, Humana Press*. 2005 571-607
45. Ornitz, D. M., J. Xu, J. S. Colvin, D. G. McEwen, C. A. MacArthur, F. Coulier, G. Gao and M. Goldfarb (1996) *Receptor specificity of the fibroblast growth factor family.* J. Biol. Chem. **271**: 15292-15297.
46. Zhang, X., O. A. Ibrahimi, S. K. Olsen, H. Umemori, M. Mohammadi and D. M. Ornitz (2006) *Receptor specificity of the fibroblast growth factor family. The complete mammalian FGF family.* J. Biol. Chem. **281**: 15694-15700.
47. Sleeman, M., J. Fraser, M. McDonald, S. Yuan, D. White, P. Grandison, K. Kumble, J. D. Watson and J. G. Murison (2001) *Identification of a new fibroblast growth factor receptor, FGFR5.* Gene **271**: 171-182.
48. Fernig, D. G. and J. T. Gallagher (1994) *Fibroblast growth factors and their receptors: An information network controlling tissue growth, morphogenesis and repair.* Progress in Growth Factor Research **5**: 353-377.
49. Baird, A., D. Schubert, N. Ling and R. Guillemin (1988) *Receptor- and heparin-binding domains of basic fibroblast growth factor.* Proc. Natl. Acad. Sci. U. S. A. **85**: 2324-2328.
50. Springer, B. A., M. W. Pantoliano, F. A. Barbera, P. L. Gunyuzlu, L. D. Thompson, W. F. Herblin, S. A. Rosenfeld and G. W. Book (1994) *Identification and concerted function of two receptor binding surfaces on basic fibroblast growth factor required for mitogenesis.* J. Biol. Chem. **269**: 26879-26884.
51. Plotnikov, A. N., J. Schlessinger, S. R. Hubbard and M. Mohammadi (1999) *Structural basis for FGF receptor dimerization and activation.* Cell **98**: 641-650.
52. Schlessinger, J., A. N. Plotnikov, O. A. Ibrahimi, A. V. Eliseenkova, B. K. Yeh, A. Yayon, R. J. Linhardt and M. Mohammadi (2000) *Crystal structure of a ternary FGF-*

*FGFR-heparin complex reveals a dual role for heparin in FGFR binding and dimerization.* Mol. Cell **6**: 743-750.

53. Pellegrini, L., D. F. Burke, F. von Delft, B. Mulloy and T. L. Blundell (2000) *Crystal structure of fibroblast growth factor receptor ectodomain bound to ligand and heparin.* Nature **407**: 1029-1034.
54. Yeh, B. K., A. V. Eliseenkova, A. N. Plotnikov, D. Green, J. Pinnell, T. Polat, A. Gritli-Linde, R. J. Linhardt and M. Mohammadi (2002) *Structural basis for activation of fibroblast growth factor signaling by sucrose octasulfate.* Mol. Cell Biol. **22**: 7184-7192.
55. Rapraeger, A. C., A. Krufka and B. B. Olwin (1991) *Requirement of heparan sulfate for bFGF-mediated fibroblast growth and myoblast differentiation.* Science **252**: 1705-1708.
56. Yayon, A., M. Klagsbrun, J. D. Esko, P. Leder and D. M. Ornitz (1991) *Cell surface, heparin-like molecules are required for binding of basic fibroblast growth factor to its high affinity receptor.* Cell **64**: 841-848.
57. Delehedde, M., M. Lyon, J. T. Gallagher, P. S. Rudland and D. G. Fernig (2002) *Fibroblast growth factor-2 binds to small heparin-derived oligosaccharides and stimulates a sustained phosphorylation of p42/44 mitogen-activated protein kinase and proliferation of rat mammary fibroblasts.* Biochem. J. **366**: 235-244.
58. Delehedde, M., M. Seve, N. Sergeant, I. Wartelle, M. Lyon, P. S. Rudland and D. G. Fernig (2000) *Fibroblast growth factor-2 stimulation of p42/44MAPK phosphorylation and IkappaB degradation is regulated by heparan sulfate/heparin in rat mammary fibroblasts.* J. Biol. Chem. **275**: 33905-33910.
59. Zhu, H., L. Duchesne, P. S. Rudland and D. G. Fernig (2010) *The heparan sulfate co-receptor and the concentration of fibroblast growth factor-2 independently elicit different signalling patterns from the fibroblast growth factor receptor.* Cell Commun. Signal **8**: 14.
60. Lundin, L., H. Larsson, J. Kreuger, S. Kanda, U. Lindahl, M. Salmivirta and L. Claesson-Welsh (2000) *Selectively desulfated heparin inhibits fibroblast growth factor-induced mitogenicity and angiogenesis.* J. Biol. Chem. **275**: 24653-24660.
61. Fannon, M., K. E. Forsten and M. A. Nugent (2000) *Potentiation and inhibition of bFGF binding by heparin: a model for regulation of cellular response.* Biochemistry **39**: 1434-1445.
62. Pantoliano, M. W., R. A. Horlick, B. A. Springer, D. E. Van Dyk, T. Tobery, D. R. Wetmore, J. D. Lear, A. T. Nahapetian, J. D. Bradley and W. P. Sisk (1994) *Multivalent ligand-receptor binding interactions in the fibroblast growth factor system produce a cooperative growth factor and heparin mechanism for receptor dimerization.* Biochemistry **33**: 10229-10248.
63. Ibrahimi, O. A., B. K. Yeh, A. V. Eliseenkova, F. Zhang, S. K. Olsen, M. Igarashi, S. A. Aaronson, R. J. Linhardt and M. Mohammadi (2005) *Analysis of mutations in fibroblast growth factor (FGF) and a pathogenic mutation in FGF receptor (FGFR) provides direct evidence for the symmetric two-end model for FGFR dimerization.* Mol Cell Biol **25**: 671-684.
64. Mohammadi, M., S. K. Olsen and R. Goetz (2005) *A protein canyon in the FGF-FGF receptor dimer selects from an a la carte menu of heparan sulfate motifs.* Curr Opin Struct Biol **15**: 506-516.
65. Sher, I., A. Weizman, S. Lubinsky-Mink, T. Lang, N. Adir, D. Schomburg and D. Ron (1999) *Mutations uncouple human fibroblast growth factor (FGF)-7 biological activity and receptor binding and support broad specificity in the secondary receptor binding site of FGFs.* J. Biol. Chem. **274**: 35016-35022.

66. Stauber, D. J., A. D. DiGabriele and W. A. Hendrickson (2000) *Structural interactions of fibroblast growth factor receptor with its ligands.* Proc. Natl. Acad. Sci. U. S. A. **97**: 49-54.
67. Mohammadi, M., S. K. Olsen and R. Goetz (2005) *A protein canyon in the FGF-FGF receptor dimer selects from an a la carte menu of heparan sulfate motifs.* Curr. Opin. Struct. Biol. **15**: 506-516.
68. Harmer, N. J., L. L. Ilag, B. Mulloy, L. Pellegrini, C. V. Robinson and T. L. Blundell (2004) *Towards a resolution of the stoichiometry of the fibroblast growth factor (FGF)-FGF receptor-heparin complex.* J. Mol. Biol. **339**: 821-834.
69. Ibrahimi, O. A., B. K. Yeh, A. V. Eliseenkova, F. Zhang, S. K. Olsen, M. Igarashi, S. A. Aaronson, R. J. Linhardt and M. Mohammadi (2005) *Analysis of mutations in fibroblast growth factor (FGF) and a pathogenic mutation in FGF receptor (FGFR) provides direct evidence for the symmetric two-end model for FGFR dimerization.* Mol. Cell Biol. **25**: 671-684.
70. Thornton, S. C., S. N. Mueller and E. M. Levine (1983) *Human endothelial cells: use of heparin in cloning and long-term serial cultivation.* Science **222**: 623-625.
71. Gospodarowicz, D. and J. Cheng (1986) *Heparin protects basic and acidic FGF from inactivation.* J. Cell Physiol. **128**: 475-484.
72. Saksela, O., D. Moscatelli, A. Sommer and D. B. Rifkin (1988) *Endothelial cell-derived heparan sulfate binds basic fibroblast growth factor and protects it from proteolytic degradation.* J. Cell Biol. **107**: 743-751.
73. Prestrelski, S. J., G. M. Fox and T. Arakawa (1992) *Binding of heparin to basic fibroblast growth factor induces a conformational change.* Arch. Biochem. Biophys. **293**: 314-319.
74. DiGabriele, A. D., I. Lax, D. I. Chen, C. M. Svahn, M. Jaye, J. Schlessinger and W. A. Hendrickson (1998) *Structure of a heparin-linked biologically active dimer of fibroblast growth factor.* Nature **393**: 812-817.
75. Faham, S., R. E. Hileman, J. R. Fromm, R. J. Linhardt and D. C. Rees (1996) *Heparin structure and interactions with basic fibroblast growth factor.* Science **271**: 1116-1120.
76. Ornitz, D. M., A. B. Herr, M. Nilsson, J. Westman, C. M. Svahn and G. Waksman (1995) *FGF binding and FGF receptor activation by synthetic heparan-derived di- and trisaccharides.* Science **268**: 432-436.
77. Zhu, X., B. T. Hsu and D. C. Rees (1993) *Structural studies of the binding of the anti-ulcer drug sucrose octasulfate to acidic fibroblast growth factor.* Structure **1**: 27-34.
78. Vlodavsky, I., J. Folkman, R. Sullivan, R. Fridman, R. Ishai-Michaeli, J. Sasse and M. Klagsbrun (1987) *Endothelial cell-derived basic fibroblast growth factor: synthesis and deposition into subendothelial extracellular matrix.* Proc. Natl. Acad. Sci. U. S. A. **84**: 2292-2296.
79. Gonzalez, A. M., M. Buscaglia, R. Fox, A. Isacchi, P. Sarmientos, J. Farris, M. Ong, D. Martineau, D. A. Lappi and A. Baird (1992) *Basic fibroblast growth factor in Dupuytren's contracture.* Am. J. Pathol. **141**: 661-671.
80. Rudland, P. S., A. M. Platt-Higgins, M. C. Wilkinson and D. G. Fernig (1993) *Immunocytochemical identification of basic fibroblast growth factor in the developing rat mammary gland: variations in location are dependent on glandular structure and differentiation.* J. Histochem. Cytochem. **41**: 887-898.
81. Baird, A. and N. Ling (1987) *Fibroblast growth factors are present in the extracellular matrix produced by endothelial cells in vitro: implications for a role of heparinase-like enzymes in the neovascular response.* Biochem. Biophys. Res. Commun. **142**: 428-435.

82. Folkman, J., M. Klagsbrun, J. Sasse, M. Wadzinski, D. Ingber and I. Vlodavsky (1988) *A heparin-binding angiogenic protein--basic fibroblast growth factor--is stored within basement membrane.* Am. J. Pathol. **130**: 393-400.
83. Flaumenhaft, R., D. Moscatelli, O. Saksela and D. B. Rifkin (1989) *Role of extracellular matrix in the action of basic fibroblast growth factor: matrix as a source of growth factor for long-term stimulation of plasminogen activator production and DNA synthesis.* J. Cell Physiol. **140**: 75-81.
84. Gallagher, J. T. (1989) *The extended family of proteoglycans: social residents of the pericellular zone.* Curr. Opin. Cell Biol. **1**: 1201-1218.
85. Kato, M., H. Wang, V. Kainulainen, M. L. Fitzgerald, S. Ledbetter, D. M. Ornitz and M. Bernfield (1998) *Physiological degradation converts the soluble syndecan-1 ectodomain from an inhibitor to a potent activator of FGF-2.* Nat. Med. **4**: 691-697.
86. Lobb, R. R., D. J. Strydom and J. W. Fett (1985) *Comparison of human and bovine brain derived heparin-binding growth factors.* Biochem. Biophys. Res. Commun. **131**: 586-592.
87. Harper, J. W. and R. R. Lobb (1988) *Reductive methylation of lysine residues in acidic fibroblast growth factor: effect on mitogenic activity and heparin affinity.* Biochemistry **27**: 671-678.
88. Thompson, L. D., M. W. Pantoliano and B. A. Springer (1994) *Energetic characterization of the basic fibroblast growth factor-heparin interaction: identification of the heparin binding domain.* Biochemistry **33**: 3831-3840.
89. Ori, A., M. C. Wilkinson and D. G. Fernig (2008) *The heparanome and regulation of cell function: structures, functions and challenges.* Frontiers in Bioscience **13**: 4309-4338.
90. Ori, A., M. C. Wilkinson and D. G. Fernig (2011) *A systems biology approach for the investigation of the heparin/heparan sulfate interactome.* J. Biol. Chem. **286**: 19892-19904.
91. Allen, B. L. and A. C. Rapraeger (2003) *Spatial and temporal expression of heparan sulfate in mouse development regulates FGF and FGF receptor assembly.* J. Cell Biol. **163**: 637-648.
92. Guimond, S., M. Maccarana, B. B. Olwin, U. Lindahl and A. C. Rapraeger (1993) *Activating and inhibitory heparin sequences for FGF-2 (basic FGF). Distinct requirements for FGF-1, FGF-2, and FGF-4.* J. Biol. Chem. **268**: 23906-23914.
93. Ostrovsky, O., B. Berman, J. Gallagher, B. Mulloy, D. G. Fernig, M. Delehedde and D. Ron (2002) *Differential effects of heparin saccharides on the formation of specific fibroblast growth factor (FGF) and FGF receptor complexes.* J. Biol. Chem. **277**: 2444-2453.
94. Ishihara, M., D. J. Tyrrell, G. B. Stauber, S. Brown, L. S. Cousens and R. J. Stack (1993) *Preparation of affinity-fractionated, heparin-derived oligosaccharides and their effects on selected biological activities mediated by basic fibroblast growth factor.* J. Biol. Chem. **268**: 4675-4683.
95. Ishihara, M. (1994) *Structural requirements in heparin for binding and activation of FGF-1 and FGF-4 are different from that for FGF-2.* Glycobiology **4**: 817-824.
96. Rahmoune, H., H. L. Chen, J. T. Gallagher, P. S. Rudland and D. G. Fernig (1998) *Interaction of heparan sulfate from mammary cells with acidic fibroblast growth factor (FGF) and basic FGF. Regulation of the activity of basic FGF by high and low affinity binding sites in heparan sulfate.* J. Biol. Chem. **273**: 7303-7310.
97. Jemth, P., J. Kreuger, M. Kusche-Gullberg, L. Sturiale, G. Gimenez-Gallego and U. Lindahl (2002) *Biosynthetic oligosaccharide libraries for identification of protein-binding heparan sulfate motifs. Exploring the structural diversity by screening for fibroblast growth factor (FGF)1 and FGF2 binding.* J. Biol. Chem. **277**: 30567-30573.

98. Kreuger, J., P. Jemth, E. Sanders-Lindberg, L. Eliahu, D. Ron, C. Basilico, M. Salmivirta and U. Lindahl (2005) *Fibroblast growth factors share binding sites in heparan sulphate.* Biochem. J. **389**: 145-150.
99. Kreuger, J., D. Spillmann, J. P. Li and U. Lindahl (2006) *Interactions between heparan sulfate and proteins: the concept of specificity.* J. Cell Biol. **174**: 323-327.
100. Sambrook, J., E. F. Fritsch and T. Maniatis *Molecular Cloning: A Laboratory Manual, 2nd ed.* 1989 Cold Spring Laboratory, Cold Spring Harbor, NY.
101. Rudland, P. S., A. C. Twiston Davies and S. W. Tsao (1984) *Rat mammary preadipocytes in culture produce a trophic agent for mammary epithelia-prostaglandin E2.* J. Cell Physiol. **120**: 364-376.
102. Uniewicz, K. A., A. Ori, R. Xu, Y. Ahmed, M. C. Wilkinson, D. G. Fernig and E. A. Yates (2010) *Differential scanning fluorimetry measurement of protein stability changes upon binding to glycosaminoglycans: a screening test for binding specificity.* Anal. Chem. **82**: 3796-3802.
103. Ori, A., P. Free, J. Courty, M. C. Wilkinson and D. G. Fernig (2009) *Identification of heparin-binding sites in proteins by selective labeling.* Mol Cell Proteomics **8**: 2256-2265.
104. Delehedde, M., M. Lyon, R. Vidyasagar, T. J. McDonnell and D. G. Fernig (2002) *Hepatocyte growth factor/scatter factor binds to small heparin-derived oligosaccharides and stimulates the proliferation of human HaCaT keratinocytes.* J. Biol. Chem. **277**: 12456-12462.
105. Duchesne, L., B. Tissot, T. R. Rudd, A. Dell and D. G. Fernig (2006) *N-glycosylation of fibroblast growth factor receptor 1 regulates ligand and heparan sulfate co-receptor binding.* J. Biol. Chem. **281**: 27178-27189.
106. Duchesne, L., D. Gentili, M. Comes-Franchini and D. G. Fernig (2008) *Robust ligand shells for biological applications of gold nanoparticles.* Langmuir **24**: 13572-13580.
107. Ron, D., D. P. Bottaro, P. W. Finch, D. Morris, J. S. Rubin and S. A. Aaronson (1993) *Expression of biologically active recombinant keratinocyte growth factor. Structure/function analysis of amino-terminal truncation mutants.* J. Biol. Chem. **268**: 2984-2988.
108. Ke, Y. Q., D. G. Fernig, J. A. Smith, M. C. Wilkinson, S. Y. Anandappa, P. S. Rudland and R. Barraclough (1990) *High-level production of human acidic fibroblast growth factor in E. coli cells: inhibition of DNA synthesis in rat mammary fibroblasts at high concentrations of growth factor.* Biochem. Biophys. Res. Commun. **171**: 963-971.
109. Lipton, S. A., J. A. Wagner, R. D. Madison and P. A. D'Amore (1988) *Acidic fibroblast growth factor enhances regeneration of processes by postnatal mammalian retinal ganglion cells in culture.* Proc. Natl. Acad. Sci. U. S. A. **85**: 2388-2392.
110. Arunkumar, A. I., T. K. Kumar, K. M. Kathir, S. Srisailam, H. M. Wang, P. S. Leena, Y. H. Chi, H. C. Chen, C. H. Wu, R. T. Wu, G. G. Chang, I. M. Chiu and C. Yu (2002) *Oligomerization of acidic fibroblast growth factor is not a prerequisite for its cell proliferation activity.* Protein Sci. **11**: 1050-1061.
111. Smith, J. A., D. P. Winslow and P. S. Rudland (1984) *Different growth factors stimulate cell division of rat mammary epithelial, myoepithelial, and stromal cell lines in culture.* J. Cell Physiol. **119**: 320-326.
112. Rapraeger, A. C., A. Krufka and B. B. Olwin (1991) *Requirement of heparan sulfate for bFGF-mediated fibroblast growth and myoblast differentiation.* Science **252**: 1705-1708.
113. Rudd, T. R., S. E. Guimond, M. A. Skidmore, L. Duchesne, M. Guerrini, G. Torri, C. Cosentino, A. Brown, D. T. Clarke, J. E. Turnbull, D. G. Fernig and E. A. Yates (2007) *Influence of substitution pattern and cation binding on conformation and activity in heparin derivatives.* Glycobiology **17**: 983-993.

114. Duchesne, L., V. Octeau, R. N. Bearon, A. Beckett, I. A. Prior, B. Lounis and D. G. Fernig (2012) *Transport of fibroblast growth factor 2 in the pericellular matrix is controlled by the spatial distribution of its binding sites in heparan sulfate.* PLoS Biol. **10**: e1001361.
115. Kinsella, L., H. L. Chen, J. A. Smith, P. S. Rudland and D. G. Fernig (1998) *Interactions of putative heparin-binding domains of basic fibroblast growth factor and its receptor, FGFR-1, with heparin using synthetic peptides.* Glycoconj. J. **15**: 419-422.
116. Ori, A., P. Free, J. Courty, M. C. Wilkinson and D. G. Fernig (2009) *Identification of heparin binding sites in proteins by selective labelling.* Mol. Cell Proteomics **8**: 2256-2265.
117. Sher, I., B. K. Yeh, M. Mohammadi, N. Adir and D. Ron (2003) *Structure-based mutational analyses in FGF7 identify new residues involved in specific interaction with FGFR2IIIb.* FEBS Lett. **552**: 150-154.
118. Wallace, B. A. and R. W. Janes (2001) *Synchrotron radiation circular dichroism spectroscopy of proteins: secondary structure, fold recognition and structural genomics.* Curr Opin Chem Biol **5**: 567-571.
119. Wallace, B. A. (2000) *Synchrotron radiation circular-dichroism spectroscopy as a tool for investigating protein structures.* J. Synchrotron Radiat. **7**: 289-295.
120. Mulloy, B. and M. J. Forster (2000) *Conformation and dynamics of heparin and heparan sulfate.* Glycobiology **10**: 1147-1156.
121. Rudd, T. R., R. J. Nichols and E. A. Yates (2008) *Selective detection of protein secondary structural changes in solution protein-polysaccharide complexes using vibrational circular dichroism (VCD).* J. Am. Chem. Soc. **130**: 2138-2139.
122. Fernig, D. G., J. A. Smith and P. S. Rudland (1990) *Appearance of basic fibroblast growth factor receptors upon differentiation of rat mammary epithelial to myoepithelial-like cells in culture.* J. Cell Physiol. **142**: 108-116.
123. Morrison, R. S., J. L. Gross, W. F. Herblin, T. M. Reilly, P. A. LaSala, R. L. Alterman, J. R. Moskal, P. L. Kornblith and D. L. Dexter (1990) *Basic fibroblast growth factor-like activity and receptors are expressed in a human glioma cell line.* Cancer Res. **50**: 2524-2529.
124. Bono, F., P. Rigon, I. Lamarche, P. Savi, V. Salel and J. M. Herbert (1997) *Heparin inhibits the binding of basic fibroblast growth factor to cultured human aortic smooth-muscle cells.* Biochem. J. **326 ( Pt 3)**: 661-668.
125. Rudland, P. S., S. J. Leinster, J. Winstanley, B. Green, M. Atkinson and H. D. Zakhour (1993) *Immunocytochemical identification of cell types in benign and malignant breast diseases: variations in cell markers accompany the malignant state.* J. Histochem. Cytochem. **41**: 543-553.
126. Hancock, J. F. and I. A. Prior (2005) *Electron microscopic imaging of Ras signaling domains.* Methods **37**: 165-172.
127. Guimond, S. E. and J. E. Turnbull (1999) *Fibroblast growth factor receptor signalling is dictated by specific heparan sulphate saccharides.* Curr. Biol. **9**: 1343-1346.